REGULATION OF THE ANTIOXIDANT GLUTATHIONE: IN THE CEREBRAL CORTEX AND THE RELATIONSHIP WITH PERIPHERAL TISSUES

by

JOAN SONG

(Under the Direction of Robert Pazdro)

ABSTRACT

Glutathione (GSH) is a ubiquitous thiol tripeptide that is well known for its antioxidant role in reducing oxidative stress and maintaining redox balance. Oxidative stress occurs when there is an imbalance between reactive oxygen species (ROS) and antioxidants in favor of ROS production, which have been implicated in disease. Previous studies have utilized inbred mice models to identify canonical GSH genes influencing GSH regulation, however, these findings do not reflect the genetic diversity of the human population. Recent studies suggest that GSH regulation is governed by tissue-specific novel genes, yet there is little understanding of the genetic mechanisms that regulate GSH levels in the brain. To address this knowledge gap, we utilized the Diversity Outbred (DO) mouse stock, which models a diverse genetic profile comparable to humans, to (1) compare levels and regulation of glutathione in the brain to other major tissues and (2) investigate genes in the genome influencing brain glutathione regulation.

INDEX WORDS: Brain, Glutathione, Redox, Genetic mapping, Diversity Outbred

REGULATION OF THE ANTIOXIDANT GLUTATHIONE: IN THE CEREBRAL CORTEX AND THE RELATIONSHIP WITH PERIPHERAL TISSUES

by

JOAN SONG

BS, New York University, 2023

A Thesis Submitted to the Graduate Faculty of The University of Georgia in Partial Fulfillment of the Requirements for the Degree

MASTER OF SCIENCE

ATHENS, GEORGIA

2025

REGULATION OF THE ANTIOXIDANT GLUTATHIONE: IN THE CEREBRAL CORTEX AND THE RELATIONSHIP WITH PERIPHERAL TISSUES

by

JOAN SONG

Major Professor:	Robert Pazdro
Committee:	Connie Rogers
	Hea Jin Park

Electronic Version Approved:

Ron Walcott
Vice Provost for Graduate Education and Dean of the Graduate School
The University of Georgia
August 2025

DEDICATION

I would like to dedicate this thesis to all my friends and family who have provided me with all the love and support throughout this process. To my loving parents and brothers, thank you for your endless encouragement, for always being there for me, and for being my number one cheerleader. To my friends, thank you for lifting me up and bringing a smile to my face. I also want to thank my dog, Kai, for providing me with all the emotional support and cuddles when I needed it the most. Lastly, I want to thank God for giving me the strength and faith to persevere during this entire journey. This would not have been possible without all your immense support.

ACKNOWLEDGEMENTS

I would like to acknowledge all of whom who have supported and guided me with this work. Firstly, I would like to thank my former lab mates, Jess Strosahl and Mary McKennon Pierce for providing me with guidance and mentorship. To my undergraduates in the Pazdro lab, Keren Song, Vivian Huynh, and Laurie Clare Jones, thank you for your commitment and assistance in this research. This truly would not have been possible without all of you. To Ching-Ting Huang of the Devos Lab, thank you for your exceptional guidance, as well as generosity to spend time answering my questions on using R/qtl. To Dr. Lauren Housley, thank you for all the mentorship you have provided me with to help shape me into a better student. To my DI cohort, thank you for bringing me joy and comfort during these two years. To Dr. Emma Laing, thank you for always radiating positive energy and for continuing to inspire others. To Dr. Dulce Minaya, thank you for ensuring my work is carried out smoothly and providing me with the resources to maintain our lab. To my major professor, Dr. Robert Pazdro, thank you for your words of encouragement and for always believing in me -- I am very proud to have been a part of the Pazdro lab. Lastly to my committee members, Dr. Connie Rogers and Dr. Hea Jin Park, thank you for your guidance and support, as well as sharing your expertise throughout this work.

TABLE OF CONTENTS

Page

LIST OF TABLES

Page

LIST OF FIGURES

Page

CHAPTER 1

INTRODUCTION

Chapter 2 serves as a literature review to provide a comprehensive overview of the background and context for the research discussed in later chapters. The review aims to bring forth a deeper understanding of complex interactions between glutathione regulation across different tissues and genetic factors, with topics in glutathione extending towards its biological function, role in redox homeostasis, regulation, and implications in disease. Moreover, an overview of mouse genetics and bioinformatics analysis establishes context and rationale with regards to research on genetic factors influencing glutathione. The purpose and significance of this thesis is presented at the end of the chapter. Chapter 3 and 4 focuses on the thesis research, with objectives of the research to: 1) identify the statistical relationship between glutathione in the brain and other peripheral tissues and 2) identify genetic variants associated with glutathione regulation in the brain. Chapter 5 provides conclusions and implications for future research.

CHAPTER 2

LITERATURE REVIEW

Introduction

Glutathione (GSH) is an essential antioxidant that plays an important role in fighting against oxidative stress and detoxifying xenobiotic compounds. To protect cells and maintain redox homeostasis, the glutathione redox system acts as the cell's antioxidant defense system, converting between the reduced thiol GSH and oxidized disulfide GSSG forms. Dysregulation of glutathione and imbalance in redox homeostasis has been implicated in various diseases such as cancer, cardiovascular disease, neurological disease, respiratory disease, diabetes, and kidney disease. Though research on glutathione has been studied extensively over the years, there is still ambiguity in understanding the intricate interplay between genetics, glutathione regulation, oxidative stress, and disease. Inbred mouse strains have been more commonly used in research to gain a better understanding on glutathione metabolism, however, studying the role of genetics is limited due to the tightly controlled genetic background of such mouse strains. For this reason, the research presented in this thesis utilizes a diversity outbred (DO) mice stock to analyze the role of genetics in glutathione regulation and more accurately reflect the genetic variation found in human populations. Findings become more translatable to human health with a broad spectrum of phenotypic variability. All in all, this thesis study expands upon previous work to define the genetic architecture of the glutathione redox system and provide further knowledge in understanding complex interactions between glutathione regulation, genetic factors, and human health.

Oxidative Stress

Mechanisms of Oxidative Stress: Oxidative stress is an imbalance between oxygen reactive species (ROS) and antioxidants in favor of ROS production, leading to an accumulation of ROS in the cell and tissues [1]. An increase of ROS and other oxidants, or a decrease in antioxidants, leads to the progression of oxidative stress due to the antioxidant defense system being unable to counteract overwhelmingly higher levels of ROS production [2]. As the production of ROS and oxidants exceeds the functional capacity of the antioxidant defense system, cellular components become damaged and dysfunctional, resulting in a downward cascade of physiological stress to the body [3]. However, when maintained at low to moderate concentrations, ROS may be beneficial in promoting human health, such as protecting against invading pathogens, facilitating cell signaling, and regulating neural activity [1]. The key to maintaining homeostasis and normal cellular activity is by achieving a balance between ROS and antioxidants [4]. Though ROS are produced under normal physiological conditions, excess levels of ROS under pathophysiological conditions lead to progressive consequences of oxidative stress [5].

Free radicals are reactive chemicals with an unpaired electron located in its outer orbit, causing them to become unstable and very reactive [6, 7]. For this reason, they can either donate or accept an electron from other molecules and act as a reductant or oxidant, respectively [8]. Free radicals are often classified as ROS or reactive nitrogen species (RNS) [9, 10], though these categories include both radical and non-radical species [7]. Commonly known oxygen free radicals include superoxide ($O_2^{\bullet-}$), hydroxyl ($OH^{\bullet}$), peroxyl ($ROO^{\bullet}$), alkoxyl ($RO^{\bullet}$), hydroperoxyl ($HOO^{\bullet}$) radicals, oxygen singlet, and peroxynitrite ($ONOO^{-}$), while nitrogen free

radicals include nitric oxide ($^{\bullet}NO$) and nitrogen dioxide ($^{\bullet}NO_2$) [7, 8]. The production of ROS requires oxygen and is regulated by enzymatic and nonenzymatic reactions [1, 7].

Nonenzymatic reactions for free radical production occur intracellularly in the mitochondrial electron transport chain (ETC), where $O_2^{\bullet-}$, the most generated ROS in mammalian cells, convert into hydrogen peroxide by the superoxide dismutase (SOD) enzyme [1, 11]. The mitochondrial ETC contains several sites that leak electrons to oxygen as electron pairs run down the ETC, which produce $O_2^{\bullet-}$ (Figure 2.1) [12, 13]. Though many of the sites produce ROS, ROS is produced largely at complex 1 and complex III, where complex I releases $O_2^{\bullet-}$ to the mitochondrial matrix and complex III releases it to the matrix and intermembrane space [12, 14]. Ubiquinone (coenzyme Q) is reduced to ubiquinol (QH_2), which drives electrons through complex I to reduce $NAD^{\pm}$ to NADH; superoxide is released by complex I during electron transport from QH_2 to $NAD^{\pm}$ [12, 15]. In complex III, ROS is produced via the autoxidation of Q located on both sides of the inner membrane [13]. Once $O_2^{\bullet-}$ is produced, it can either reduce cytochrome c in the intermembrane space or convert to H_2O_2 and O_2 in the matrix and intermembrane space [13].

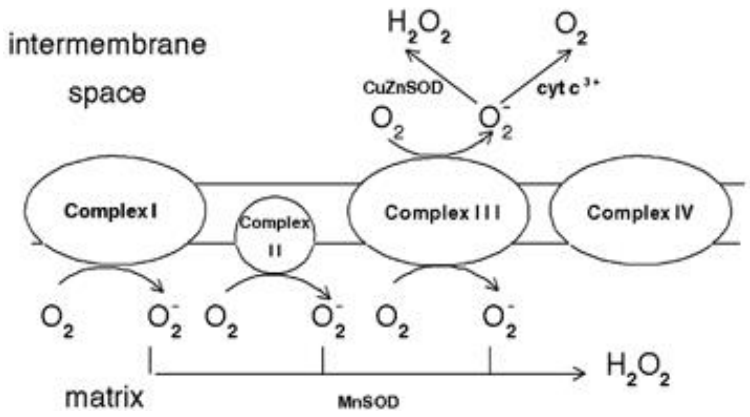

Figure 2.1. Sites of superoxide formation in the respiratory chain. Figure adapted from Turrens. (2003) [13].

Enzymatic reactions generating $O_2^{\bullet-}$ involve NADPH oxidase, xanthine oxidase, and peroxidases [1, 11]. Through several reactions, $O_2^{\bullet-}$ is converted to other non-radical reactive species, such as H_2O_2, hypochlorous acid (HOCl), hypobromus acid (HOBr), and $ONOO^-$ [1, 7]. Essentially, ROS is produced by a sequential reduction of electrons (Figure 2.2) [16]. H_2O_2 is produced from $O_2^{\bullet-}$ through enzymes superoxide dismutase (SOD), cytochrome P450, D-amino acid oxidase, acetyl coenzyme A oxidase, or uric acid oxidase [7, 11]. Oxidants with stronger oxidant potential, $ONOO^-$, can also be produced by the reaction between NO and $O_2^{\bullet-}$ as a result [7]. RNS formed through this reaction is dangerous in that it causes damage to nucleic acids, lipids, and proteins [10, 17].

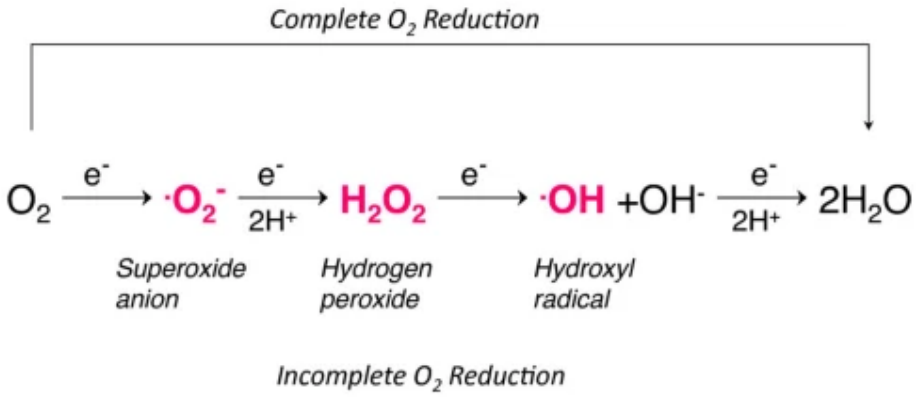

Figure 2.2. Complete and incomplete reduction of molecule oxygen. Figure adapted from Bartz and Piantadosi. (2010) [16].

The Fenton reaction involving H_2O_2 and $O_2^{\bullet-}$ and using ferrous ion (Fe^{2+}) or cuprous ion (Cu^+) as its reaction catalyst, forms $OH^\bullet$ [1]. $OH^\bullet$ is the most powerful ROS oxidant and is formed during the Haber-Weiss reaction, either through the Fenton reaction or decomposition of $ONOO^-$ [18]. During the Fenton reaction, Fe^{2+} oxidizes to ferric ion (Fe^{3+}) while simultaneously producing $OH^\bullet$ and a hydroxide ion (OH^-) through the interaction between Fe^{2+} and H_2O_2; the Fe^{2+} is then reduced back to Fe^{3+} by obtaining an electron from $O_2^{\bullet-}$ (Figure 2.3) [18]. Compared to other ROS, $OH^\bullet$ is more attracted towards smaller biomolecules (i.e. amino acids, nucleotides, and monosaccharides), which leads to the most severe damage to biological systems [19].

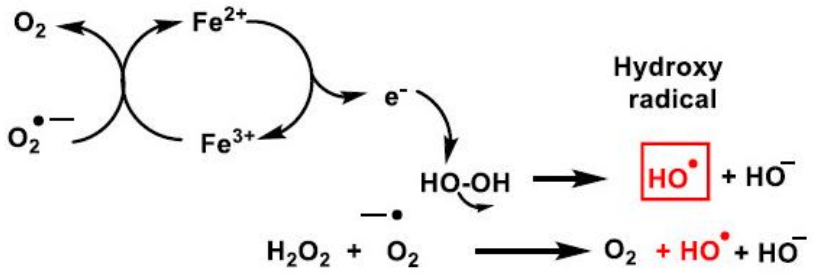

Figure 2.3. The Fenton reaction. Figure adapted from Juan, *et al*. (2021) [18].

Free radicals are generated from both endogenous and exogenous sources [1]. Endogenous production of free radicals derives from various factors such as the mitochondria, cytochrome P450 metabolism, peroxisomes, immune cell activation, inflammation, ischemia, infection, cancer, excessive exercise, mental stress, and aging [1, 20]. Production of exogenous free radicals occur from factors including environmental pollutants, heavy metals, drugs, chemicals, cigarette smoke, alcohol, and radiation [1].

Impact on Cellular Components (Lipids, Proteins, Carbohydrates, DNA): Due to excess levels of ROS mediating oxidative stress, essential biomolecules progressively become damaged and no longer carry normal function [8]. Though carbohydrates are targeted as well, the highly unstable and reactive nature of ROS primarily targets lipids, nucleic acids, and proteins [8].

Lipids: Cell membranes are prone to oxidative damage due to the sensitivity of polyunsaturated fatty acid (PUFA) residues of its phospholipids [10, 18]. Phospholipid contact with ROS oxidizing agents result in lipid peroxidation, where unsaturated fatty acid chains become oxidized by free radicals; this generates a hydroperoxidized lipid and an alkyl radical [18]. Lipid peroxidation results in non-enzymatic damage to the integrity of the cell membrane, altering its fluidity and permeability [21]. The process of lipid peroxidation occurs in three stages: initiation, propagation, and termination (Figure 2.4) [22]. During the initiation step, prooxidants (e.g., hydroxyl radical) remove a hydrogen atom from a lipid molecule at its allylic position and form a carbon-centered lipid radical ($L^{\bullet}$); once initiated, chain reactions will continue until termination products are formed [22]. Oxidation of PUFAs can be initiated by enzymes such as lipoxygenase, myeloperoxidase, and cyclooxygenase [23]. The propagation step involves the $L^{\bullet}$ to react with an oxygen molecule to generate a peroxyl radical ($LOO^{\bullet}$), which

then causes a hydrogen to be removed from another lipid molecule and generate a new $L^{\bullet}$ and lipid hydroperoxide (LOOH) [22]. This step acts as a chain reaction of $L^{\bullet}$ production with the peroxyl radical as the principal chain-carrying species [22, 23]. During the termination step, antioxidants (e.g., vitamin E) donate a hydrogen atom to $LOO^{\bullet}$ and produce a corresponding antioxidant radical that reacts with another $LOO^{\bullet}$ to form a nonradical products [22]. Lipid peroxidation produces primary and secondary oxidation products. Primary products include LOOH, and secondary products include aldehyde, such as malondialdehyde (MDA), propanal, hexanal, F2-isoprostanes, and 4-hydroxynonenal (4-HNE) [22]. F2-isoprostanes are products from the peroxidation of arachidonic acid esterified in phospholipids and are widely used as a biomarker of oxidative stress [24]. 4-HNE is a strong oxidant and the most significantly produced product derived from hydroperoxides; it harms signal transduction pathways and alters phenotypic characteristics of cells [20, 22].

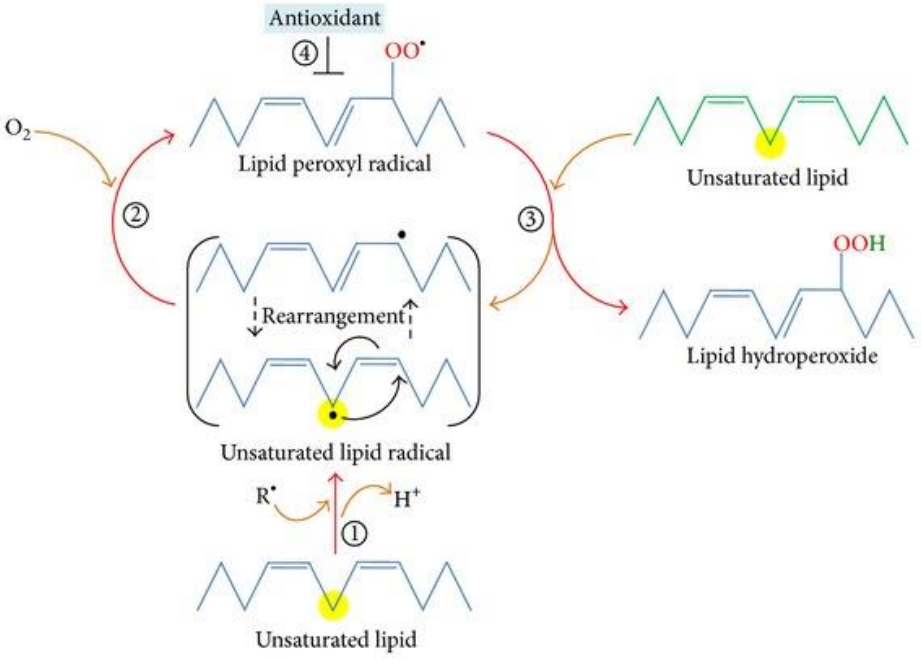

Figure 2.4. Lipid peroxidation process. Figure adapted from Ayala, *et al*. (2014) [22].

Proteins: The process of protein oxidation is complex in which oxidative damage in proteins can be categorized in three ways: oxidation of amino acids, cleavage of peptide bonds, and aggregation between proteins due to reactions with lipid peroxidation products [8, 18]. The side chains of amino acids are susceptible to oxidation, especially particular amino acids such as methionine, cysteine, arginine, and histidine [8, 10]. Peroxyl radical is the primary culprit for oxidation of proteins, and damage to proteins can disrupt enzyme activity, receptors, and membrane transport [8]. The peroxyl radical are then converted to alkyl peroxides by reacting with a protonated superoxide [20]. The oxidation process can occur through direct or indirect reactions. The direct mechanisms include ROS attack, metal-catalyzed oxidation (MCO), and oxidative cleavage of the protein backbone [25]. The indirect reaction (secondary mechanism) involves reactions between reactive products of other biomolecules (lipids, nucleic acids, and carbohydrates) and proteins, which result in a cross-linkage of amino acid side chains and carboxylate the protein [25, 26].

Carbohydrates: Advanced glycation end products (AGEs) are a complex group of compounds that are formed non-enzymatically through the Maillard reaction, where reducing sugars react with amino acids in proteins, lipids, or DNA [27]. The formation of endogenous AGEs can be divided into three main stages: glycation, Amadori rearrangement, and non-enzymatic peptide cross-linking [27]. During the glycation step, the Maillard reaction involves condensation between a carbonyl group from a reducing sugar and a side chain of an amino group (e.g., lysine side chain), and thereby producing a reversible Schiff base (aldimine) [28, 29]. Amadori products can then be produced through the reaction of Schiff base molecules between the amino group and glucose; formation of Amadori products is favored in the presence

of alkaline pH values and phosphate ions [27, 29]. Amadori products irreversibly rearrange and form into AGEs without regulation and following both oxidative and non-oxidative pathways [27, 29]. In the non-enzymatic peptide cross-linking stage, Amadori products further react with protein or amino acid residues to form additional AGEs [27]. Other pathways can contribute to the formation of endogenous AGEs, such as glucose autoxidation. Glucose autoxidation occurs when glucose reacts directly with proteins and lipids to form AGEs [27]. Due to covalent cross-linkage, the formation of AGEs causes impairments in protein structure and result in protein oligomerization and aggregation [30]. The binding of AGEs to the receptor for advanced glycation end-products (RAGE), a multi-ligand receptor, is implicated in the pathology of diabetic complications, neurodegenerative disorders, inflammation, oxidative stress, and cell death [27, 30]. The interaction between AGEs molecules and RAGE triggers a downstream signaling pathway that leads to the activation of the nuclear factor-kB (NF-kB) signaling pathway[27].

Nucleic Acids: ROS are important mediators of oxidative damage to nucleic acids. The hydroxyl radical is especially known to cause damage to - and react with - the purine base, pyrimidine bases, and deoxyribose backbone of the DNA molecule [10]. Damage to the DNA molecule leads to base and/or sugar alterations, sugar-base cyclization, DNA-protein cross-links, and intra- and interstrand cross-links, which can in turn generate DNA strand breaks [31]. By-products of DNA oxidation are base modifications including 8-oxoguanine (8-oxo-G or 8-hydroxygunanine), 2,6-diamino-4hydroxy-5-formamidopyrimidine (FapyGua), uracil glycol, and 5-hydroxycytosine [31, 32]. Guanine possesses low oxidation potential, making it more susceptible to singlet oxygen and thus form into 8-oxo-7,8-dihydroguanine (8-oxoG) [32]. 8-oxoG can lead to the disruption of cellular function through the formation of apurinic site (AP

site) or mispairing with adenine to alter DNA structure and promote mutagenesis [33]. Although DNA is considered the major target, RNA is also susceptible to oxidative damage. RNA, such as messenger RNA and ribosomal RNA, are more vulnerable to oxidative damage than DNA due to its single-stranded structure and lack of protective proteins [34, 35].

Repair Systems of Oxidative Damage: Essential maintenance repair systems are established to remove or repair biomolecules damaged by low-level oxidative damage from ROS, before they accumulate and lead to permanent damage [6]. Each biomolecule category has its own unique repair system to protect against oxidative stress: damaged nucleic acids are repaired by specific enzymes, oxidized proteins are removed by proteolytic systems, and oxidized lipids are repaired by peroxidases, phospholipases, and acyl transferases [6].

Three enzymatic activities are involved in repairing lipids from oxidative damage: (1) peroxidase with substrates hydrogen peroxide, short chain hydroperoxides, and phospholipid hydroperoxides; (2) phospholipase A_2 (PLA_2); and (3) lysphosphatidylcholine acyl CoA transferase (LPCAT) [36]. Peroxidase activity of peroxiredoxin 6 (Prdx6) can catalyze the reduction of its hydroperoxide substrates through the catalytic triads (peroxidation, resolution, and recycling) [36]. Prdx6 also exhibits PLA_2 activity, enabling it to selectively recognize and hydrolyze peroxidized fatty acids in the phospholipid membrane [37, 38]. The reduced phospholipid can then be regenerated by the LPCAT activity of Prdx6 by acylating the lost fatty acid with a free fatty acid (CoA derivative) [36]. This complete system of enzymatic activities provides protection to the integrity of the cell membrane.

Proteolytic enzymes, such as the 20S proteasome and the mitochondrial Lon protease, can recognize, degrade, and remove oxidized polypeptides from cells prior to aggregation and cross-linkage [38, 39]. The 20S proteasome is of the ubiquitin-proteasome system, a system in

the cytoplasm that plays an important in detecting and degrading misfolded and defective proteins [39, 40]. The 20S proteosome is an active core complex of the 26S proteosome that directly degrades substrates and consists of four stacked rings: two inner rings related to beta-subunits and two outer rings related to alpha-subunits [40]. The mitochondrial Lon protease is in the mitochondrial matrix and has a similar function to that of the 20S proteasome and degrades oxidized proteins [39]. The Lon protease is involved in maintaining the integrity of the mitochondrial genome and carries multiple functions, such as DNA binding and chaperone activity [39]. Taking these two proteolytic enzymes together, they act as key players in restoring the mitochondrial genome from oxidative stress.

To maintain genomic integrity, there are many major DNA repair pathways, such as the base excision repair (BER), nucleotide excision repair (NER), mismatch repair (MMR), homologous recombination (HR), and non-homologous end joining (NHEJ) [41]. The BER pathway repairs 8-oxoG and other base modifications, where the 8-oxoG is snipped off by 8-oxoguanine DNA glycosylase to leave an AP site [33]. The AP-endonuclease 1 (APE1) then processes AP sites into single strand breaks [33]. In the final step, the base and additional nucleotides are replaced by long patch and short patch base excision repair [33]. In a similar fashion, the NER pathway can also remove and repair DNA base lesions from the genome through two sub-pathways: global genomic NER (GG-NER) and transcription-coupled NER (TC-NER) [42]. The GG-NER detects and eliminates bulky damage in the entire genome, while the TC-NER repairs damage to transcribed DNA strands that limit transcription activity [43]. Both pathways can recognize damage of DNA with their corresponding proteins; TC-NER is activated by the stopping of RNA polymerase II at damaged sites of the transcribed strand, and GG-NER is controlled by XPC, a protein factor that reveals damage [43]. The transcription

factor II H (TFIIH) plays an important role during repair in these pathways by unwinding DNA, recruiting downstream repair factors, and verifying bulky lesions [43, 44]. This allows for DNA incision, DNA repair synthesis, and DNA strand ligation in both pathways [43].

Physiological Activities of ROS: When maintained at low or moderate amounts, ROS play a beneficial role in maintaining normal physiological function [1]. ROS are known to support crucial physiological processes as secondary messengers and participate in cell signaling and proliferation during cell adhesion and gene expression [45]. Additionally, they have a pivotal role in synthesizing cellular structures, fighting off pathogens, modulating proper blood flow, and regulating the redox system [1, 45]. The most significant effect of ROS in cell signaling is in the mitogen-activated protein kinase (MAPK) pathway, which involves the activation of nuclear transcription factor NF-kB [10]. NF-kB controls the expression of protective genes that participate in the repairment of damaged DNA, immunity, apoptosis, inflammation, cell growth, cell survival, and differentiation [10]. Furthermore, NF-kB is a DNA binding protein that interacts with a dimer of two members of the NF-kB/Rel/Dorsal (NRD) family of proteins; there are five NRD members, RelA (p65), cRel, RelB, p50 (NF-kB1) and p52 (NF-kB2) [10]. The inhibitory (IkB) family binds to NF-kB and keeps it inactive in the cytoplasm, however, the removal of IkB allows NF-kB to enter the nucleus and bind to kB regulatory elements [10]. The activation of NF-kB involves two major signaling pathways -- the canonical and noncanonical (or alternative) pathways (Figure 2.5) [46]. The canonical pathway responds to various stimuli, including cytokine receptors and TNF receptors, that trigger a multi-subunit IkB kinase (IKK) complex composed of catalytic subunits IKKα and IKKβ, and a regulatory subunit called NF-kB essential modulator (NEMO or IKKγ) [46]. Once activated, IKK can then phosphorylate IkBα and activates the ubiquitin-dependent degradation of IkBα in the proteosome, leading to the

nuclear translocation of dimers of the canonical NF-kB, p50/RelA and p50/c-Rel dimers [46]. On the other hand, the noncanonical pathway selectively responds to specific stimuli, such as ligands of the TNF receptor family [46]. NF-kB-inducing kinase (NIK) is the central signaling molecule that activates IKKα to mediate the phosphorylation of the NF-kB2 precursor protein, p100, and eventually induce p100 ubiquitination and processing [46, 47]. p100 requires degradation into mature NF-kB2 p52, in which then the noncanonical NF-kB complex p52/RelB is translocated into the nucleus [46].

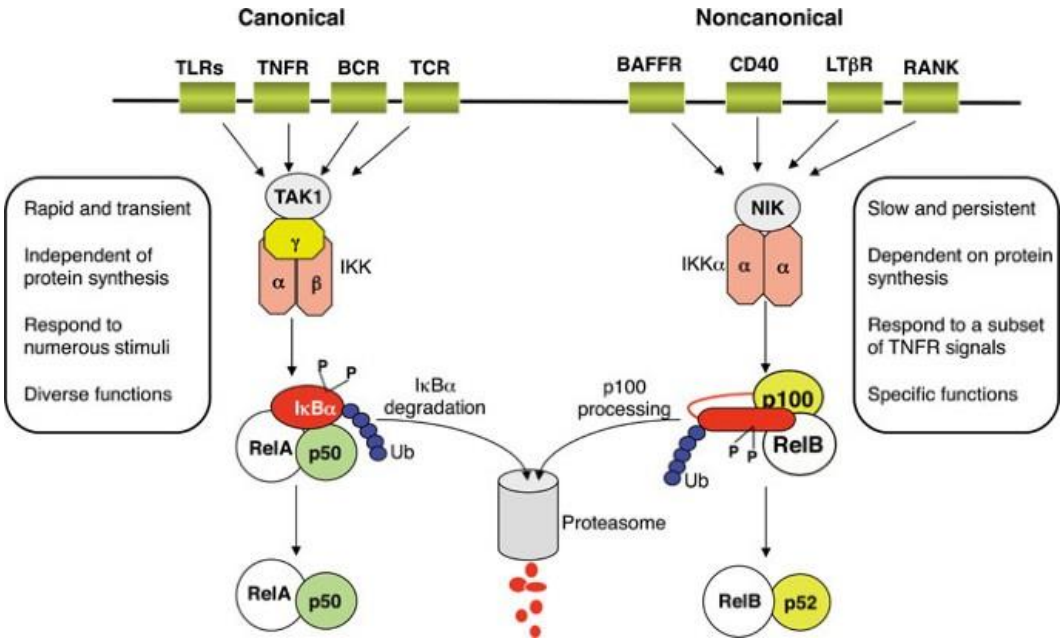

Figure 2.5. Canonical and non-canonical NF-kB signaling pathways. Figure adapted from Sun (2010) [47].

Endogenous oxidants can act as secondary messengers and trigger a cascade of intracellular responses that activate expression of antioxidant and detoxifying enzymes to regulate cellular redox status [2]. ROS are critical regulators of the Kelch-like ECH-associated protein (Keap1) to Nuclear factor erythroid 2-related factor 2 (Nrf2) signaling pathway that is

responsible for the transcription of antioxidant genes (Figure 2.6) [48]. Nrf2 regulates cellular responses against oxidative stress by regulating the expression of antioxidant genes, but is suppressed by Keap1, a substrate adaptor protein that binds to Nrf2 for polyubiquitination by Cullin 3 (Cul3) E3 ubiquitin for proteasomal degradation [48]. During times of oxidative stress, cysteine residues on Keap1 are modified and the protein structure is altered; ultimately, these changes prevent the ubiquitination of Nrf2 by Cul3 [48]. This allows Nrf2 to translocate to the nucleus, where it will heterodimerize with musculoaponeurotic fibrosarcoma (sMaf) proteins and bind to the ARE to activate the transcription of antioxidant genes [48].

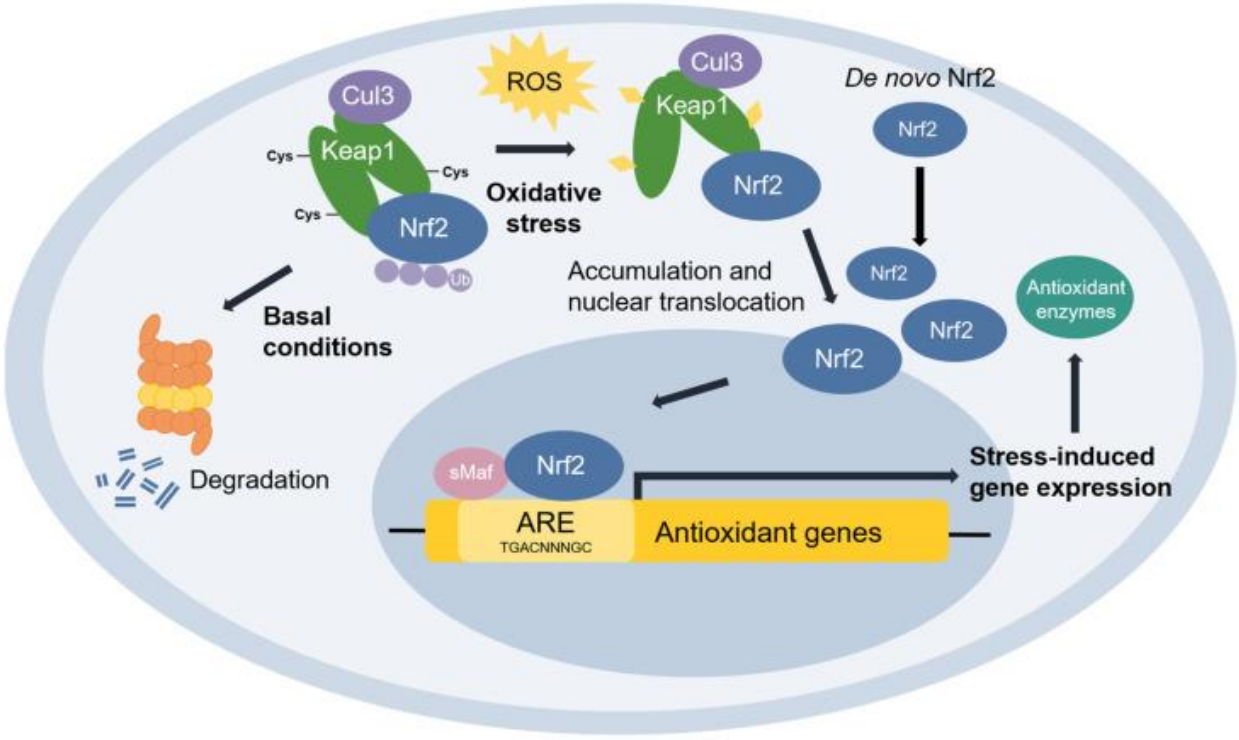

Figure 2.6. The Keap1-Nrf2 pathway. Figure adapted from Ngo & Duennwald (2022) [48].

Protective role of antioxidants against oxidative stress

Antioxidants of each class (endogenous and exogenous) possess a protective role in fighting against oxidative stress in the cell. The cell has developed a highly intricate endogenous antioxidant system to counteract ROS that can be further categorized into non-enzymatic and enzymatic groups [49]. Exogenous sources of antioxidants can play a supporting role in the cell's antioxidant defense system by directly neutralizing free radicals or enhancing endogenous activity [50].

Exogenous Antioxidants: Exogenous sources of antioxidants obtained from the diet or supplements can be characterized into three categories: the first category is vitamins (A, E, C, K); the second is carotenoids (lutein, B-carotene, lycopene) and polyphenols (flavonoids, phenolic acid); and the third is minerals (selenium, zinc) [51]. Vitamins A, E, and K are fat-soluble vitamins that carry out mechanisms of action towards mitigating oxidative stress [52]. Vitamin A includes retinol, retinal, and retinoic acid and possesses antioxidant properties by directly scavenging ROS and supporting antioxidant enzymatic activity [53]. All-trans-retinoic acid is the primary mediator of vitamin A's antioxidant abilities and regulates many genes involved in the cell's antioxidants processes, such as superoxide dismutase (SOD) [53]. Vitamin E is known to directly scavenge free-radicals and protect polyunsaturated fatty acids from oxidative damage, with α-tocopherol as its most active form; less active forms include β-tocopherol, γ-tocopherol, and α-tocotrienol [52]. Vitamin K is not a classical antioxidant; however, it has been discovered that vitamin K1 and K2 (menaquinone-4) can inhibit oxidative cell death caused by glutathione depletion [54]. Unlike vitamins A, E, and K, vitamin C is a water-soluble vitamin but can also act as a ROS scavenger and combat oxidative stress by

stimulating the biosynthesis and activation of antioxidant enzymes (e.g., SOD) and promote several transcription factors (e.g., Nrf2) that enable the expression of antioxidant genes [55, 56].

Carotenoids are the most abundant lipid-soluble phytochemicals and exhibit antioxidant properties, such as enhancing the translocation of Nrf2 into the nucleus and activating antioxidant enzymes [51, 57]. Specific carotenoids also act as a precursor to vitamin A. β-carotene is a provitamin A carotenoid that can convert to retinoids (vitamin A), however, other carotenoids (lutein and lycopene) cannot and are referred to as non-provitamin A carotenoids [52, 58]. Polyphenols carry multiple phenol groups that are effective in preventing lipid oxidation and can be broadly classified into flavonoids and phenolic acid [51, 59]. Flavonoids are the largest group within the family of plant-derived polyphenolic compounds, while phenolic acids are a dominant category under the non-flavonoid class and exist in plants either in their free form or esterified form [59]. In addition to its antioxidant properties, polyphenols have also been demonstrated to possess anti-inflammatory and anti-carcinogenic properties [59].

Trace minerals such as selenium and zinc are also important to the cell's antioxidant defense system. Selenium is an essential cofactor to form selenium dependent antioxidant enzymes (e.g., selenoproteins) such as glutathione peroxidase [7]. Selenocysteine forms a predominant residue of selenoproteins and during protein synthesis, the selenocysteine residue is co-translationally recognized by the UGA termination codon [60]. Selenium can be found in organic (selenocysteine, selenomethionine) and inorganic (selenite, selenate) compounds that are readily metabolized to various forms of Se metabolites in the body [60]. Zinc is a cofactor of SOD and inhibits lipid peroxidation by preventing copper ion and iron ion-initiated lipid oxidation [3]. Additionally, zinc regulates glutathione metabolism, inhibits the nicotinamide adenine dinucleotide phosphate-oxidase enzyme, and modulates metallothionein expression [61].

Dietary sources of antioxidants are critical in countering oxidative stress and the production of ROS, and growing evidence suggests that malnutrition in previously mentioned exogenous antioxidants give rise to oxidative damage to essential biomolecules and prevent numerous diseases [7]. A range of dietary patterns have been associated with the role of oxidative stress, with some dietary patterns linked with decreased oxidative stress and others vice versa [62]. The Mediterranean diet has been widely recommended to optimize antioxidant levels due to its composition of mainly plant-based foods rich in antioxidants, such as polyphenols [62]. It has also been demonstrated that the Mediterranean diet can prevent type 2 diabetes, stroke, cardiovascular disease, and Alzheimer's disease [62]. A high-fat and high-carbohydrate diet on the other hand, has been associated with elevated levels of protein carbonylation and lipid peroxidation and decreased antioxidant defense status [62]. Furthermore, these diets may alter oxygen metabolism, and as lipid deposits are accompanied by ROS production, this further exacerbates effects of oxidative stress and disease progression [62]. Adopting an antioxidant-rich dietary pattern and incorporating dietary supplements may help support and maintain the body's antioxidant system, thereby reducing the risk of adverse health outcomes.

Endogenous Antioxidants: Endogenous, small-molecule antioxidants include ascorbic acid, glutathione, melatonin, tocopherols and tocotrienols (vitamin E), uric acid, bilirubin, coenzyme Q, and alpha lipoic acid [3, 8]. The enzymatic group includes SOD, catalase, glutathione peroxidase (GPx), glutathione reductase (GR), and glutathione S-transferase (GST) [3, 8]. SOD is a metalloenzyme that catalyzes the breakdown of the superoxide anion into oxygen and hydrogen peroxide and requires a metal cofactor, such as iron (Fe), zinc (Zn), copper (Cu), and manganese (Mn) [8, 63]. SOD exists in three forms: cytosolic Cu, Zn-SOD, mitochondrial Mn-SOD, and extracellular-SOD [8, 50]. SODs neutralize superoxide ions

through successive oxidative and reductive cycles of transition metal ions at its active site [50]. Although SOD reduces the superoxide anion to hydrogen peroxide, hydrogen peroxide is still a harmful by-product to metabolic processes and must be converted into other, less harmful molecules [8]. The catalase enzyme reduces the hydrogen peroxide produced by SOD to less dangerous molecules, water and molecular oxygen, which completes the detoxification process following SOD [63]. GPx is a selenocysteine peroxidase that catalyzes the oxidation of glutathione (GSH) into oxidized glutathione (GSSG) and breaks down hydrogen peroxides to water by utilizing GSH as its electron donor, protecting the cell from lipid peroxidation and oxidative stress [63, 64]. There are at least eight GPx enzymes in humans, GPx1-GPx8, with GPx1-GPx4 and GPx6 being the only GPx enzymes to be selenoproteins [65]. GPx1 is the most abundant selenoperoxidase among the glutathione peroxidases and is found in the cytosol and mitochondria of all cells [63, 65]. GPx2 is commonly present in the gastrointestinal tract of the intestine [63], and GPx3 can be found in the plasma and primarily in renal tissue relative to other tissues [63, 65]. GPx4 is often referred to as a phospholipid hydroperoxide, because of its ability to break down lipid hydroperoxides and protect the cell membrane from oxidative damage [63, 66]. GPx6 is expressed in the olfactory epithelium but has different implications in humans and rats [64, 65]. GPx5, GPx7, and GPx8 are independent of selenium, where GPx5 is characterized as a secreted protein in the epididymis, and GPx7 and GPx8 are CysGPxs with low GPx activity [65]. GPx7 is known to improve non-alcoholic steatohepatitis by regulating oxidative stress, and GPx8 has shown to inhibit the oxidative stress response of hepatocellular carcinoma cells [66]. Oxidized glutathione through GPx can then convert back into reduced GSH through the GR enzyme by using NADPH as its reducing agent, maintaining the homeostasis of the glutathione

cycle [67]. GST enzymes can also fight against oxidative stress by reducing lipid hydroperoxides through selenium independent GPx enzymes [68].

Glutathione and redox homeostasis

Overview of Glutathione (Background, Metabolism, and Function): Glutathione (GSH) is a ubiquitous tripeptide composed of cysteine, glutamic acid, and glycine that directly acts as an antioxidant to protect the body from oxidative stress [69]. GSH was discovered in 1888 by J. de Rey-Pailhade, but its precise composition as γ-L-glutamyl-L-cysteinyl-glycine was established later in 1935 by Harington and Mead [70, 71]. GSH mostly exists in two forms: its thiol-reduced form and its disulfide-oxidized form (GSSG) [72]. GSH is the most abundant non-protein thiol in cells, however, unlike vitamins, it can be synthesized intracellularly through ATP-dependent enzymatic steps [69]. The first step of GSH biosynthesis is the rate-limiting step catalyzed by glutamate cysteine ligase (GCL) and coupled with ATP hydrolysis, which binds glutamate with cysteine to form γ-glutamyl-L-cysteine (Figure 2.7) [73, 74]. The next step is catalyzed by GSH synthetase (GS), which combines γ-glutamyl-L-cysteine with L-glycine to produce the GSH tripeptide [73]. Under normal physiological conditions, the rate of the enzymatic process for GSH synthesis is largely dependent on the availability of its precursor cysteine and GCL activity [72, 73].

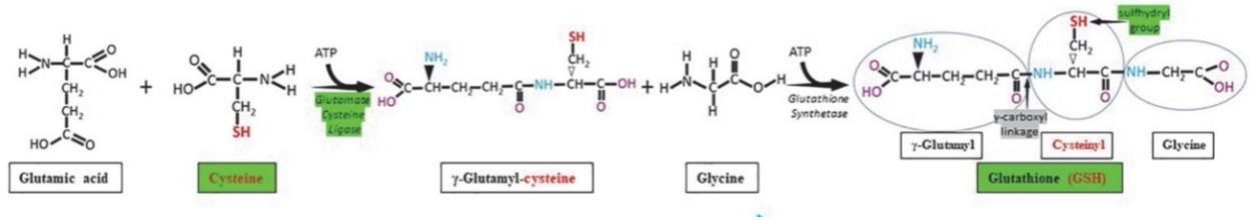

Figure 2.7. Glutathione (GSH) synthesis and redox cycle. Figure adapted from Labarrere & Kassab (2022) [74].

The predominant form of glutathione is GSH and represents at least 98% of total cellular glutathione [72]. Two molecules of GSH may be combined to form the disulfide-oxidized form (GSSG), a step typically coupled with GPx-mediated conversion of hydrogen peroxides to water [73]. GSSG can then form back into two molecules of GSH through the GR enzyme at the expense of NADPH produced by the pentose phosphate pathway, thereby forming a redox cycle [72, 73]. Apart from the redox cycle, organic peroxides can be reduced by either GPx or GST enzymes as two molecules of GSH convert to GSSG [73]. GSH is also involved in the γ-glutamyl cycle, which is critical to glutathione homeostasis and transportation to other cells (Figure 2.8) [75, 76]. γ-glutamyl transferase (GGT) is the first major enzyme of the γ-glutamyl cycle that regulates the metabolism of GSH; GGT breaks down extracellular GSH into its constituent amino acids, γ-glutamyl compounds and cysteinylglycine [75, 76]. These constituent amino acids are taken up by cells and are necessary for intracellular resynthesis of GSH [76]. Cysteinylglycine further breaks down into cysteine and glycine as cofactors for γ–glutamylcysteine synthetase and GSH synthetase, respectively [75, 76]. Through γ-glutamyl cyclotransferase, the γ-glutamyl amino acid is catalyzed into 5-oxoproline, which then is catalyzed into glutamate through 5-oxoprolinase [75]. Glutamate conjugates with cysteine to form γ–glutamylcysteine and is directly utilized for GSH biosynthesis [76]. This γ-glutamyl

cycle can act to bypass the rate-limiting step catalyzed by GCL and maintain levels of GSH in cells [76].

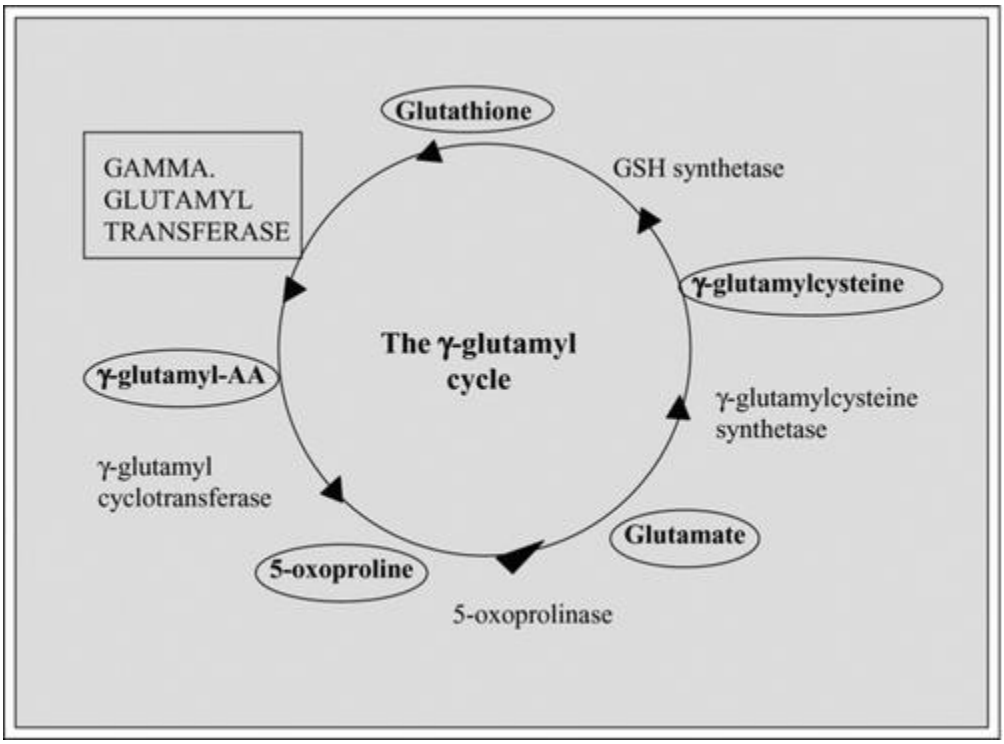

Figure 2.8. The γ-glutamyl cycle. Figure adapted from Mistry & Stockley. (2010) [75].

GSH functions as an antioxidant primarily as a component of the enzymatic processes involving GPx, GR, and GST [69, 72]. GSH also functions independently and directly reacts with a variety of free radicals and pro-oxidants, as well as directly interacting with damaged biomolecules for repairment [69, 72]. The GSH/GSSG couple coordinates with other redox couples, $NADP^+$/NADPH and FAD/$FADH_2$, in maintaining cellular redox homeostasis [77]. These redox couples have oxidizing or reducing capabilities in different capacities, depending on their standard redox potential: -240 mV (GSH/GSSG), -315 mV ($NADP^+$/NADPH), and –219 mV (FAD/$FADH_2$) [77]. The redox state of the GSH/GSSG couple serves as an important

indicator of the redox environment [74]. In addition to its role as an antioxidant in cellular redox reactions, GSH also participates in detoxifying xenobiotics, protecting protein thiols from crosslinking and oxidation, regulating the cell cycle, and storing cysteine [78].

Digestion, Absorption, and Transportation Mechanisms: Glutathione can be orally administered via diet or supplementation and is primarily absorbed in the upper jejunum, where GSH breaks down into its constituent amino acids through the GGT enzyme [79, 80]. However, oral GSH supplementation is not efficient due to hydrolysis of GSH by GGT, leading to poor absorption from the gastrointestinal tract [79, 81]. So while GSH is largely resistant to intracellular degradation, extracellular GSH is rapidly metabolized by cells expressing GGT on the external surface [82]. For these reasons, supplementation of individual GSH precursors has been suggested to improve intracellular GSH status [80]. Cellular GSH is compartmentalized into different organelles and other subcellular locations-- GSH exists mostly in the cytosol (70-85%), with 10-15% in the mitochondria and a very small percentage in the endoplasmic reticulum (ER) [74, 82]. GSSG on the other hand, is mainly found extracellularly [74]. Many factors affect levels of intracellular GSH, including presence of heavy metals, high glucose concentrations, heat shock, oxidative stress, inflammatory cytokines, cancer, ionizing radiation, enzymatic antioxidant activity, availability of constituent amino acids, and diet [83, 84]. While GSH synthesis only takes place in the cytosol, it is distributed to various organelles via transporters [83]. Porins on the outer membrane of the mitochondria allow GSH to enter, while dicarboxylate and oxoglutarate transporters in the inner membrane facilitate its movement within [83]. Though not clearly established, GSH can also be transported in the nucleus, where Bcl-2 proteins facilitate the translocation of GSH through Bcl2-associated athanogene pores [83, 85]. Translocation into the ER occurs though facilitated diffusion of the Sec61 protein-conducting

channel, however in the sarcoplasmic reticulum membrane of skeletal muscles, it has been speculated that the ryanodine receptor calcium channel type 1 plays a role in GSH transport [83, 85]. In the cell plasma membrane, the exchange between extracellular and intracellular GSH occurs through ATP-dependent transporters: the organic-anion-transporting polypeptide, the drug resistance-associated proteins, and cystic fibrosis transmembrane conductance regulator [83]. However, the uptake of "intact" GSH into the cell remains controversial due to degradation by the GGT enzyme on the external surface [85]. The half-life of intracellular GSH ranges from 3 hours (in rat liver), 4 days (in human red blood cells), to minutes (in the plasma), resulting in continuous turnover of GSH in cells [72].

Measurement Techniques: GSH and GSSG can be quantified and measured using several different techniques such as ultra-violet (UV) absorbance, fluorescence, spectrophotometry, electrochemical, and tandem mass spectroscopy, however, there are limitations to each [86]. The high-performance liquid chromatography (HPLC) coupled with UV presents issues with specificity and sensitivity detection, restricting widespread application [86, 87]. Furthermore, UV and fluorescence techniques require derivatization of GSH prior to detection due to the susceptibility of GSH degradation and oxidation, as well as instability of derivatized GSH [86]. Derivatization is a chemical structure modification that is used to enhance detectability for the target analytes, but this method has significant drawbacks due to its time-sensitive and time-consuming approach, and its risk for incomplete or excess derivatization reagents in the detection process [88, 89]. Although the use of HPLC coupled with electrochemical detection is expensive and requires a high potential to measure GSSG, this method is simple and requires no derivatization [86, 87]. The technique using liquid-chromatography coupled with tandem mass

spectroscopy is another method that does not require derivatization steps; however, it is costly and complex to use [90, 91].

Biosynthetic Precursors: The precursor cysteine is a key determinant and limiting factor of GSH synthesis [73]. Cysteine can be synthesized from methionine via the transsulfuration pathway in tissues (i.e. liver) that possess the enzymes to catalyze the reactions [92]. Alternatively, most cells are supplied with cysteine through a transporter, encoded by solute carrier family 7 member 11, the cystine (oxidized cysteine) and glutamate antiporter system xCT [92, 93]. Along with its role as a precursor for GSH synthesis, cysteine thiols can also scavenge free radicals and directly react with ROS like nitric oxide [94, 95]. The reduced form of the sulfur atom of a cysteine residue is susceptible to oxidative modifications, therefore making cysteine highly reactive, especially when its thiol side chains are in its deprotonated thiolate form (S^-) [96, 97]. Its nucleophilic properties allow thiolate groups to donate electrons and participate in non-redox reactions [96]. Due to the unstable nature of cysteine, sulfenylated cysteine can promote disulfide bond formations with ROS and stabilize protein structure [96].

N-acetylcysteine (NAC), a synthetic derivative of L-cysteine and a precursor of GSH, is a widely used antioxidant to protect against oxidative stress [98, 99]. NAC is a safe and inexpensive medication that is well tolerated when administered orally and has a dual role as a nucleophile and –SH donor, allowing it to promote detoxification and directly scavenge for free radicals [100, 101]. Additionally, NAC serves as a more efficient source of sulfhydryl thiol groups compared to cysteine and can cross the plasma membrane of cells to then rapidly convert to cysteine intracellularly [98]. Administration of NAC can stimulate GSH synthesis, boost levels of GSH, and therefore become beneficial in the context of diseases and disorders [100, 102]. NAC's mechanism of action, however, is still not fully understood. Many studies have

used animal disease models, cell culture experiments, and clinical studies, to explore the pharmacological use of NAC and decipher its potential role as a therapeutic [98, 103].

In animal experiments, NAC has been implicated to serve as a potential therapeutic for diseases such as liver disease [104, 105], cataracts [106], neurological disorders [107-110], diabetes [104, 111-113], and cardiovascular disease [112, 114]. Falach-Malik, *et al*. utilized a KK-Ay (genetic model of type 2 diabetes) and high fat diet (HFD)-fed C57BL/6 (diet-induced glucose intolerance) mice to demonstrate that, after the administration of NAC, glucose tolerance was improved in both the KK-Ay mice and HFD-fed mice, and insulin sensitivity was increased in the KK-Ay mice [104]. Additional animal studies have shown NAC to attenuate gestational diabetes mellitus and to hold a possible molecular mechanism against insulin resistance and the development of type-2 diabetes by improving glucose tolerance, insulin sensitivity, inflammation, and lipid profile [110-112]. Furthermore, in a study conducted by Falach-Malik, *et al*., NAC-treated mice exhibited micro-steatosis compared to the control mice with macro-steatosis in the liver, demonstrating a protective effect of NAC [104]. Har-Zahav, *et al*. built onto this theme using a Mdr2-/- cholestatic mouse model and demonstrated that NAC improved liver fibrosis [105]. Several other studies using rodent models highlight the potential of NAC for attenuating the pathology of Parkinson's disease, Alzheimer's disease, stroke, traumatic brain injury, and cognitive dysfunction, particularly by counteracting oxidative stress [107-110]. More, *et al*. used an amyloid beta oligomers (AβOs) induced rat model to demonstrate that after NAC treatment, spatial learning and memory was improved [110]. Various animal models, such as apolipoprotein E knockout mice and aging LDLR-/- mice, have also reported NAC to attenuate the progression of atherosclerosis by reducing oxidative stress [114]. Although there is

significant evidence in animal models that NAC can improve the pathogenesis of several diseases, the clinical application of NAC is still undergoing investigation.

Currently, NAC is an approved drug by the Food and Drug Administration (FDA) for the treatment of acetaminophen overdose only, yet NAC has been used as an over-the-counter nutritional supplement for respiratory diseases, toxicity, psychiatric disorders, and cardiovascular disease [114]. There is still limited evidence to approve NAC as a treatment for various other diseases despite its potential therapeutic role suggested by numerous studies. Clinical trials investigating the effects of NAC administration have reported improvements in fertility [100, 115-117], neurodegenerative diseases [107, 118-120], psychiatric disorders [101, 118, 121-123], liver diseases [118, 124, 125], respiratory diseases [118, 126, 127], eye disease [118], cardiovascular diseases [114, 118], diabetes [113], cancer [113, 118], and kidney disease [128]. Notably in a 2015 systemic review on the effects of NAC in neurodegenerative diseases and psychiatric disorders, evidence from numerous clinical studies leads NAC into a positive direction [129]. However, due to inconsistent findings and few controlled trials, further research is warranted to clearly define the efficacy of NAC.

NAC therapy has also been reported to produce different responses among individuals who harbor specific genotypes. A clinical trial conducted by Oldham, *et al*. investigates genes *TOLLIP* and *MUC5B* and their interactions with NAC therapy in individuals with idiopathic pulmonary fibrosis (IPF) [130]. This study found significant interactions between *TOLLIP* and NAC; individuals with a TT genotype were associated with significant beneficial effects with NAC, while individuals with a CC genotype were associated with harmful effects from NAC [130]. It is highly recommended that clinical trials consider and study the genetic predisposition

of individuals and the efficacy of NAC. Taking the study of NAC in this context can expand future research and interventions in genetic influences on other diseases beyond IPF.

Cysteamine (CA) is also involved in the production of GSH by enhancing the uptake of the precursor cysteine [131]. CA possesses a thiol group that allows CA to directly scavenge free radicals and other ROS, thereby reducing oxidative stress [131]. Due to its antioxidant role, it has been used as a common treatment for cystinosis and hypothyroidism, and a potential treatment for renal dysfunction, hyperpigmentation, cancer, malaria, sickle-cell anemia, and neurodegenerative disorders [131]. The therapeutic potential of CA in neurodegenerative disorders is attributable to its ability to traverse the blood brain barrier [132]. Although CA is implicated to be a beneficial therapeutic for neurodegenerative disorders, a detailed investigation of its molecular mechanisms is still needed to clarify its cytoprotective role [132].

Several precursors have been discussed to enhance levels of GSH and directly react with free radicals, however, many studies have demonstrated that direct administration of GSH via oral, intraperitoneal, and intranasal routes increases GSH levels [133-136]. Other routes of GSH administration include intravenous, however, the efficacy of this route of treatment appeared to be ineffective [133]. Furthermore, oral administration of GSH remains controversial due to the poor absorption of GSH; GSH is enzymatically degraded by GGT within the intestine [80, 137]. However, because oral administration of GSH is degraded within the intestine, a sublingual formulation of GSH can be delivered [137]. GSH is well absorbed in the mucosa, and the sublingual route can bypass the hepatic first-pass metabolism [137]. Schmitt, *et al*. demonstrated that participants who received the sublingual form of GSH had significantly increased GSH levels compared to those who received oral GSH administration [137]. With regards to this,

further research should be conducted to determine the optimal route of GSH administration to enhance the body's stores of GSH.

Influence of Individual Exogenous Antioxidants and Amino Acids in GSH Homeostasis: Although certain routes of GSH administration appear to be effective in some studies, oral GSH is known to be the most convenient and safe method of GSH ingestion [137]. However, due to the poor absorption and bioavailability of oral GSH, studies have focused on supplementation of individual antioxidants and amino acids to directly or indirectly increase GSH levels [80]. Several antioxidants and amino acids are interconnected with the GSH pathway and therefore are under investigation to clarify their impacts on GSH status [80].

α-Tocopherol (Vitamin E): Vitamin E and GSH are closely related, in which vitamin E can enhance the antioxidant power of GSH. Animal studies have demonstrated that after dietary supplementation with vitamin E, GSH concentrations were increased, and lipid peroxidation was inhibited [138]. In humans, similar effects from oral supplementation of vitamin E were shown to increase GSH levels [138]. Jain, *et al*. demonstrated that diabetic patients supplemented with vitamin E (100 IU/day) exhibited increased GSH concentrations by 9% and decreased lipid peroxidation [138]. Moreover, Barbagallo, *et al*. presents similar findings in their double-blind, randomized study, showing increased levels of GSH after vitamin E administration (600 mg/day) [139]. However, it has been shown in a 2022 systematic review of the effects of vitamin E supplementation in polycystic ovary syndrome (PCOS) that three clinical studies did not demonstrate significant improvement in GSH after vitamin E supplementation (400 mg/day) in patients with PCOS [140]. This implies that vitamin E may have different effects in a variety of conditions, meaning that more research on vitamin E supplementation should be conducted in different contexts of disease to further understand its role.

Pyridoxine (Vitamin B_6): Pyridoxal 5'-phosphate (PLP), the biologically active form of Vitamin B_6, is a coenzyme involved in the transsulfuration pathway of homocysteine to cysteine [141]. While vitamin B_6 can directly react with and scavenge free radicals and inhibit lipid peroxidation, it may also indirectly serve as a coenzyme in GSH homeostasis by enhancing GSH synthesis [141]. Hsu, *et al*. demonstrated that in an animal model, BALB/c mice given a vitamin B_6-supplemented diet exhibited lower levels of plasma GSH compared to BALB/c mice given a vitamin B_6-deficient diet, as well as those given a homocysteine diet [141]. However, hepatic GSH was the lowest in mice given vitamin B_6-deficient diet, and the highest in mice given the homocysteine diet, indicating a shift in GSH distribution from the plasma to liver [141]. These findings entail that supplementation of vitamin B_6 was not affected by the transsulfuration pathway. Though this study shows no significant impact on GSH levels from vitamin B_6 supplementation, one study has shown that homocysteinemic mice supplemented with vitamin B_6 exhibited increased levels of GSH compared to homocysteinemic mice with no supplement [142]. Additionally, renal GSH levels increased in chromium-induced rats compared to the control group [143]. In clinical trials, the findings have also been mixed. Lai, *et al*. explored the impact of several supplementations in patients with liver cirrhosis: vitamin B_6, GSH, and vitamin B_6 and GSH combined [144]. No significant improvements in plasma GSH were observed in all groups, but the authors explained the results via the redistribution of GSH from plasma to liver due to liver cirrhosis patients requiring more GSH to protect from damaged liver function [144]. On the other hand, DiFrancisco-Donoghue, *et al*., explored the impact of vitamin B_6 supplementation with vitamin B_{12} and folic acid supplementation in patients with Parkinson's disease, and their findings demonstrate that GSH levels can be improved with vitamin B_6, vitamin B_{12}, and folic acid

supplementation [145]. Because of the inconsistent findings, further research is recommended, given the potential benefits it can serve for GSH status improvement.

Ascorbate (Vitamin C): Ascorbate is the reduced active form of vitamin C and is a potent antioxidant that is interconnected with GSH by also playing a pivotal role in neutralizing free radicals [146]. Throughout the process of stabilizing and neutralizing free radicals, ascorbate is oxidized into dehydroascorbate and then transported across cell membranes of different cellular compartments to be regenerated into vitamin C [146]. Due to the mutual relationship between vitamin C and GSH of the antioxidant defense system, studies have investigated the effects of vitamin C supplementation on GSH status [147]. In rodent studies, it appeared that GSH levels in homocysteinemic mice supplemented with vitamin C were higher compared to homocysteinemic mice given no supplement [142]. Furthermore, vitamin C supplementation in aging rats showed increased levels of GSH [148]. However, in weanling rats, the group receiving high supplementation of the vitamin had significantly decreased erythrocyte (RBC) levels of GSH but significantly increased GPx activity in RBC and plasma [149]. A similar effect of increased GPx activity was seen in the heart of male guinea pigs given a high vitamin C supplementation [150]. Decreased levels of GSH may be explained by toxicity due to high doses of vitamin C given. In healthy adults who took 500 or 1000 mg/day of vitamin C supplements, GSH in lymphocytes increased by 18% [151]. Another clinical study demonstrates a 50% increase of GSH in RBC after 500 mg/day of vitamin C supplementation [152]. Many studies have also found vitamin C supplementation to be more effective when used in conjunction with other antioxidants, such as vitamin E [153, 154]. Based on clinical trials, ascorbate appears to be effective in improving GSH status, though more research is needed to explore its applicability in a variety of disease states.

Selenium (Se): Se is an essential cofactor required by GPx, a selenoprotein that is responsible for neutralizing free radicals and oxidizing GSH [7]. Given the role of Se in GPx expression, it is presumed that increased levels of Se lead to an increase in GPx activity and expression [155]. In a 2014 meta-analysis on the effects of selenium supplementation on GPx activity in various tissues of animals and humans, it was found that selenium-enriched foods are more effective at increasing GPx activity compared with selenomethionine [156]. When exploring the impact of Se supplementation on GPx activity, higher *GPx1* expression was seen in the liver of Se supplemented rat pups compared to the control group [157]. In another rodent study, Se supplementation increased GPx activity in the heart and liver [158]. In humans, varying results on the effects of Se supplementation have been documented. A randomized clinical trial demonstrated that patients with chronic kidney disease who received 200 mcg/day of Se supplementation for three months presented increased GPx activity in RBC [159]. Similar results are found in patients with chronic renal failure who increased GPx activity in RBC after treatment with Se for three months [160]. However, in another study of Se supplementation in healthy adults, only platelet GPx increased, while GPx in the plasma and erythrocytes did not [161]. This implies that there may be tissue-specific targets of GPx from Se supplementation or selenium-enriched foods [156].

Zinc: Zinc is an essential trace element that carries antioxidant potential through several mechanisms, such as but not limited to, regulating oxidant production and metal-induced oxidative damage, mediating the induction of the zinc-binding protein metallothionein, and playing a part in the regulation of GSH metabolism and thiol redox status [162, 163]. Zinc cannot directly participate in redox reactions; however, zinc can indirectly regulate redox status by its involvement in proteins such as metallothionein, a protein that scavenges for oxidants through the release of zinc (Figure 2.9) [163, 164]. Although zinc is unable to directly participate in redox reactions, the

released zinc can directly regulate transcription factors and activities of enzymes (phosphatases and kinases) involved in redox signaling [163]. In addition, zinc can indirectly affect cell redox homeostasis and redox signaling by affecting GSH synthesis through the modulation of the transcription factor Nrf2 [163]. Due to its capacity in modulating the activity of protein redox function, zinc is known to have both a direct and indirect role in regulating oxidative damage [163, 164]. A rodent study conducted by Zhou, *et al*., demonstrated that zinc supplementation in metallothionein-knockout mice increased GSH concentrations in the cytosol and mitochondria in the liver, as well as partially inhibited the decrease in GPx activity [165]. Moreover, zinc supplementation increased GPx activity in the serum, liver, and kidney of rats chronically exposed to cadmium, a toxic trace element [166]. A 2021 systematic review and meta-analysis of randomized controlled trials highlights three out of six studies that have demonstrated increased GSH after zinc supplementation, which have been shown in pregnant women with gestational diabetes, hemodialysis patients, and patients with diabetic foot ulcer [162]. In the other three studies, zinc supplementation appeared to have no significant effect on GSH levels in women with PCOS, pregnant women, and elderly individuals [162]. Given the varying effects of zinc supplementation, further research should help personalize recommendations to specific individuals in different health conditions.

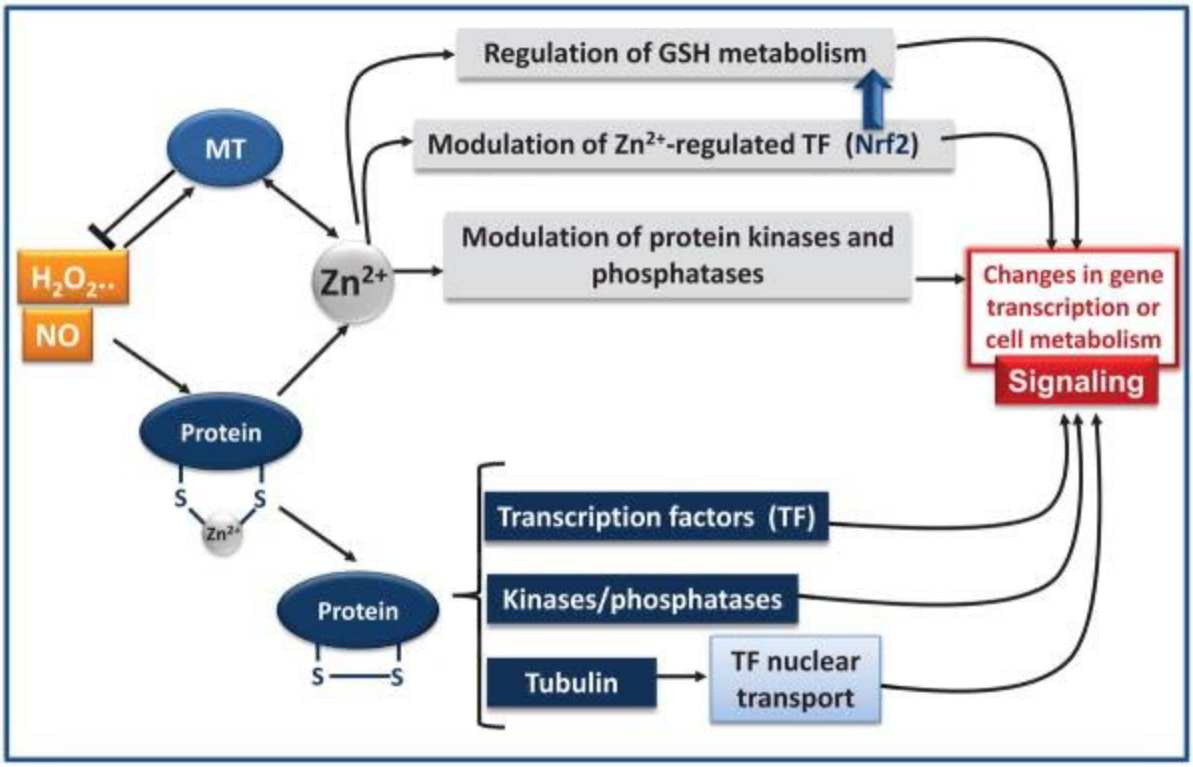

Figure 2.9. Zinc in the regulation of redox signaling. Figure adapted from Oteiza. (2013) [163].

L-Glutamine: L-glutamine is the most abundant amino acid and can deaminate by phosphate-activated glutaminase, producing glutamate and ammonia [167]. Glutamate is a precursor to glutathione and therefore be utilized for GSH synthesis [167]. This leads to the presumption that supplementation of glutamine may increase GSH synthesis and attenuate oxidative damage. A rodent study subjected to exercise showed that groups given the L-glutamine and L-alanine supplementation exhibited increased GSH levels in the soleus muscle and liver compared to the control group, however, it is unclear whether the results were because of L-glutamine or L-alanine [168]. In malnourished rats during inflammatory shock, glutamine supplementation restored glutathione stores in the gut [169]. Similar results can be seen in endotoxemic mice, where groups fed a glutamine-enriched diet presented with increased GSH

content in Peyer's patches [170]. Conversely in canine models, glutamine supplementation failed to modify erythrocyte and duodenum GSH concentrations, alongside results showing a decreased GSH synthesis rate [171]. The authors of this study suggest that glutamine availability may not affect plasma GSH, while in contrast in the duodenum, glutamine may help preserve the GSH pool by decreasing GSH synthesis [171]. In humans, glutamine supplementation appears to enhance plasma glutathione in the resting state of patients receiving parenteral nutrition [167]. Additionally, it was found that GPx activity increased in HDL-c lipoproteins after glutamine supplementation in exercising older individuals [172]. A common theme of increased GSH levels after glutamine supplementation is also found in HIV positive patients [173]. Contrary to these findings, Valencia, *et al*. found that individuals who took oral glutamine did not observe an increase in plasma GSH [174]. A further investigation of glutamine supplementation is called for to clarify its effects on GSH status.

L-Glycine: Glycine is a rate-limiting amino acid for GSH synthesis and constitutes as one out of the three amino acids required for GSH formation [102]. It has been well-documented that glycine supplementation increases GSH synthesis, and its dietary form is proposed to produce the same effect [102]. In a 2018 review, it is discussed that in animal studies, glycine supplementation increased tissue GSH levels in milk-fed piglets and in rats with burn injury, alcohol-induced liver injury, and fructose-induced metabolic syndrome [102, 175-178]. In clinical trials exploring the effects of glycine and NAC as a joint supplement, total GSH remained unchanged, however, subjects experiencing high oxidative stress and low GSH status responded with increased GSH generation [179, 180]. According to another study, combined glycine and cysteine supplementation markedly increased GSH concentrations in elderly subjects

[181]. Due to limited studies on the individual effect of cysteine supplementation, more research is warranted to delineate its discrete role on GSH status.

Implications in Disease

GSH is a powerful antioxidant that is implicated as a marker for human disease and potential therapeutic for disease treatment due to its ability to mitigate oxidative stress. Common diseases in discussion for GSH therapy include cardiovascular disease, diabetes, renal disease, hepatic disease, neurodegenerative disorders, and cancer [182, 183].

Cardiovascular Disease (CVD): CVD is a highly prevalent disease that carries a high mortality rate around the world and encompasses different types of CVD, such as occlusion of coronary arteries, hypertensive heart diseases, and stroke [184]. The pathology of CVD includes accumulating levels of oxidative stress and free radicals that lead to the decline in an individual's health [184]. In a 2021 review, GSH redox homeostasis is known to play a preventive role in hypertension, atherosclerosis, cardiac hypertrophy, ischemia-reperfusion injury, and heart failure [184]. Across both animal and human studies, there is accumulating evidence showing the beneficial effects of GSH on CVD. *ApoE* -/- mice given an oral GSH supplementation produced reduced levels of lipid peroxides and oxidation of LDL [185]. Similar effects are seen when given an OTC supplement that supplies cysteine residues [186]. In mice on a high saturated fat diet, oral supplementation of NAC increased levels of GSH and reduced cholesterol levels in the plasma and liver [187]. It is documented in human studies that individuals with stroke or myocardial infarction [188], however, there is limited evidence in humans whether GSH supplementation or supplementation of GSH precursors alleviates CVD pathology. It is advised for future studies to explore the effects of GSH supplementation or NAC and determine the efficacy of GSH as a form of treatment.

Diabetes: Along with CVD, diabetes is another highly prevalent disease worldwide and is responsible for the cause of blindness, end-stage renal disease, and amputations [189]. In several human studies, GSH has been shown to prevent and help manage type 2 diabetes (T2D) [190]. In non-insulin-dependent diabetic patients, it was demonstrated that oral supplementation of NAC increased GSH concentrations and decreased plasma vascular cell adhesion molecules, suggesting that NAC may slow down the progression of vascular damage [191]. It was also found that dietary supplementation with cysteine and glycine in diabetic patients significantly increased GSH synthesis and concentrations, as well as significantly decreased oxidative stress and lipid peroxides [189]. Although one study shows no benefit in glycemic control, glucose tolerance, insulin resistance, or oxidative stress markers [192], a combined supplementation of NAC and glycine showed decreased insulin resistance, improved GSH deficiency, and reduced markers of oxidative stress [193, 194]. Combined NAC and glycine appear to be more effective than NAC by itself, therefore future double-blind studies should further clarify the effects of NAC and glycine on diabetes.

Renal Disease: Kidney disease is prevalent in individuals who have diabetes or CVD, in which it is likely that the effects of NAC and/or GSH supplementation on diabetes and CVD may also influence renal function, and there is current evidence documenting the direct effects of NAC on the kidney. In mice subjected to renal injury, NAC administration led to decreased interstitial fibrosis and reperfusion injury [195]. In humans, a 2016 systematic review and meta-analysis highlights 86 randomized controlled trials that have demonstrated a small beneficial effect on contrast-induced nephropathy after NAC administration [196]. In chronic hemodialysis patients receiving NAC administration, homocysteine levels and other inflammatory markers were decreased, as well as improved renal anemia [197-199]. Additionally, greater decrease in

homocysteine levels were found in the NAC group with residual renal function compared to the anuria group [197], which share similar findings with another study showing improved glomerular filtration rate after NAC treatment [200].

Hepatic Disease: NAC is approved by the FDA for the treatment of acetaminophen overdose [114]. Patients given an oral NAC treatment within 16 hours of acetaminophen ingestion showed improved hepatic function and no deaths caused by acetaminophen [201]. NAC treatment has also shown improvements in non-acetaminophen in acute liver failure (NAI-ALF) [202], with one study also showing improvements in transplant-free survival in NAI-ALF [203]. Additionally in chronic liver disease, NAC has demonstrated to attenuate the pathology of hepatitis B, with Wang, *et al*. demonstrating decreased total bilirubin, and improved intrahepatic cholestasis and coagulation dysfunction [204]. In a combined GSH and entecavir therapy, chronic hepatitis B patients produced decreased aminotransferase (ALT), total bilirubin, hyaluronic acid, type III collagen, and laminin, with increased albumin and improved liver fibrosis grades, however it is not clear whether the effects were due to GSH [205]. In patients with non-alcoholic fatty liver disease, NAC treatment decreased ALT and significantly decreased the span of the spleen [206]. Similar results can be seen using GSH treatment, with significantly decreased ALT levels presented [207]. One rodent study using rat subjected to alcohol-induced oxidative stress, decreased aspartate aminotransferase and ALT after NAC administration, demonstrating that ethanol-induced liver damage can be alleviated with NAC [208].

Neurodegenerative Disorders: The dysregulation of GSH homeostasis, alterations of GSH-dependent enzyme activities, and neuronal GSH loss are all closely associated with the progression of neurodegenerative diseases, such as Alzheimer's disease (AD) and Parkinson's disease (PD) [209, 210]. Before Aβ deposition, APP/PS-1 knock-in mice orally administered

NAC demonstrated decreased protein and lipid oxidation and increased GPx [211]. Similarly, AD rat models reveal NAC treatment revered cognitive deficits and reduced oxidative stress in the hippocampus and prefrontal cortex, as well as improved levels of neurofibrillary tangles and Aβ deposition [212]. In PD mice models, NAC attenuated the loss of dopaminergic terminals and decreased levels of toxic α-synuclein [213]. In clinical trials, NAC has been shown to improve AD and PD pathology. In a randomized controlled trial, patients with PD exhibited increased dopamine transporter binding activity, along with significantly improved PD symptoms [214]. In AD individuals, NAC administration improved nearly all outcome measures after 3 and 6 months of treatment, though significant results were found in subsets of cognitive tasks [120]. These findings suggest that NAC may help resolve certain neurodegenerative diseases by increasing antioxidant potential and reducing oxidative stress, however more research is needed to better understand its potential therapeutic effects.

Cancer: Disturbances in the GSH antioxidant system and homeostasis have been implicated in tumor initiation, progression, and treatment response, suggesting that GSH may have both a protective and pathogenic role [215]. It is reported in a clinical trial that NAC supplementation possesses metabolic and anti-proliferative effects in breast cancer [216]. Additionally, NAC has shown an ability to inhibit cancer cell proliferation and tumor growth by targeting the Notch2 malignant signaling [217]. Despite the beneficial effects of NAC, it is well documented that GSH can also play a role in chemotherapy resistance and cancer progression [215, 218]. For instance, NAC supplementation significantly increased tumor progression and reduced survival in mouse models induced with lung cancer [219], as well as increase lymph node metastases and invasive properties of malignant melanoma cells in a mouse model of malignant melanoma [220]. Due to the contradictory results of NAC and potential harmful

effects in cancer, further research is warranted in animal and cell models before the initiation of clinical trials.

Regulation of the Glutathione Redox System

GSH is a tightly-regulated peptide as it serves many vital functions, such as detoxification and scavenging of free radicals, maintaining thiol status of proteins, regulating cysteine, and modulating essential cellular functions (e.g., DNA synthesis, immune function) [73]. It was previously discussed that GSH is regulated by various factors, namely levels of oxidative stress, availability of constituent amino acids, activity of regulatory enzymes, GSH synthesis, dietary factors (antioxidants and amino acids), and degradation and transportation within cells. However, due to the complex nature of GSH, other factors may regulate the GSH redox systems: hormones, tissue specific, and genetic factors.

Hormonal Regulation: Regulation of GSH is suggested to be carried out by hormonal-mediated mechanisms [221]. Hormones are known to take part in signaling pathways that affect the regulation of influx and efflux of GSH and its regulatory enzymes across different cells. Key hormones that have been documented to influence GSH regulation are thyroid hormone, glucagon, sex hormones, and growth hormone.

Thyroid Hormone (TH): A decline in GSH levels was found to be one of the earliest manifestations in hypothyroidism [222]. In a rodent study conducted by Rahaman, *et al*., it was found that progressive hypothyroidism of postnatal development exhibited an increase in superoxide dismutase and catalase enzyme activity and decreased GSH levels [223]. This led the authors to postulate that the TH is involved in the regulation of GSH status. To investigate the role of TH on GSH homeostasis, Dasgupta, *et al*. studied the effects of TH on gamma-glutamyl transpeptidase (GGT), an enzyme heavily involved in catalyzing GSH [228]. Intraperitoneal

injections of TH of rats produced results in which GGT activity increased in astrocytes [224]. However, due to the incompatibility of TH and GGT in the presence of down regulated GSH, it is presumed that other regulatory enzymes such as glutamate cysteine ligase (GCL), may be involved as well [222, 224]. Dasgupta, *et al*., discovered that hypothyroidism led to the decline in GCL activity of the rat brain, but with the administration of TH, an increase in GCL activity was observed [222]. Additionally, a stark increase in GSH levels was seen in astrocytes [222]. In rat hepatocytes, however, have exhibited significant reductions in total glutathione S-transferases (GST) activity after administration of tri-iodothyronine (T3) and thyroxine (T4) [225]. Given the distinct responses seen in different regulatory GSH enzymes with TH, this indicates future research to account for the differences in TH compatibility with individual enzymes.

Glucagon: Glucagon is a hormone documented to be involved in GSH regulation, especially in the context of diabetes. Elevated levels of glucagon and oxidative stress are often seen in diabetes, which leads researchers to speculate that glucagon may play a role in GSH homeostasis [226, 227]. It has been reported by Patarrão, *et al*. that glucagon decreases hepatic GSH levels, which in turn promotes insulin resistance [226]. A similar pattern was observed by Kim, *et al*., where cellular GSH levels in the liver were significantly decreased by glucagon [228]. These results suggest that glucagon may be responsible for GSH efflux in the liver, thereby decreasing hepatic GSH in diabetic individuals [226, 228]. GST expression and GSH synthesis has also been noted to be inhibited by glucagon in rat hepatocytes, however due to mixed findings in GST expression, the effect of glucagon on GST expression remains unclear [227, 229].

Sex Hormones (Estrogen and Testosterone): It has been evident through clinical and experimental studies that females have higher GSH levels compared to males due to higher

levels of estradiol [230]. A 2020 review summarized three studies that have shown estrogen to regulate the expression and activity of GSH reductase (GR) and GPx in several tissues [231-233]. Women who underwent estrogen replacement therapy (ERT) produced higher levels of GSH and lower levels of GSSG, resulting in decreased blood GSSG/GSH ratio 30 days after ERT [232]. Like humans, rodent studies demonstrate increased GR, GPx, and γGT activity, as well as increased GSH levels after estradiol treatment [233, 234]. Results of the effects of testosterone on the regulation of the glutathione redox systems are rather mixed. While Zhang, *et al*., documents that testosterone treatment mice produced increased activity of superoxide dismutase and GPx in cardiomyocytes [235], Moreira-Lopes, *et al*., reports that testosterone induces ROS generation via NADPH oxidase-dependent mechanisms [236]. Proinflammatory effects of testosterone may be dependent on the specific receptor it is binded to [231]. Alongside the positive and negative effects of testosterone, it is also shown to have little effect on total GST activity [225]. Although the effects of estrogen are clear, more research is warranted to better understand the positive and negative effects of testosterone.

Growth Hormone (GH): Low amounts of GH have been associated with stress resistance and increase longevity and have been implicated in the cell's redox defense system [237]. GH administration in rodent studies has demonstrated significantly decreased GST activity in the kidney, little effect on GST activity in the liver, [237, 238] and suppressed GGT activity in the heart and liver [238]. Similarly, Coecke*, et al*., demonstrates little effect on total GST activity by GH [225]. In the brain, levels of GGT and GST were unchanged by GH treatment but suppressed the degradation and utilization of GSH [238]. Furthermore, γ-glutamylcysteine synthetase, an enzyme responsible for GSH synthesis, was not altered by GH treatment in the liver, but was increased in the kidneys and suppressed in the heart [238]. It is also seen that GH regulates levels

of cytosolic GST in specific tissues in rats [239]. In another rodent study, GH administration to aged rats produced no effect on GSH levels in the hippocampus of the brain, but produced a significant decrease in GSSG concentrations and significant increase in GSH/GSSG ratio [240]. In the frontal cortex however, there were no significant effects [240]. These results imply that the regulation of these enzymes is tissue-specific and can therefore explain varying levels of GSH in different tissues.

Tissue Specificity: Documentation of tissue specificity of the GSH pathway has been made clear in studies evaluating the effects of hormones in a variety of tissues. In addition to this, further research reveals that hepatic and renal GSH/GSSG are significantly correlated across 30 inbred strains [241]. Studies have found that a striking difference in GSH levels in tissues; GSH in the liver is observed to be the highest, while the lung, spleen, and kidneys contain a quarter of GSH found in the liver [242]. Gould, *et al*., further explored the pattern of GSH levels in tissues across 19 mouse strains, with the liver exhibiting the highest total GSH levels, and subsequently the striatum, kidney, cerebral cortex, heart and with pancreas exhibiting the lowest total GSH levels [243]. Statistical analysis was also conducted to identify significant correlations between GSH phenotypes in tissues, where total GSH levels of the liver were positively correlated with those of the heart, cerebral cortex, and striatum [243]. Furthermore, total GSH levels of the kidney were found to be positively correlated with those of the heart, as well as total GSH levels of the pancreas positively correlated with those of the striatum [243]. Correlations of GSH levels among tissues were also found, however, there were fewer significant correlations of GSSG levels between tissues [243]. Tissue-specific results were also seen in obesity-prone mouse strains given a high-fat diet [244]. Given the discovery of tissue-specific GSH regulation

among different mouse strains, it was speculated that genetic factors may heavily influence the regulation of the GSH redox systems.

Genetic Regulation: GSH levels and redox status are heritable. It was found in a heritability estimate of 12 mouse strains that GSH phenotypes were moderately heritable in old mice [243], findings that aligned with the heritability estimates found in young-adult mice [241] and in human erythrocytes [245]. Studies using classical inbred mouse strains have also uncovered that C57BL/6 (B6) mice exhibited significantly higher GSH/GSSG ratios than those of DBA/2 (D2) mice in several brain regions [246], as well as B6 mice exhibiting higher erythrocyte GSH/GSSG ratios than D2 mice [247]. In 14 diverse inbred mouse strains, Tsuchiya, *et al*. has also discovered significant variations in GSH phenotypes [248]. Moreover, Zhou, *et al*. utilized 30 genetically diverse inbred mouse strains and found GSH phenotypes to produced threefold ranges and moderate to high heritability [241]. The estimated heritabilities gathered from this study were like those found in humans [245], which bring forth the relevance of findings from mouse studies to human health.

Mouse Genetics

The laboratory mouse has been used to investigate human health due to its similarities of human physiology and disease [249]. By innovative genetic engineering and selective breeding, a large variety of mouse models have been generated to model specific human diseases [249]. Not only do mice have similar biological components as humans, but its genetic makeup is also nearly 80 percent identical to humans [249]. The mouse model is ideal for conducting experiments under controlled conditions and to elucidate the relationship between gene and phenotype [250, 251]. The first emerging inbred strains, called the DBA inbred stock, were initiated in 1909 by C.C. Little, who investigated the pathology of cancer [252]. The DBA strain

has evolved over time, developing a new family of unique inbred strains through selection and inbreeding techniques [252]. Throughout time, roughly over 450 inbred strains of mice have been developed for 90 years and used to study the different genotypes and phenotypes in many contexts of disease research [253]. Although inbred mouse strains have used in biomedical research for many years due to the decreased within-strain phenotypic variability [254], it does not accurately reflect the genetic variation found in the human population.

Diversity Outbred (DO) mice: The DO mouse population has been developed to model the high level of genetic diversity and complex traits found in the human population [255]. The DO mice is a heterogenous stock derived from the same eight founder strains (A/J, C57BL/6J, 129S1/SvImJ, NOD/ShiLtJ, NZO/HlLtJ, CAST/EiJ, PWK/PhJ, and WSB/EiJ) as the Collaborative Cross inbred strains (Figure 2.10) [255, 256]. To create new generations, mice are randomly assigned to a breeding pair, which gives rise to the current generation, G10, containing high levels of allele diversity and unlimited novel allele combinations [255].

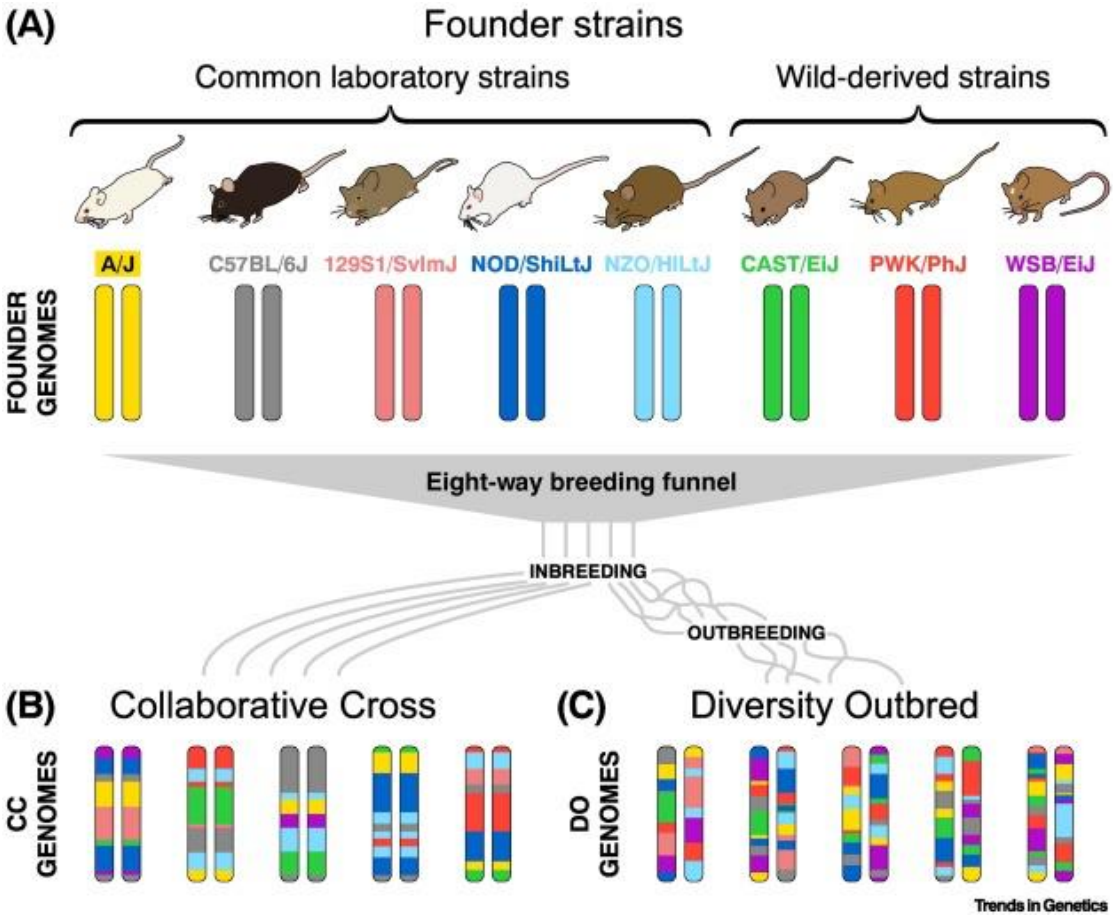

Figure 2.10. Development of the Diversity Outbred (DO) mice stock. Figure adapted from Saul, *et al*. (2019) [256].

The DO mice stock has been used in quantitative trait loci (QTL) mapping analysis to investigate complex traits through high-precision genetic mapping, in which data gathered from DO QTL studies can be found in a repository at the Jackson Laboratory (https://dodb.jax.org) [256, 257]. Data gathered from DO mice are also reusable in the Mouse Phenome Database (https://phenome.jax.org/), which can be used for initial exploration, trait correlation, and discovery of genetics [256]. Methods to conduct QTL analysis are well established, especially the R/qtl package, a statistical software for estimating genetic maps, identifying genotyping

errors, performing QTL genome scans, and calculating genotype probabilities to phenotype data [258, 259].

Previous Studies on GSH using DO mice stock: Previous studies have used the R/qtl software to explore genetic variations involved in GSH regulation. Using 347 DO mice samples, Gould, *et al*. utilized the R/qtl2 software for QTL mapping analysis of GSH in both the liver [260] and kidney [261]. Subsequently after identifying specific candidate genes (i.e. *Socs1, Aifm1)* associated within a suggested locus, an integrative bioinformatics approach that included databases for expression, phenotypic, and functional annotations were used [260, 261]. Due to limited studies investigating the genetic architecture of the GSH antioxidant system in various tissues, it is critical to facilitate research in other tissues, such as the brain.

Bioinformatics Analyses

Bioinformatics is an essential tool for managing and interpreting biological data, including genomic and phenotypic data analysis [262]. It is difficult to find all data information in one location, but with the growing number of databases accessible to the public, it is becoming a highly valuable resource to researchers [262]. Depending on the database, it can provide comprehensive descriptions of diseases, identify genetic mutations or polymorphisms that bring risk to a certain disease, or enable a search for genes associated with a particular disease [262]. Typically, databases will have their respective roles as genome-wide association studies, or phenome-wide association studies, but databases can also serve as both to allow for the exploration of genotypic and phenotypic data all in one place.

Genome-Wide Association Studies (GWAS): GWAS test thousands of genetic variants across different genomes to identify statistically associated polymorphisms with a given phenotype [263]. As sample size increases, GWAS associates a greater number of variants to the

phenotype and has a wide range of applications when generating results, such as gaining a better understanding of the biology of the phenotype, estimating its heritability, calculating genetic correlations, and predicting clinical risk or potential causal relationships between risk factors and health outcomes [263]. A phenotype of interest with genomic predictor variables such as single nucleotide polymorphisms (SNPSs), predicted gene expression, or genetic risk score, can be inputted into GWAS analysis to find significant associations [264]. Although GWAS is a powerful tool that links variants with specific phenotypes, it presents limitations particularly because most traits are influenced by many other causal variants, including both causal and non-causal variants; this can lead to unclear inferences between the variants and phenotypes [263].

The UK Biobank is a large, open-access population biobank that contains around 500,000 genotyped individuals who have been phenotyped for quantitative traits, namely anthropometric traits, blood cell traits, metabolites, cognitive traits, brain imaging traits, and depressive symptoms for GWAS [263]. GWAS can be conducted using data from the UK Biobank, which has been used frequently in previous studies. Berg *et al*. demonstrated that the polygenic selection of height using the UK Biobank produced better results in GWAS than when using GIANT consortium and replication studies [265]. Elliot, *et al*. and Smith, *et al*. both demonstrate the UK Biobank to be a wealth of data and found 148 replicated clusters of associations between genetic variants and brain imaging phenotypes, as well as 692 newly found associations [266, 267]. GWAS data from the UK Biobank provides a range of opportunities to discover new genetic associations, which have clearly been documented in many other research studies [268-270].

Phenome-Wide Association Studies (PheWAS): In PheWAS, a genetic or clinical variable can be used to find associations in phenomes derived from information in the electronic health

record (EHR) for analysis [264]. PheWAS can be used to link certain genetic variants with disease and adverse events associated with a specific behavior [264]. Studies prove PheWAS to be an important tool for analyzing biological test results, for example, in the study conducted by Neuraz, *et al*., the authors found that high methyltransferase expression was associated with diabetes and iron-deficiency anemia in a group of 442 individuals [271]. Furthermore, Diogo, *et al*., found through PheWAS methods that the A928V variant of tyrosine kinase 2 is associated with an increased risk of pneumonia [272]. As in GWAS, the UK Biobank data can be analyzed through PheWAS, which will link phenotypic data obtained from questionnaires and other phenotyping methods (notably the EHR data) to link genetic information [273]. PheWAS has made important contributions to many more discoveries found in studies, proving it to be a valuable biological data tool [274, 275].

Expression Quantitative Loci Analysis (eQTL): eQTL analysis can be utilized in tandem with GWAS to prioritize target genes for a GWAS locus [263]. The loci of causal variants from GWAS can be identified by using high-precision mapping of highly correlated SNPs, which can help narrow down variants associated with the phenotype of interest [263]. A highly accessible QTL catalogue available for use is the Genotype-Tissue Expression (GTEx) resource, containing eQTL and splicing QTL for 49 tissues [263]. This resource provides both *cis*-eQTL and *trans*-eQTL associations with data from roughly 30,000 donors and can serve as a framework for not only GWAS, but also transcriptome-wide association studies that analyze associations between gene expression levels from GWAS with a trait [263]. Although eQTL analysis can help identify loci associated with RNA expression, it inevitably possesses limitations such as that the statistical associations identified do not signify a causal relationship [263]. For this reason, eQTL analysis should be integrated with GWAS data using co-localization techniques to identify loci

where regulatory associations and disease associations coincide with the same causal variant [263]. Additionally, eQTLs affect more than several genes which can make it difficult to prioritize genes that are associated with disease; however, the use of other data sources or annotations can alleviate some of those challenges [263].

Purpose and Significance

It has been made evident through many studies that the GSH redox system is heavily influenced by genetic factors. Although studies have made tremendous successes in defining genetic variants underlying GSH homeostasis, their use of inbred mouse models do not accurately reflect the genetic variation found in humans and therefore cannot entirely translate its findings into human health. Studies on the genetic regulation of GSH remain limited and based on the observed tissue-specific differences in GSH levels, it is predicted that genetic variants govern regulation of GSH in a tissue specific manner.

Purpose of Thesis Research: This thesis research aims to build upon previous knowledge on the investigation of the genetic architecture of the GSH antioxidant system. Previous work has found candidate genes associated with GSH regulation in the liver and kidney, however, there is no documentation of studies investigating other tissues such as the brain. This research will further explore genetic players in GSH regulation and provide a comprehensive list of all candidate genes that influence the tissue specific nature of GSH regulation. The hypothesis of this research foresees distinct genes responsible for tissue-specific GSH variation, which will be achieved by narrowing down and prioritizing key genetic variants associated with GSH. Furthermore, previous studies show correlations between the liver, kidney, and heart GSH, and this thesis research expands on correlations between different peripheral tissues by introducing the brain into the paradigm. This research will help bring forth a better understanding of the role

of genetics in GSH regulation and contribute to the advancement of potential therapeutics developed for human health and disease.

CHAPTER 3

CONSTRUCTING A CORRELATION MODEL OF GLUTATHIONE STATUS BETWEEN CORTICAL, RENAL, AND HEPATIC GLUTATHIONE REDOX SYSTEMS[1]

[1] Song J. and Pazdro R. Constructing a correlation model of glutathione status between cortical, renal, and hepatic glutathione redox systems. To be submitted to a peer-reviewed journal

Abstract

Glutathione is an essential antioxidant with pivotal roles in maintaining redox homeostasis and eradicating free radicals. Glutathione exists in its reduced (GSH) and oxidized form (GSSG) and are recycled between these two forms to neutralize free radicals in the cell. The brain is abundant in GSH due to its high oxygen consumption and rich contents of unsaturated fatty acids. Due to the essential role of GSH in the brain, altered GSH status has been associated with numerous cases of neurodegenerative disease, in which it is still unknown whether regulation of GSH acts uniquely among genetically distinct individuals. To investigate the impact of genetic regulation in GSH status, this study utilizes a Diversity Outbred (DO) mice stock to mirror the genetic diversity found in the human population. GSH and GSSG concentrations were quantified in the cerebral cortex and subsequently screened for statistical associations between each GSH phenotype, where we found significant variation in each GSH phenotype and significant correlations between several measurements. Cortical GSH phenotypes were then statistically correlated with renal and hepatic GSH phenotypes, which revealed a significant relationship between the cortical and renal GSH systems but not between the cortical and hepatic GSH systems. This study presents key findings and provides a better understanding into the genetic background of GSH regulation in the brain.

Introduction

Glutathione (GSH), a ubiquitous tripeptide composed of cysteine, glutamic acid, and glycine, is an essential antioxidant that protects major tissues of the body from oxidative stress [69]. Glutathione is the most abundant non-protein thiol in cells and can be found in its reduced form and oxidized form, GSH and GSSG, respectively [69, 72]. GSSG can be recycled to GSH with NADPH as the reducing agent driving the reaction[67]. GSH is present at high concentrations in the brain, and amounts can vary depending on the region of the brain, where the highest amounts are located in glial cells of the cortex followed by the hippocampus, cerebellum, striatum, and substantia nigra [276, 277]. In the central nervous system, GSH serves to modulate cellular differentiation and proliferation, promote apoptosis, activate enzymes, transport metals in cells, aid in neurotransmission, and act as a source of cysteine during protein synthesis [276].

Due to its high oxygen consumption and high proportion of polyunsaturated fatty acids, the brain is highly sensitive to the generation of reactive oxygen species (ROS) and oxidative stress [277, 278]. With growing evidence that glutathione plays an important role in detoxifying counteracting oxidative stress in disease, it is expected that impaired GSH synthesis and metabolism can worsen neurodegenerative diseases [210, 277, 279]. In patients with Alzheimer's disease (AD), it has been demonstrated that GSH levels are decreased in the cortex region of the brain compared to healthy controls [280, 281]; a similar effect was also observed in the hippocampus [282, 283]. Additionally, crucial enzymes for GSH metabolism, glutathione peroxidase (GPx) and glutathione-S-transferase (GST) activity, were seen to decrease in patients with AD [276, 284-286]. In Parkinson's disease, patients were found to have depleted levels of GSH in the substantia nigra of the brain [287, 288]. In contrast, supplementation with N-acetyl

cysteine (NAC), which increases GSH levels, led to symptom improvements in neurodegenerative diseases and disorders [107-110]. Furthermore, in mouse models, deleting several enzymes involved in GSH metabolism have been shown to influence the progression of neurodegeneration and cognitive impairment. Compared to control mice, GPx knockout mice were shown to exhibit neurodegeneration and memory impairment [289, 290]. Neuron-specific knockout of glutamate-cysteine ligase (GCL) similarly induced progressive neurodegeneration and marked neuroinflammation [210].

Levels of GSH appear to vary in different tissues, with the liver and small intestine containing the highest amount of GSH concentrations (1-6 mM) [291], followed by the kidney (2-5 mM) [292], brain (2-3 mM) [293], blood (~1 mM) [294], and lung epithelial cells (0.42 mM) [295]. Moreover, a mice study using 19 inbred strains quantified levels of GSH in several major tissues, finding that total glutathione levels were the highest in the liver ($\bar{x}$ = 30.72 ± 3.09 nmol/mg protein), followed by the striatum ($\bar{x}$ = 25.96 ± 3.84 nmol/mg protein), then the kidney ($\bar{x}$ = 15.93 ± 1.49 nmol/mg protein), cerebral cortex ($\bar{x}$ = 14.25 ± 0.94 nmol/mg protein), heart ($\bar{x}$ = 10.01 0.78 nmol/mg protein), and pancreas ($\bar{x}$ = 9.93 ± 1.26 nmol/mg protein) [243]. It is evident that GSH concentrations vary among different tissues in inbred mice models, however due to their lack of genetic variability, there is limited translatability in the human population. Research on the statistical relationship of GSH in the brain and other peripheral tissues are scarce, especially in a genetically diverse model. In view of the limited evidence on this, investigating the regulation of GSH in the brain and its overlap with other major tissues may bring important insight on GSH variation in the brain and its role in neurodegenerative diseases.

This study seeks to utilize the Diversity Outbred (DO) mice stock to evaluate how genetic influence can impact GSH variation in the cerebral cortex. The rationale is that the DO mice

stock is derived from eight founder strains as the Collaborative Cross inbred strains, which provides a diverse genetic profile and can easily be translatable to human populations [256]. Our results contrast GSH concentrations in the cerebral cortex against those previously found in the liver [260] and kidney [261], which will provide key insight into the genetic regulation of cortical GSH and whether those mechanisms differ from the peripheral tissues.

Materials and Methods

Animals: Male and female Diversity Outbred (DO) mice (J:DO; JAX® #009376) from The Jackson Laboratory (Bar Harbor, ME USA) were delivered to the University of Georgia. All mice arrived at 4 weeks of age and were kept under the same conditions: on a 12-hour light/dark cycle and given *ad libitum* access to water and standard chow diet (LabDiet®, St. Louis, MO USA, product 5053). Mice were fasted for 3-4 hours before sacrifice at 5-6 months of age and euthanized humanely by cervical dislocation for tissue harvesting. In total, 351 mice (172 males, 175 females) were sacrificed. All methods and procedures involving animals were approved by The University of Georgia Institutional Animal Care and Use Committee (IACUC) in accordance with the ethical standards of the institution (AUP #A2016 07-016).

Assessment of cortical total glutathione, GSH, GSSG, GSH/GSSG ratio, and redox potential: Brain tissue samples from the cerebral cortex were isolated from each mouse after human euthanasia and rinsed with ice-cold PBS, blotted on a paper towel, and flash-frozen in liquid nitrogen. Brain tissues were processed within 12 h and homogenized in PBS comprised of 10 mM diethylenetriaminepentaacetic acid (DTPA), and subsequently acidified with an equal volume of ice-cold 10% perchloric acid (PCA) containing 1 mM DTPA based on previous studies [243, 296]. Next, acidified samples were centrifuged at 15,000 RPM and 4°C for 15 min for collection and filtration of the acidified supernatant. At -80°C, the filtered supernatant

samples were stored for future analysis. GSH and GSSG concentrations of each sample were quantified by using high performance liquid chromatography (HPLC) coupled with electrochemical detection (Dionex Ultimate 3000, Thermo Fisher Scientific, Waltham, MA USA) based on a previous study [296]. The mobile phase comprised of 4.0% acetonitrile, 0.1% pentafluoropropionic acid, and 0.02% ammonium hydroxide with a flow rate set at 0.22 mL/min and an injection volume of 5.0 μL. Settings of the HPLC were placed in the following: conditioning cell (+500 mV), boron-doped diamond cell (+1475 mV), cleaning potential (+1900 mV) between samples. Concentrations of GSH and GSSG of each generated peak were quantified using standards of known concentrations, external calibration, and the Chromelion chromatography Data System Software (Dionex Version 7.2, Thermo Fisher Scientific, Waltham, MA USA). Concentrations of GSH and GSSG were standardized to total protein (Pierce BCA Protein Assay, Thermo Fisher Scientific, Waltham, MA USA) and denoted in nmol/mg protein. Concentrations of total glutathione were calculated using the equation: [GSH]+[2GSSG]. The GSH/GSSG ratio was calculated using $\frac{[GSH]}{[GSSG]}$ and the redox potential (E_h) of the GSH-GSSG pair ($2GSH \rightarrow GSSG + 2e^- + 2\text{H}+$) was determined in each brain sample through the Nernst equation: $E_h = E0 + RTnFln[(ox)(red)]$. E_h = measured cell potential, E0 = standard electrode potential for GSSG/2GSH (-264 mV at pH 7.4 [297-299]), R = gas constant (8.3145 J x mol x K^{-1}), T = temperature in Kelvin (40°C = 313.15 K), n = number of electrons transferred (2), F = Faraday's constant (96485 C x mol^{-1}), ox = molar concentrations of oxidant (GSSG), and red = molar concentration of reducant (GSH). The final equation for calculating redox potential is: $E_h(mV) = -264 + 31\log[\frac{(GSSG)}{(GSH)^2}]$.

Statistical analysis: RStudio version 2025.05.0+496 (RStudio, PBC., Boston, MA) and R version 4.3.2 (R Foundation for Statistical Computing, Vienna, Austria) were used to normalize

data, determine descriptive statistics, and identify correlations between variables. Spearman's rho (ρ) was computed to report each correlation. Correlations with a p-value less than 0.05 were considered statistically significant.

Results

Cortical GSH phenotypes vary significantly among DO mice: We measured cortical concentrations of GSH and GSSG, GSH/GSSG ratio, and redox potential in a large cohort of DO mice (N = 187) and discovered considerable variation across all GSH phenotypes (Table 3.1), which can also be visually represented by histograms in Figure 3.1. Cortical total glutathione concentrations varied widely (1.897-78.273 nmol/mg), as well as cortical GSH concentrations (0.428-70.391 nmol/mg). Other GSH phenotypes exhibited significant variation, such as cortical GSSG concentrations (0.064-8.551 nmol/mg) and cortical GSH/GSSG values (0.268-97.618). Cortical redox potential also varied, ranging from -362.734 to -234.821 mV. Phenotypes by sex were also analyzed, in which there were no significant sex differences observed (Tables 3.2 and 3.3).

Phenotype	N	x̄	Median	SD	Min	Max
Total Glutathione (nmol/mg)	187	14.772	11.477	11.921	1.897	78.273
GSH (nmol/mg)	187	10.879	8	10.987	0.428	70.391
GSSG (nmol/mg)	187	1.946	1.557	1.411	0.64	8.551
GSH/GSSG	187	9.696	5.684	13.286	0.268	97.618
E_h (mV)	187	-309.878	-314.693	29.716	-362.734	-234.821

Table 3.1. Descriptive statistics for cortical GSH concentrations and redox status in DO mice. Cortical concentrations of GSH (nmol/mg protein) and GSSG (nmol/mg protein) were quantified in samples collected from DO mice (93 males; 94 females) by HPLC. Total glutathione concentrations were then calculated (GSH + 2GSSG), as well as GSH/GSSG and E_h (mV). Basic descriptive statistics were determined in RStudio.

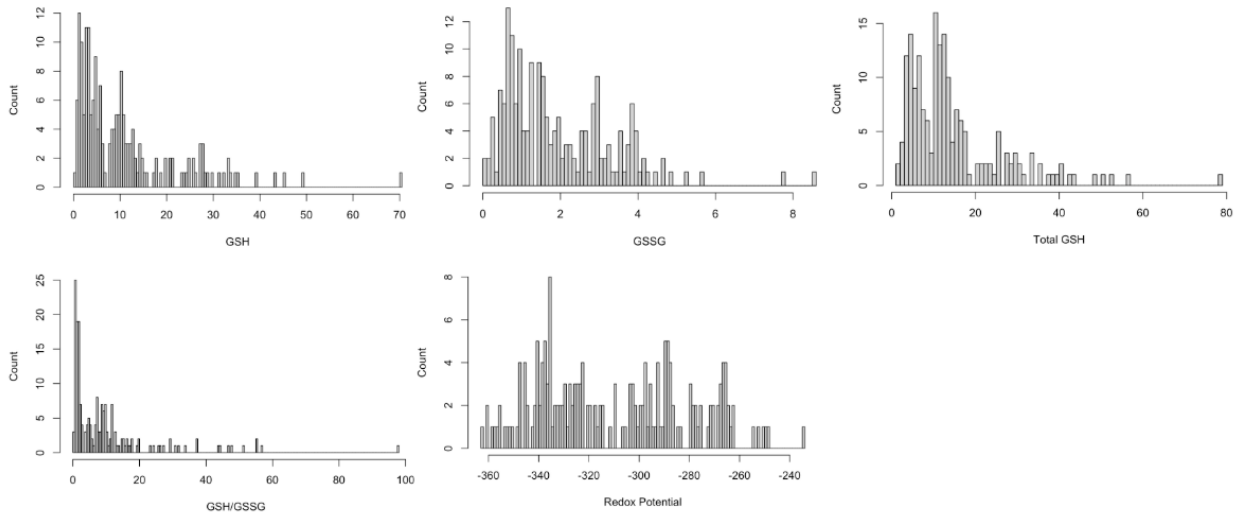

Figure 3.1. Variations in cortical GSH phenotypes. GSH, GSSG, and Total GSH were standardized as nmol/mg protein. Redox potential was expressed in millivolts (mV). Histograms were generated in RStudio.

Statistical correlations were screened between cortical GSH phenotypes and numerous significant associations were discovered among variables (Table 3.4; Figure 3.2). Cortical GSH concentrations were positively correlated with cortical GSSG concentrations ($\rho = 0.22$, $p = < 0.01$), cortical total glutathione concentrations ($\rho = 0.97$, $p = < 0.001$), cortical GSH/GSSG levels ($\rho = 0.34$, $p = < 0.001$), and negatively correlated with cortical E_h levels ($\rho = -0.75$, $p = < 0.001$). Similarly, cortical total glutathione concentrations were positively correlated with cortical GSSG concentrations ($\rho = 0.44$, $p = < 0.001$), cortical GSH/GSSG levels ($\rho = 0.21$, $p = < 0.01$), and negatively correlated with cortical E_h levels ($\rho = -0.65$, $p = < 0.001$). Cortical GSSG concentrations exhibited an additional positive correlation with cortical E_h levels ($\rho = 0.19$, $p = < 0.01$) and negative correlation with cortical GSH/GSSG levels ($\rho = -0.43$, $p = < 0.001$). Lastly, cortical GSH/GSSG levels were negatively correlated with cortical E_h ($\rho = -0.67$, $p = < 0.001$).

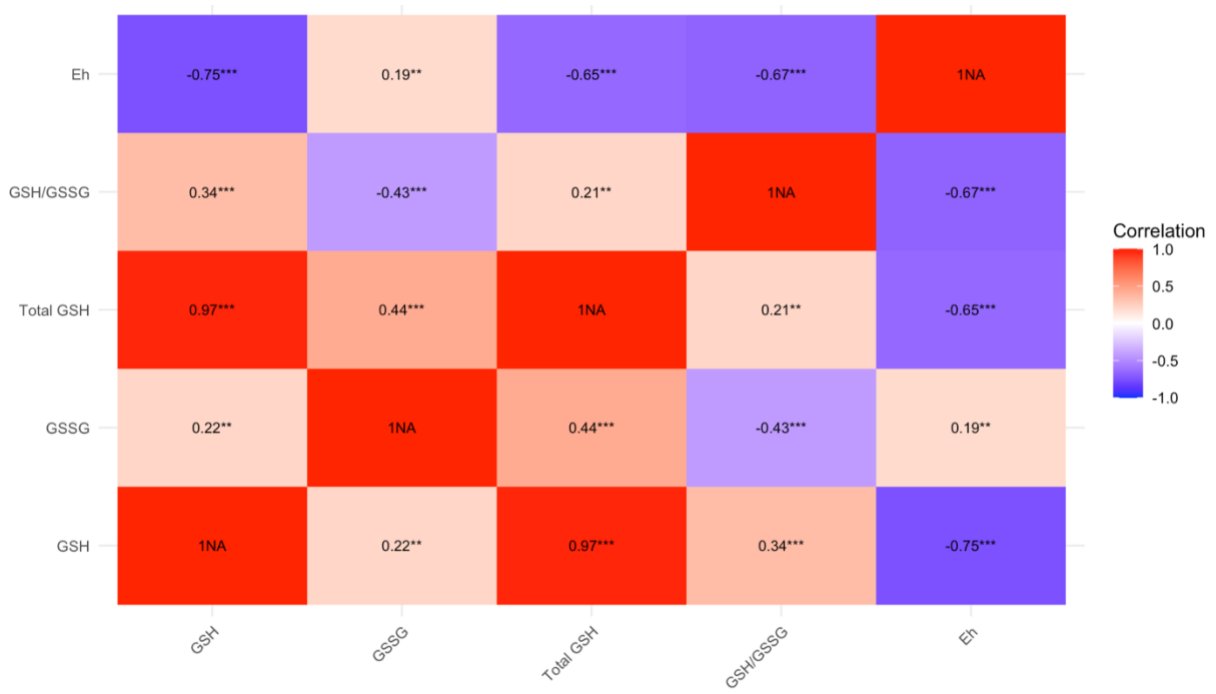

Figure 3.2. Correlations among cortical GSH phenotypes in the DO population. Spearman's rho (ρ) was calculated for each variable combination and listed within each corresponding box. GSH, GSSG, and total glutathione concentrations were standardized as nmol/mg protein. E_h was expressed as mV. P-values are denoted by the following: *** < 0.001, ** < 0.01, * < 0.05. Heatmaps were generated in RStudio.

The cortical GSH system is significantly correlated with the renal GSH systems but not the hepatic GSH system: We screened for statistical correlations between the cortical GSH variables measured in the present study and those measured in the livers and kidneys of the same DO population [260, 261]. Cortical GSH variables were significantly associated with multiple renal GSH variables (Figure 3.3) but not with the hepatic GSH system (Figure 3.4). Cortical GSSG was negatively correlated with renal GSH (ρ = -0.3, p = < 0.001), renal GSSG (ρ = -0.22, p = < 0.01), renal total glutathione (ρ = -0.3, p = < 0.001), and positively correlated with renal E_h levels (ρ = 0.2, p = < 0.01). Cortical total glutathione was negatively correlated with renal GSSG (ρ = -0.8, p = < 0.05), and cortical GSH/GSSG was negatively correlated with renal E_h levels (ρ = -0.15, p = < 0.05). Moreover, cortical E_h levels were negatively correlated with renal GSH (ρ = -0.2, p = < 0.01), renal total glutathione (ρ = -0.2, p = < 0.01), renal GSH/GSSG (ρ = -0.22, p = <

0.01), and positively correlated with renal E_h levels ($\rho = 0.25$, $p = < 0.001$). There is limited correlation between the cortical GSH system and hepatic GSH system. Cortical GSH was negatively correlated with hepatic GSH ($\rho = -0.15$, $p = < 0.05$), hepatic GSSG ($\rho = -0.16$, $p = < 0.05$), and hepatic total glutathione ($\rho = -0.15$, $p = < 0.05$). Furthermore, cortical total glutathione was negatively correlated with hepatic GSH/GSSG ($\rho = -0.15$, $p = < 0.05$).

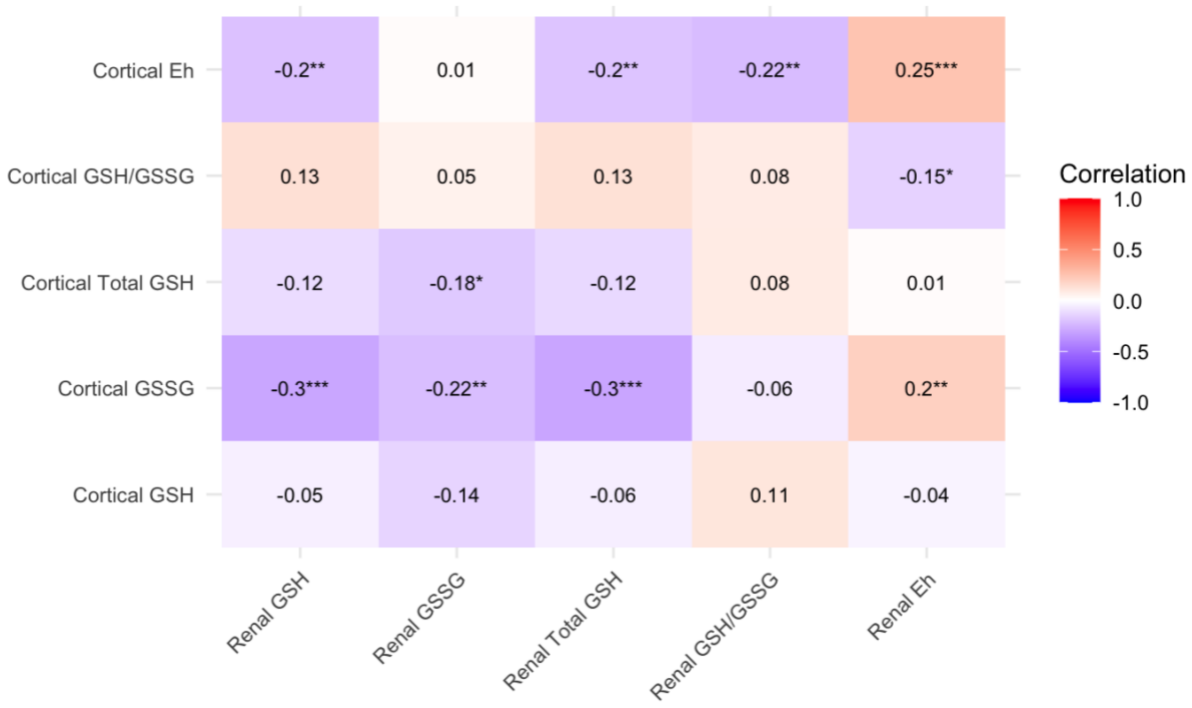

Figure 3.3. Cortical GSH variables are significantly correlated with renal GSH variables within the same cohort of DO mice. Spearman's rho (ρ) was calculated for each variable combination and listed within each corresponding box. GSH, GSSG, and total glutathione concentrations were standardized as nmol/mg protein. E_h was expressed as mV. P-values are denoted by the following: *** < 0.001, ** < 0.01, * < 0.05. Heatmaps were generated in RStudio.

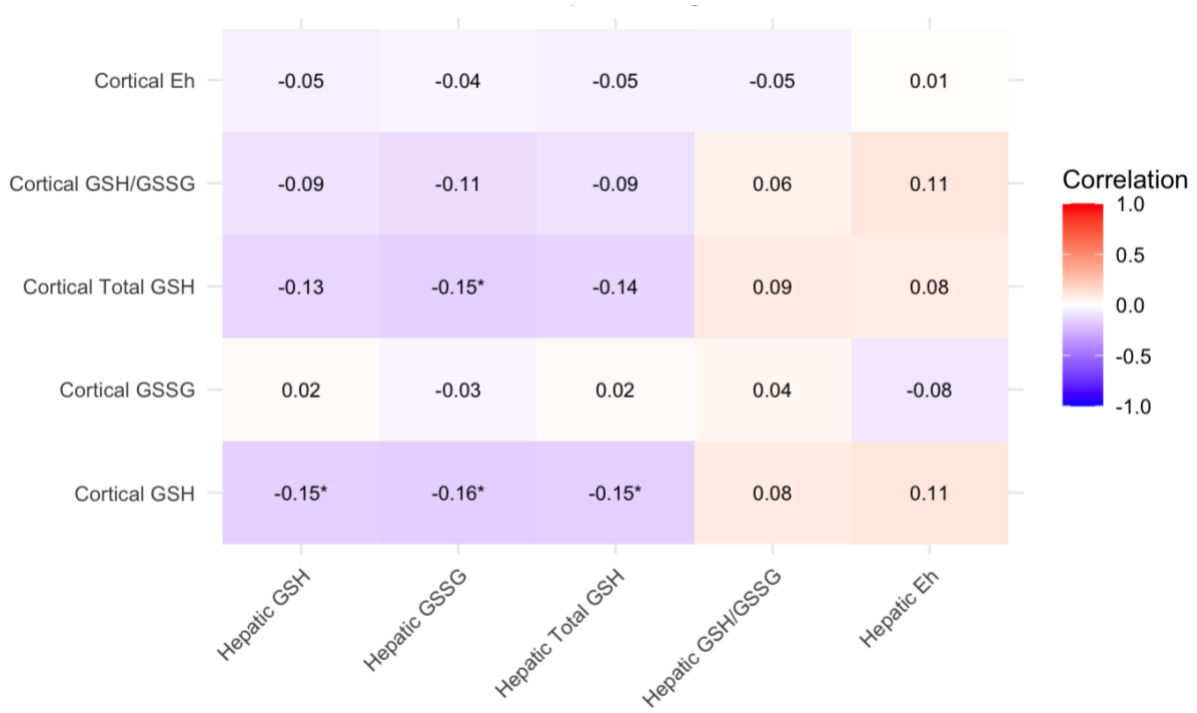

Figure 3.4. Cortical GSH variables are not significantly correlated with hepatic GSH variables within the same cohort of DO mice. Spearman's rho (ρ) was calculated for each variable combination and listed within each corresponding box. GSH, GSSG, and total glutathione concentrations were standardized as nmol/mg protein. E_h was expressed as mV. P-values are denoted by the following: *** < 0.001, ** < 0.01, * < 0.05. Heatmaps were generated in RStudio.

Discussion

GSH carries a pivotal role in protecting the brain and health, however there is currently limited understanding of how genetic variation influences cortical GSH status, and potential influential genes and loci on GSH status in the brain remain unknown. In this study, we utilized the genetically diverse DO stock to examine the impact of genetic variation on GSH phenotypes of the brain and compared GSH regulation in the cerebral cortex to other major tissues to determine the relationship between cortical, renal, and hepatic GSH. Overall, this study screened for statistical relationships and found variations across cortical GSH phenotypes, as well as discerning correlations between GSH status in the brain, liver, and kidney.

Significant variations were found among multiple GSH phenotypes of the cortical GSH system and independent of sex, where total glutathione values ranged from 1.897 to 78.272, GSH values ranged from 0.428 to 70.391, GSSG values ranged from 0.64 to 8.551, GSH/GSSG ratio ranged from 0.268 to 97.618, and redox potential ranged from –362.734 to –234.821. In a study conducted by Rebrin, *et al.,* B6 mice given ad libitum chow exhibited a mean GSH value of about 14 nmol/mg protein, a mean GSSG value of about 0.12 nmol/mg protein, and a mean GSH/GSSG ratio of 123, and DBA/2 mice given ad libitum chow exhibited a mean GSH value of about 14 nmol/mg protein, a mean GSSG value of about 0.14 nmol/mg protein, and a mean GSH/GSSG ratio of 98 [246]. GSSG results demonstrate that values below one can be found in the cerebral cortex under oxidative stress, however, it is not known for certainty that values below one are normal among GSH and GSH/GSSG due to unclear ranges of GSH and GSH/GSSG phenotypes in the current literature. It can be postulated however, that certain limitations of this study can lead to values lower than one. Limitations to this study include inaccurate measurements due to technical HPLC issues as it aged, oxidation of samples in the autosampler at 4ºC while running within 4 hours, and oxidation of samples placed in a -80 ºC freezer for about 5-6 years. Future studies should investigate variations of glutathione in the cerebral cortex by using rodent models to help clarify the validity of significantly low phenotypic values. Despite the limitations of this study, utilizing a DO mouse stock allows results to represent how cortical GSH varies in a highly diverse population, such as those of humans.

Within the same DO cohort, we also discovered significant correlations between cortical and renal GSH phenotypes, however, there were limited significant correlations between cortical and hepatic GSH phenotypes. The hepatic GSH phenotypes, however, had numerous significant correlations with the renal GSH phenotypes, as demonstrated in a previously published study on

the statistical relationship between renal and hepatic GSH systems [261]. Between the cortical and renal GSH systems, multiple statistical correlations were found, such as cortical GSSG concentrations negatively correlated with renal GSSG concentrations ($\rho = -0.22$, $p < 0.01$) and cortical E_h values positively correlated with renal E_h values ($\rho = 0.25$, $p < 0.001$). The strong correlation found between the cortical and renal GSH systems can also be reflected to a study by Gould, *et al.,* where it was discovered that several inbred strains, such as the B6 mice strain, had higher GSH/GSSG ratios in the kidneys and cerebral cortex but lower GSH/GSSG ratios in the liver [243]. For example, the B6 mice strain exhibited a mean GSH/GSSG ratio of about 60 in the kidneys and about 65 in the cerebral cortex, while the GSH/GSSG ratio was about 38 in the liver [243]. This implies that cortical and renal GSH systems may be under the influence shared genetic factors, in which further research is warranted. As with between the cortical and hepatic GSH systems, there were very limited correlations observed. These findings were similar to the results displayed by Gould, *et al.,* in which compared to the kidney GSH/GSSG ratios, liver GSH/GSSG ratios were further from cerebral cortex GSH/GSSG ratios [243].

Based on our current findings from this study, disease risk or protection may be determined by the variation of glutathione in different tissues of the body. For instance, disease susceptibility of the brain and kidneys may be closely related, in which disruption of renal function may impact levels of glutathione in the cerebral cortex or vice versa. Glutathione levels in the cerebral cortex or kidneys may provide insight of GSH status in the other and serve as a useful tool to be implemented into personalized medicine for treatment or monitoring of certain diseases. This can in turn, change the course of our current understanding on complex disease processes and revolutionize precise therapeutic interventions. On the other hand, the weak relationship between the cerebral cortex and liver implies that they are largely regulated

independently from each other. It is speculated however, that the cerebral cortex and liver may be under the influence of some shared regulation, as seen in the few significant correlations between the cerebral cortex and hepatic phenotypes of this study. GSH synthesis takes place in the cytosol of all cells, the liver plays a role in synthesizing GSH and exporting GSH to other tissues of the body through plasma and bile and can impact levels of glutathione in the brain. Within the interorgan GSH transport system, GSH from the liver can translocate from the plasma to the brain via the blood brain barrier [277]. Due to limited data in the current literature, more research is needed to clarify the relationship between the regulation of cortical and hepatic GSH status.

Although there were no significant differences in variation between equal numbers of males and females of this current study, it was observed that male mice had overall higher mean values across all glutathione phenotypes than those in female mice. For example, male mice had a mean GSH value of 13.202 nmol/mg protein, while female mice had a mean GSH value of 8.58 nmol/mg protein. It was found by Wang, *et al.,* that GPx protein expression was higher in the male cerebral cortex than females at postnatal day 30 of Sprague-Dawley rats [300]. Contrary to these findings however, Wang, *et al.,* discovered that GSH content was higher in female mouse cortical tissues (84.5 ± 2.3) than in male mouse cortical tissues (79.3 ± 2.2) [301]. These findings could be influenced by distinct hormonal regulation of males and females, but due to inconsistent findings between studies, additional studies are needed to discern differences in cortical GSH status among sex.

To complete our understanding of GSH variation across different tissues, future research efforts should study other tissues that have not been investigated yet in a DO mouse stock, such as the adipose and pancreatic tissues. Moreover, future studies should explore other parts of the

DO mouse brain, such as the cerebellum and olfactory bulb, to connect with findings discovered in the cerebral cortex of this current study and determine relationships with one another. All in all, discoveries from this study builds a better understanding of GSH regulation and reveals a tissue-specific component of GSH variation. Future research is warranted in human populations to expand our understanding in the variation and regulation of GSH status, as well as its potential impact on human health.

Conclusion

Little is known on the genetic background of GSH status in the brain but is a crucial component to better understand the regulation of GSH. This present study showcases the analysis of cortical GSH within a large DO cohort, along with statistical correlations found between the cortical GSH phenotypes and GSH phenotypes of other major tissues. Although correlations between cortical GSH status and hepatic GSH status were not meaningful, the strong relationship shown between cortical and renal GSH status highlights shared genetic regulatory mechanisms. Overall, the findings of this study contribute to bridging the knowledge gap between GSH regulation in the brain and understanding of genetic influence. This supports the next phase of this thesis in identifying genetic variants involved in cortical GSH regulation, which will help develop potential therapeutic interventions to alleviate oxidative stress in neurodegenerative disease.

Table 3.2. Descriptive statistics for cortical GSH concentrations and redox status in male mice. Cortical concentrations of GSH (nmol/mg protein) and GSSG (nmol/mg protein) were quantified in samples collected from DO mice (93 males) using HPLC. Total glutathione concentrations were then calculated (GSH + 2GSSG), as well as GSH/GSSG and E_h (mV).

Phenotype	N	$\bar{x}$	Median	SD	Min	Max
Total Glutathione (nmol/mg)	93	17.568	13.235	12.694	3.625	78.273
GSH (nmol/mg)	93	13.202	10.078	12.272	0.428	70.391
GSSG (nmol/mg)	93	2.183	1.739	1.55	0.427	8.551
GSH/GSSG	93	10.099	7.341	11.211	0.268	55.2
E_h (mV)	93	-314.77	-322.067	29.926	-362.734	-234.821

Table 3.3. Descriptive statistics for cortical GSH concentrations and redox status in female mice. Cortical concentrations of GSH (nmol/mg protein) and GSSG (nmol/mg protein) were quantified in samples collected from DO mice (94 females) using HPLC. Total glutathione concentrations were then calculated (GSH + 2GSSG), as well as GSH/GSSG and E_h (mV).

Phenotype	N	$\bar{x}$	Median	SD	Min	Max
Total Glutathione (nmol/mg)	94	12.005	8.931	10.454	1.897	48.538
GSH (nmol/mg)	94	8.58	5.134	9.038	0.502	39.328
GSSG (nmol/mg)	94	1.712	1.246	1.222	0.064	4.605
GSH/GSSG	94	9.296	4.502	15.111	0.459	97.618
E_h (mV)	94	-305.039	-302.919	28.854	-358.14	-248.798

Table 3.4. Statistical correlations between markers of the cortical GSH system. Spearman's rho (ρ) was calculated to understand relationships between cortical GSH system markers. Cerebral cortex GSH and GSSG concentrations were calculated using HPLC and standardized as nmol/mg protein. Concentrations were then used to calculate total glutathione (GSH + 2GSSG), GSH/GSSG, and E_h (mV).

Phenotype		**ρ**	**p-value**
GSH	GSSG	0.22	$p < 0.01$
GSH	Total GSH	0.97	$p < 0.001$
GSH	GSH/GSSG	0.34	$p < 0.001$
GSH	E_h	-0.75	$p < 0.001$
GSSG	Total GSH	0.44	$p < 0.001$
GSSG	GSH/GSSG	-0.43	$p < 0.001$
GSSG	E_h	0.19	$p < 0.01$
Total GSH	GSH/GSSG	0.21	$p < 0.01$
Total GSH	E_h	-0.65	$p < 0.001$
GSH/GSSG	E_h	-0.67	$p < 0.001$

CHAPTER 4

HIGH-RESOLUTION GENETIC MAPPING DISCOVERS NOVEL GENETIC LOCI TIED TO THE CORTICAL GSH SYSTEM AND REDOX BALANCE[2]

[2] Song J. and Pazdro R. Constructing a correlation model of glutathione status between cortical, renal, and hepatic glutathione redox systems. To be submitted to a peer-reviewed journal

Abstract

Glutathione is a master antioxidant essential to the cell's antioxidant defense system for combating oxidative stress and maintaining homeostasis. The thiol-reduced form (GSH) is converted to its disulfide-oxidized form (GSSG) in a redox cycle that neutralizes free radicals. Oxidative stress is caused by an imbalance between reactive oxygen species (ROS) and antioxidants in favor of ROS production. Genetic mutations in the antioxidant defense pathway have been associated with the progression of neurodegenerative diseases, implying that increased understanding of the genetic background of GSH metabolism may support therapeutic targets to mitigate oxidative stress in neurodegenerative disease. Current literature has focused on canonical GSH genes, but little is known of potential loci or genes influencing the cortical GSH system outside of the canonical GSH pathway. The present study utilizes high-resolution genetic mapping with the Diversity Outbred (DO) mouse stock to identify novel loci and genes underlying variation in cortical GSH status. Results from genetic mapping identify a suggestive locus associated with cortical GSH on murine chromosome 13 at 87.365 Mbp, and bioinformatics analysis identified two plausible candidate genes: *transmembrane protein 161B* (*Tmem161b*) and *X-ray repair complementing defective repair in Chinese hamster cells 4* (*Xrcc4*). Overall, these results build upon current knowledge of the GSH redox system and reveal novel genetic players in cortical GSH regulation, proposing candidate genes to be further investigated in future mechanistic studies.

Introduction

Glutathione (GSH) is a ubiquitous thiol tripeptide made up of cysteine, glutamate, and glycine that is known for its role in protecting the body against oxidative stress [69]. GSH is synthesized through a number of ATP-required enzymatic steps [69]. The first step involves the rate limiting step catalyzed by glutamate cysteine ligase (GCL), coupled with ATP hydrolysis, to form γ-glutamyl-L-cysteine, and is followed by glutathione synthetase (GS) to form the GSH tripeptide [73]. Glutathione exists primarily in its thiol-reduced form (GSH) and its disulfide-oxidized form (GSSG) [72]. Two molecules of GSH can convert to GSSG through the glutathione peroxidase (GPx) enzyme to neutralize hydrogen peroxides [73]. In turn, GSSG can be recycled to form GSH through the glutathione reductase (GR) enzyme by the expense of NADPH, thus completing the redox cycle [73].

The depletion of glutathione is associated with the progression of neurodegenerative diseases [210] due to the imbalance between reactive oxygen species (ROS) and antioxidants in favor of ROS production, which increases oxidative stress in the brain [302]. Additionally, genetic mutations in the antioxidant defense pathway have highlighted the relevance of glutathione in preventing or alleviating neurodegenerative processes. Knockout of several enzymes responsible for glutathione synthesis and metabolism in mice models have shown to contribute to neurodegeneration and cognitive impairment. For example, in conditional GCLC-conditional knockout mice, there seemed to be progressive neurodegeneration and inflammation in the brain [210]. GPx mutations in mice have also exhibited cognitive impairment and neurodegeneration [289, 290, 303, 304]. In humans of non-smokers and non-abusers of alcohol, it was discovered that several single nucleotide polymorphisms (SNPs) of the gamma-glutamyl transferase (GGT1) gene conferred protection against ischemic stroke [305]. In patients with

schizophrenia, it was found that the GPx-1 polymorphisms rs1050450 and rs1800668 were associated with schizophrenia [306]. Furthermore, patients with Parkinson's disease (PD) demonstrated loss of GSH as early as in the beginning stages of PD [288, 307]. These findings imply that GSH related polymorphisms may play a role in placing genetic risk in individuals for neurodegenerative diseases and disorders. Despite the critical role of GSH genes, to our knowledge, there is currently no research showing the genetic variants that directly regulate GSH dynamics in the brain.

To gain a better understanding on key genes and variants involved in brain GSH metabolism, high-precision genetic mapping of quantitative trait loci (QTL) was performed in a large Diversity Outbred (DO) mouse stock to reflect the genetic diversity found in the human population. Previous work completed in our lab have discovered novel loci and genes associated with GSH status in both the liver [260] and kidney [261], though the brain has not been investigated yet. This current work utilizes the same DO mouse stock to characterize the genetic architecture of cortical GSH. We sought out genetic loci and candidate genes associated with cortical GSH and contrasting findings from the renal and hepatic GSH systems [260, 261] to identify genetic overlap between these major tissues. As it currently stands, this is the first largest high-precision genetic mapping study on the genetic regulation of cortical GSH, which will provide novel insight into candidate genes that will pave the way for future studies on the GSH systems and redox status.

Materials and Methods

Animals: Male and female Diversity Outbred (DO) mice (J:DO; JAX® #009376) from The Jackson Laboratory (Bar Harbor, ME USA) were delivered to the University of Georgia. All mice arrived at 4 weeks of age and were kept under the same conditions: on a 12-hour light/dark

cycle and given *ad libitum* access to water and standard chow diet (LabDiet®, St. Louis, MO USA, product 5053). Mice were fasted for 3-4 hours before sacrifice at 5-6 months of age and euthanized humanely by cervical dislocation for tissue harvesting. In total, 351 mice (172 males, 175 females) were sacrificed. All methods and procedures involving animals were approved by The University of Georgia Institutional Animal Care and Use Committee (IACUC) in accordance with the ethical standards of the institution (AUP #A2016 07-016).

Genotyping: DNA was collected at sacrifice from tail tips of all 351 mice. Samples were processed by GeneSeek (Neogen Genomics, Lincoln, NE USA, 68504) for genotyping using the third-generation Mouse Universal Genotyping Array (GigaMUGA) [308], which is a 143K-probe array built on the Illumina Infinium II platform for genetic mapping in the DO mouse stock.

Quantitative trait loci (QTL) mapping: Genome scans were performed in 187 (93 males, 94 females) DO samples. 164 of the 351 samples were excluded from QTL mapping due to technical HPLC machine issues. The R/qtl2 software was used to conduct QTL analysis [309] and sex was included as additive covariates in the genome scan. To normalize data, each phenotype were rank-z-score transformed [310], and kinship was accounted for among DO mice using the "leave one chromosome out" (LOCO) method [309, 311]. Each genome scan underwent 1000 permutations to establish phenotype-specific significance thresholds [309, 312, 313]. A suggestive threshold (p-value ≤ 0.20) was applied for reporting QTL loci [313], and a 95% Bayesian credible interval was identified for each peak located close to the reported QTL position [309, 312]. The Best Linear Unbiased Predictors (BLUPs) model was utilized to determine the effect level of the eight founder allele strains [314]. Genes within intervals were plotted using the database found in Mouse Genome Informatics (MGI).

Candidate gene analysis: To prioritize candidate genes, databases for expression, functional, and phenotypic annotations were utilized based on methods used in previous studies [315, 316]. Protein-coding genes within the significant QTL intervals ± 1 Mbp were collected and reported through the Mouse Genome Informatics (MGI) database [317]. Genes not expressed in adult rodent cortical tissue were excluded based on gene expression annotations from the Gene eXpression Database (GXD) [318] through MGI [317], as well as EBI Expression Atlas (EEA) through the European Molecular Biology Laboratory European Bioinformatics Institute (EMBL-EBI) [319]. Candidate genes were further narrowed down by using Gene Ontology (GO) annotations [320, 321] through MGI [317] to identify gene function relevant to the brain. Phenotypic data were also collected from mammalian phenotype (MP) [322] and PheWeb (PW) [323].

Results

QTL mapping of cortical GSH phenotypes: We performed QTL genome-wide analysis using R/qtl2 on cortical total glutathione, GSH, GSSG, GSH/GSSG, and redox potential (Figure 4.1). We ran 1000 permutation tests in each QTL scan to determine LOD score thresholds to assess significance ($p < 0.05$). There were no peaks greater than the LOD score thresholds, however, several peaks surpassed the suggestive LOD score threshold of 6 ($p \leq 0.20$) (Table 4.1). The genome-wide scans for cortical GSH concentrations revealed a suggestive QTL peak on mouse chromosome 13 at 87.365 Mbp (LOD score 6.452). The genome-wide scan for cortical total glutathione concentrations revealed a suggestive QTL peak on mouse chromosome 13 at 87.317 Mbp (LOD score 6.781). Five suggestive peaks for cortical GSH/GSSG were revealed on mouse chromosome 6 at 112.423 Mbp, chromosome 6 at 112.491 Mbp, chromosome 6 at 112.524 Mbp, chromosome 11 at 90.585 Mbp, and chromosome 19 at 58.739 Mbp (LOD scores

6.091, 7.284, 6.299, 6.674, and 6.153, respectively). Two suggestive peaks for cortical redox potential were revealed on mouse chromosome 11 at 90.585 Mbp and chromosome 19 at 58.743 Mbp (LOD scores 7.154 and 6.321, respectively). Given that the peak position and QTL intervals were the same between the two genome scans, cortical GSH scans are included in Figure 4.2 and cortical total glutathione scans are found in Figure 4.3. Founder allele effects from other suggestive peaks can be found in Figures 4.4-4.8.

Figure 4.1. QTL mapping results of cortical GSH concentrations and redox status. Genome-wide scans were generated for cortical **A)** total glutathione concentrations (GSH + 2GSSG, expressed as nmol/mg protein); **B)** GSH concentrations (nmol/mg protein); **C)** GSSG concentrations (nmol/mg protein); **D)** GSH/GSSG; and **E)** redox potential of the GSSG-GSH couple (E_h, expressed as mV). Permutation-derived significant thresholds for each scan were indicated by colored lines at significant (α) levels 0.05 (blue), 0.1 (red), and 0.2 (purple).

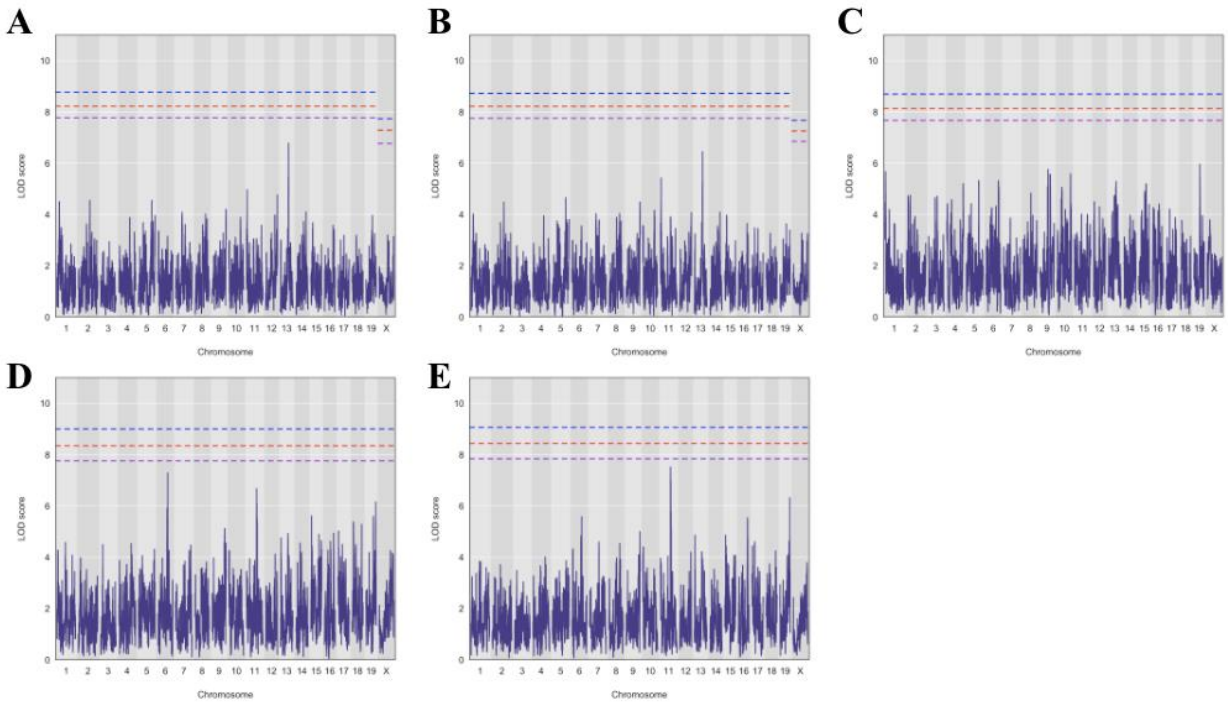

Figure 4.2. High-resolution association mapping for cortical GSH concentrations reveals a suggestive peak on chromosome 13. A) Genome-wide scan of cortical GSH concentrations (nmol/mg protein) exhibits a QTL with a peak LOD score 6.452 at 87.365 Mbp (45.155 cM) on mouse chromosome 13. Permutation-derived significance thresholds are indicated by colored lines at significance (α) levels 0.05 (blue), 0.1 (red), and 0.2 (purple). **B)** The founder allele QTL effects indicate that the PWK, 129, NOD, and WSB alleles contribute to a higher cortical GSH concentration (nmol/mg protein), while the NZO and B6 alleles contribute to a lower cortical GSH concentration (nmol/mg protein). Each colored line represents one of eight DO founder alleles as indicated in the legend. The differences between strains are considered significant when the LOD score (bottom plot) crosses significance thresholds established in panel A. **C)** Candidate genes found within the QTL interval relative to the MGI database. The cortical total glutathione genome scan resulted in the same suggestive QTL interval on mouse chromosome 13 compared to cortical GSH (Figure 4.3)

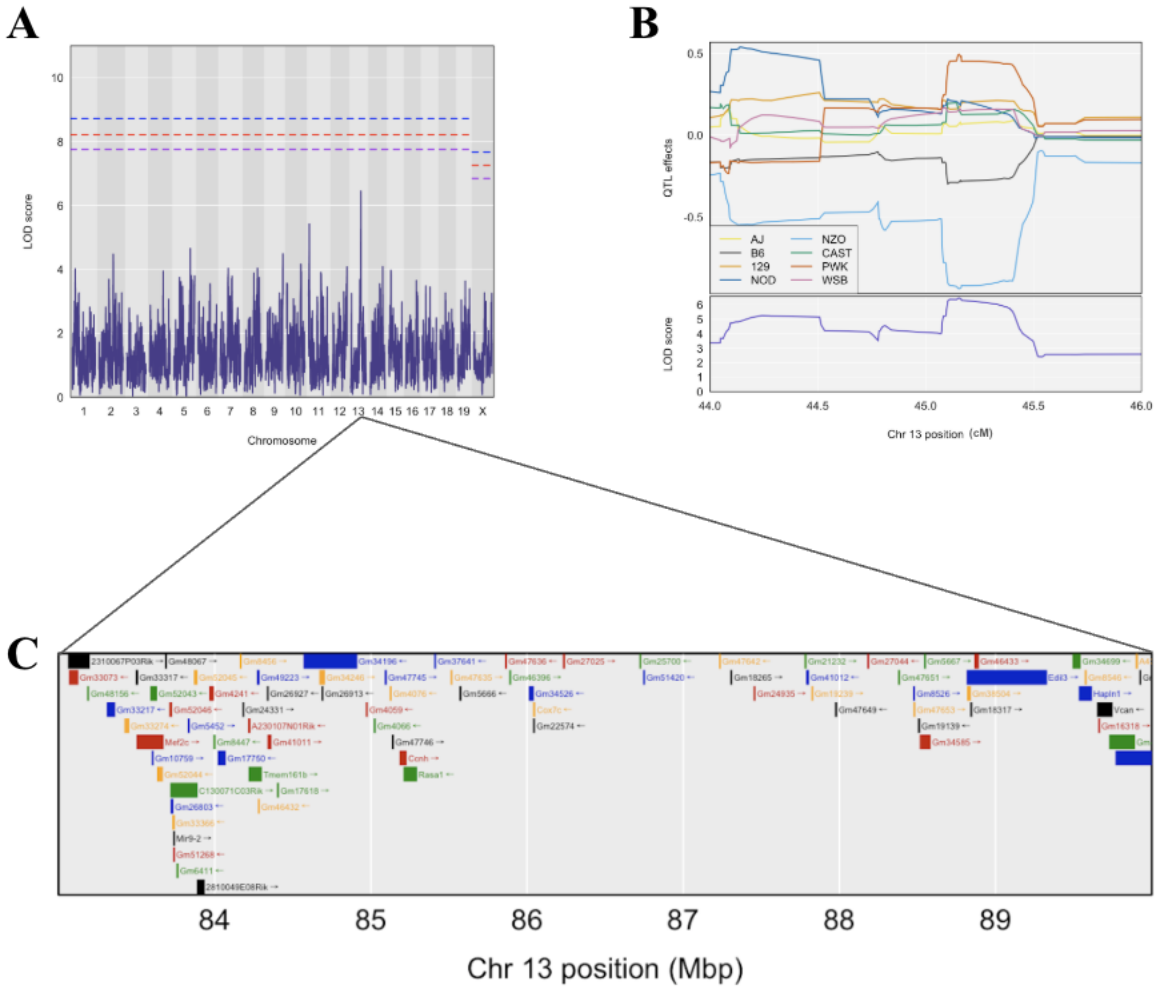

The highest peak (LOD score 6.452) on mouse chromosome 13, associated with cortical total glutathione and GSH concentrations, was further investigated and defined by the following location: 87.365 Mblp with a QTl interval of 83.909-89.354 Mbp (Figure 4.2A). Founder allele effects revealed that the PWK, 129, NOD, and WSB alleles contribute to a higher cortical total glutathione and GSH concentration, while the NZO and B6 alleles contribute to a lower cortical total glutathione and GSH concentration (Figure 4.2B). R/qtl was then utilized to plot genes located within the interval $\pm$ 1 Mbp (Figure 4.2C). Functional RNA and protein coding genes were screened based on available expression, functional, and phenotypic data (Tables 4.2 and 4.3). The QTL interval contained 81 possible candidate genes: 13 protein-coding genes, 1 non-coding RNA gene, 67 pseudogenes, 27 lncRNA genes, 3 unclassified genes, 5 miRNA genes, 1 snoRNA gene, and 1 snRNA gene. 31 of the 81 candidate genes were excluded due to limited brain expression annotations from EMBL-EBI and MGI. Out of the remaining 50 candidate genes, 44 genes were excluded due to limited functional annotations from GO. Of the remaining 6 genes, 2 had phenotypic annotations related to brain function or redox metabolism from MP and PW: *transmembrane protein 161B* (*Tmem161b*) and *X-ray repair complementing defective repair in Chinese hamster cells 4* (*Xrcc4*). *Tmem161b* A query in Ensembl Biomart revealed that *Tmem161b* is associated with abnormal stratification in cerebral cortex (MP:0000790) in mice. In humans, *TMEM161b* was linked with major depressive disorder [324-327], as well as neocortical polymicrogyria and intellectual disability [328]. In both mice and humans, *Tmem161b* and *TMEM161* was implicated in regulating cerebral cortical gyration, Sonic Hedgehog signaling, and ciliary structures in developing the central nervous system [329]. A

query in Ensembl Biomart also revealed that *Xrcc4* is associated with abnormal cerebral cortex morphology (MP:0000788), increased neuron apoptosis (MP:0003203), and thin cerebral cortex (MP:0006254) in mice. Existing literature shows that mutations in *XRCC4* in humans are linked to marked neurological manifestations [330] and susceptibility in schizophrenia [331, 332]. It is notable that mutations in *XRCC4* are linked to the risk of autism spectrum disorder (ASD), where brain tissues from ASD patients showed higher levels of oxidative stress and DNA damage [333]. Furthermore, *XRCC4* has been associated with increased risk of gliomas [334] and shown to be associated with the APTX gene, a gene that causes neurological disorders when mutated [335].

Comparison of the cortical, renal, and hepatic GSH systems: We compiled all significant loci and other QTL associated with either renal or hepatic GSH phenotypes to screen for genetic overlap with cortical QTL intervals (Table 4.4). There were no overlapping QTL intervals found between the cortical GSH system and the renal and hepatic GSH systems.

Discussion

This work sought to define the genetic regulation of the cortical GSH system by using high-precision QTL mapping in a genetically diverse mouse model. We documented novel loci associated with cortical GSH and subsequently identified candidate genes within the QTL interval. Candidate genes were then narrowed down by using expression, functional, and phenotypic annotations. Through comprehensive genetic mapping, we establish further understanding of genetic regulation of the cortical GSH system.

QTL mapping of cortical GSH suggested a novel locus on mouse chromosome 13 at 87.365 (83.909 – 89.354) Mbp. Bioinformatics analyses revealed two potential candidate genes within the QTL: *Tmem161b* and *Xrcc4*. These two candidate genes were all validated through

expression, functional, and phenotypic annotations due to their relevance to brain function and oxidative stress, therefore we concluded these two genes to most likely influence cortical GSH regulation. Although its exact biological functions are unknown, *TMEM161b* has been implicated in neurological disorders in humans [324-328]. Notably, this gene is shown to be involved in developing the central nervous system and regulating cerebral cortical folding and gyration in animal and human models [329]. Brains with greater gyrification patterns are known to be associated with increased Gpx and superoxide dismutase (SOD) activity, which serve as markers of cognitive improvement [336]. Chui, *et al*., demonstrated that oxidative stress levels progressively increase in the developing mouse cortex under normal conditions [337], and given the suggested role of *Tmem161b,* this gene is likely to be involved in brain antioxidant activities and should be further explored in future studies. The function of the second candidate gene, *Xrcc4*, is also ambiguous, however, mutations in this gene is suggested to contribute to defects in neurogenesis and severe neuronal apoptosis in mice [338, 339]. Furthermore, *XRCC4* has been associated with a spectrum of neurological disorders in humans [330-333], as well as glioma [334]. *XRCC4* is also known to interact with DNA ligase IV and repair DNA double strand breaks caused by oxidative stress [340], in which reduced DNA end joining activity has been observed in AD patients [341]. Despite its involvement in brain function, more research is warranted to further define its role in the cortical redox system.

In addition to non-canonical genes influencing cortical GSH status, other distinct non-canonical genes have also been found to regulate renal, hepatic, and cardiac GSH status. In the renal GSH system, Gould, *et al.,* discovered *Aifm1* as a potential genetic regulator for renal GSH [261]. In the hepatic GSH system, Koch, *et al.,* found *Cdh2* to be associated with hepatic steatosis [342] and *Socs1* as a potential genetic regulator for hepatic GSH/GSSG [260]. In the

cardiac GSH system, several potential candidates, *MiR-208a, Myh6, Myh7, and Nfatc4,* were identified for cardiac GSH regulation [manuscript under review]. Discoveries of genes outside of the GSH pathway suggest to us that the GSH pathway is not the only player affecting GSH pathology in many major tissues.

To further validate the roles of these genes in regulating GSH status in their respective tissues, future studies should utilize methods, such as gene manipulation (knockout or overexpression) or profiling gene expression in tissues by using RNA-seq, to observe GSH status in response to gene expression patterns or vice versa. In humans, it was found that UCP2-silencing $KRAS^{mut}$ cell lines exhibited decreased GSH/GSSG ratios compared to wild-type counterparts [343]. In a mice study conducted by Qiu, *et al.*, it was discovered through the use of RNA-seq, livers from *Sirt1* liver-specific knockout (*LKO)* mice enriched glutathione metabolism and elevated the expression of GST family genes by increasing Nrf2 levels, a regulator of glutathione metabolism, which therefore increased GSH/GSSG ratios and GSH [344]. Furthermore, a mice study conducted by Chen, *et al.,* found that Nrf2-knockout mice exhibited altered glutathione homeostasis and decreased expression of genes involved in GSH biosynthesis, regeneration, utilization, and transport in the liver, and that Ucp2-knockout mice exhibited altered glutathione homeostasis in the liver, spleen, and blood [345]. There is evidence of other genes known to influence GSH status, however, future research using similar methods to further speculate novel non-canonical genes found in this current study and its connected studies is warranted.

Although a suggestive threshold of 6 ($p < 0.20$) was applied to report QTL loci, we hypothesize that with a greater sample size, there may be QTL peaks surpassing or meeting the significance threshold of $p < 0.05$, $p < 0.1$, or $p < 0.2$. Despite no peaks reaching the significance

threshold in this current study, a sample size of 187 DO mice provides close to substantial power to identify QTL peaks with considerable effects, as suggested by power analysis demonstrating that studies with as few as 200 DO mice can detect loci with large effects [346]. A study by Svenson, *et al.,* utilized a smaller DO mouse population to conduct high-resolution genetic mapping, which involved 150 DO mice in their study [310]. This sample size of 150 provided sufficient power for identifying QTL intervals in their mapping resolution, suggesting that a sample size of 187 mice samples may also be sufficient for QTL mapping.

There is substantial evidence in the current literature that canonical GSH genes regulate GSH status. To test our hypothesis that the cortical GSH system is regulated by distinct, novel genetic regulation outside of canonical GSH genes involved in GSH synthesis and metabolism, we utilized R/qtl2 to visualize founder allele effects for *glutathione peroxidase 1 (Gpx1), glutathione cysteine ligase – catalytic subunit (Gclc), glutathione cysteine ligase – modifier subunit (Gclm), glutathione synthetase (Gs), and glutathione reductase (Gr)* in each GSH phenotype (Figures 4.9-4.13). According to our results, there were no significant differences between the eight founder strains. This supports our hypothesis that variation in cortical GSH concentrations and redox status are controlled by novel loci and genes outside of the canonical GSH pathway. By identifying and validating non-canonical genes outside of the GSH pathway, it can help us to determine disease susceptibility and resistance in the human population and pave the way for personalized medicine and treatment strategies.

Conclusion

In this study, we identified a novel QTL underlying cortical total glutathione and GSH concentrations on chromosome 13 using a large cohort of DO mice. We identified *Tmem161b* and *Xrcc4* as the most plausible gene within the locus and validated its relevance to brain

function through functional and phenotypic annotations. These two genes have shown great potential as key genetic players in GSH synthesis and metabolism. Future studies will further investigate the mechanisms of *Tmem161b* and *Xrcc4* as a genetic regulator of the cortical GSH system, thus expanding our knowledge of the genetic architecture of the glutathione redox system.

Table 4.1. Results for high-resolution association mapping of cortical GSH redox system.

QTL peaks with LOD scores > 6 are listed within the table. Peak information includes LOD score, QTL position (in Mbp) on mouse chromosome, and respective Bayesian credible intervals. Specific marker identification from the GigaMUGA listed for each peak.

Phenotype	LOD	Chr	QTL Position (Mbp)	Marker ID
GSH	6.452	13	87.364942 (83.908994 - 89.354169)	UNCJPD005456
Total Glutathione	6.781	13	87.316743 (83.983279 - 89.354169)	UNCHS036670
GSH/GSSG	6.091	6	112.422549 (104.813291 - 112.481351)	JAX00145465
GSH/GSSG	7.284	6	112.491205 (112.481351 - 112.496201)	UNCHS018579
GSH/GSSG	6.299	6	112.523643 (112.498928 - 112.967579)	UNCHS018581
GSH/GSSG	6.674	11	90.585428 (90.188681 - 93.674856)	UNCHS031836
GSH/GSSG	6.153	19	58.73912 (48.103472 - 59.07224)	UNCHS048099
E_h	7.154	11	90.585428 (90.218619 - 91.74591)	UNCHS031836
E_h	6.321	19	58.743035 (58.653947 - 59.053912)	UNCHS048100

Table 4.2. Cortical GSH candidate genes and their relevant annotations (Chr13: 83.909 − 89.354 ± 1 Mbp; GRCm38/mm10).[a]

[a] Resource abbreviations: **EEA**, EBI Expression Atlas; **PW**, PheWeb; **GO**, Gene Ontology; **GXD**, Gene eXpression Database; **MGI**, Mouse Genome Informatics; **MP**, Mammalian Phenotype.

				Expression		Functional	Phenotypic	
MGI Gene Symbol	**Genome Coordinates (strand)**	**MGI Gene/Marker ID**	**Feature Type**	**EEA (EMBL-EBI)**	**GXD (MGI)**	**GO (MGI)**	**MP**	**PW**
2310067P03Rik	Chr13:83065457-83194347 (+)	MGI:1917536	lncRNA gene	**X**	**X**	**X**		
Gm33073	Chr13:83071742-83120537 (-)	MGI:5592232	lncRNA gene					
Gm48156	Chr13:83189565-83189709 (-)	MGI:6097525	Pseudogene	**X**	**X**			
Gm33217	Chr13:83314533-833564 (-)	MGI:5592376	lncRNA gene					
Gm33274	Chr13:83427681-83446408 (-)	MGI:5592433	lncRNA gene					
Gm33317	Chr13:83498349-83503901 (-)	MGI:5592476	lncRNA gene					
Mef2c	Chr13:83504017-8366708 (+)	MGI:99458	protein coding gene	**X**	**X**			
Gm52043	Chr13:83592977-83625269 (-)	MGI:6366025	lncRNA gene					
Gm10759	Chr13:83601246-83602668 (+)		unclassified gene					
Gm52044	Chr13:83636274-83662307 (-)	MGI:6366027	lncRNA gene					
Gm48067	Chr13:83687222-83687441 (+)	MGI:6097396	Pseudogene	**X**	**X**			
Gm52046	Chr13:83714932-83721655 (-)	MGI:6366031	lncRNA gene					
C130071C03Rik	Chr13:83721381-83884194 (+)	MGI:2443574	lncRNA gene	**X**	**X**			

Gm26803	Chr13:83723442-83729582 (-)	MGI:5477297	lncRNA gene	**X**	**X**			
Gm33366	Chr13:83734709-83738535 (-)	MGI:5592525	unclassified non-coding RNA gene	**X**	**X**			
Mir9-2	Chr13:83738814-83738885 (+)	MGI:3619442	miRNA gene		**X**			
Gm51268	Chr13:83738821-83738876 (-)	MGI:6364935	miRNA gene					
Gm6411	Chr13:83761132-83762335 (-)	MGI:3643659	Pseudogene	**X**	**X**			
Gm5452	Chr13:83832241-83833845 (+)	MGI:3645281	Pseudogene	**X**	**X**			
Gm52045	Chr13:83872776-83883184 (-)	MGI:6366029	lncRNA gene					
2810049E08Rik	Chr13:83891208-8392871 (+)	MGI:1919927	lncRNA gene	**X**	**X**			
Gm4241	Chr13:83971355-83987991 (-)	MGI:3782418	lncRNA gene	**X**	**X**			
Gm8447	Chr13:83987991-83998485 (-)	MGI:3647954	Pseudogene	**X**	**X**			
Gm17750	Chr13:84025297-84064774 (-)	MGI:5009828	lncRNA gene	**X**	**X**			
Gm8456	Chr13:84166453-84166911 (+)	MGI:3647453	Pseudogene	**X**	**X**			
Gm24331	Chr13:84182278-84182344 (+)	MGI:5454108	miRNA gene					
A230107N01Rik	Chr13:84219581-84219581 (-)	MGI:2445042	lncRNA gene	**X**	**X**			
Tmem161b	Chr13:84222195-84296141 (+)	MGI:1919995	protein coding gene	**X**	**X**	**X**	**X**	**X**
Gm49223	Chr13:84274844-84280817 (+)	MGI:6118679	lncRNA gene	**X**	**X**			
Gm46432	Chr13:84281176-84281876 (-)	MGI:5826069	Pseudogene	**X**	**X**			

Gm26927	Chr13:84339149-84340113 (-)	MGI:5504042	Pseudogene	**X**	**X**	
Gm41011	Chr13:84343893-84357771 (+)	MGI:5623896	lncRNA gene			
Gm17618	Chr13:84404839-84405472 (+)		protein coding gene			
Gm34196	Chr13:84573766-84906191 (-)	MGI:5593355	lncRNA gene			
Gm34246	Chr13:84675411-84699672 (+)	MGI:5593405	lncRNA gene			
Gm26913	Chr13:8469021-84690941 (-)	MGI:5504028	Pseudogene	**X**	**X**	
Gm4059	Chr13:84973709-84974317 (-)	MGI:3782234	Pseudogene	**X**	**X**	
Gm4066	Chr13:85024162-85025436 (-)	MGI:3782241	Pseudogene	**X**	**X**	
Gm47745	Chr13:85094335-85095373 (+)	MGI:6096889	Pseudogene	**X**	**X**	
Gm4076	Chr13:8512655-85127514 (-)	MGI:3782251	Pseudogene	**X**	**X**	
Gm47746	Chr13:8514072-85141102 (+)	MGI:6096890	Pseudogene		**X**	
Ccnh	Chr13:85189377-85223469 (+)	MGI:1913921	protein coding gene	**X**	**X**	**X**
Rasa1	Chr13:85214699-85289486 (-)	MGI:97860	protein coding gene	**X**	**X**	
Gm37641	Chr13:85411681-85411919 (-)	MGI:5610869	unclassified gene		**X**	
Gm47635	Chr13:85516402-85516619 (+)	MGI:6096708	Pseudogene	**X**	**X**	
Gm5666	Chr13:85572776-85573677 (-)	MGI:3648664	Pseudogene	**X**	**X**	
Gm47636	Chr13:85865112-85865333 (-)	MGI:6096709	Pseudogene	**X**	**X**	
Gm46396	Chr13:85891742-85892128 (+)	MGI:5826033	Pseudogene	**X**	**X**	

Gm34526	Chr13:86017038-86037981 (-)	MGI:5593685	lncRNA gene			
Cox7c	Chr13:86044798-86046904 (-)	MGI:103226	protein coding gene	**X**	**X**	**X**
Gm22574	Chr13:86044989-86045048 (-)	MGI:5452351	snoRNA gene	**X**	**X**	
Gm27025	Chr13:86235827-86237727 (+)	MGI:5504140	Pseudogene		**X**	
Gm25700	Chr13:86725823-86725932 (-)	MGI:5455477	miRNA gene			
Gm51420	Chr13:86748548-86748616 (-)	MGI:6365007	Pseudogene			
Gm47642	Chr13:87234439-87234594 (-)	MGI:6096719	Pseudogene	**X**	**X**	
Gm18265	Chr13:87307726-87308524 (+)	MGI:5010450	Pseudogene	**X**	**X**	
Gm24935	Chr13:87456778-87456887 (+)	MGI:5454712	miRNA gene			
Gm21232	Chr13:87782971-87783976 (+)	MGI:5434587	Pseudogene	**X**	**X**	
Gm41012	Chr13:87793851-87799957 (-)	MGI:5623897	lncRNA gene			
Gm19239	Chr13:87826532-87827257 (+)	MGI:5011424	Pseudogene	**X**	**X**	
Gm47649	Chr13:87977497-87980299 (-)	MGI:6096731	unclassified gene	**X**	**X**	
Gm27044	Chr13:88184661-88185456 (-)	MGI:5504159	Pseudogene	**X**	**X**	
Gm47651	Chr13:88382346-88382622 (+)	MGI:6096734	Pseudogene		**X**	
Gm8526	Chr13:8847858-88479054 (+)	MGI:3645225	Pseudogene	**X**	**X**	
Gm47653	Chr13:88480632-88480791 (+)	MGI:6096737	Pseudogene	**X**	**X**	
Gm19139	Chr13:8850928-88511428 (-)	MGI:5011324	Pseudogene	**X**	**X**	

Gm34585	Chr13:8852119-88578175 (+)	MGI:5593744	lncRNA gene	**X**	**X**			
Gm5667	Chr13:88547216-8854827 (+)	MGI:3648667	Pseudogene	**X**	**X**			
Edil3	Chr13:88821472-89323225 (+)	MGI:1329025	protein coding gene	**X**	**X**			
Gm38504	Chr13:88824224-8883612 (+)	MGI:5621389	lncRNA gene					
Gm18317	Chr13:88843574-88844576 (+)	MGI:5010502	Pseudogene					
Gm46433	Chr13:88870746-88887998 (+)	MGI:5826070	lncRNA gene					
Gm34699	Chr13:8949922-89539669 (-)	MGI:5593858	lncRNA gene					
Hapln1	Chr13:89539796-89611832 (+)	MGI:1337006	protein coding gene	**X**	**X**	**X**		
Gm8546	Chr13:89576959-89578463 (-)	MGI:3647346	Pseudogene	**X**	**X**			
Vcan	Chr13:89655309-89743027 (-)	MGI:102889	protein coding gene	**X**	**X**			
Gm16318	Chr13:89662669-89663573 (+)	MGI:3826563	Pseudogene	**X**	**X**			
Gm4117	Chr13:89733697-89887166 (+)	MGI:3782293	lncRNA gene	**X**	**X**			
Xrcc4	Chr13:89774027-90089608 (-)	MGI:1333799	protein coding gene	**X**	**X**	**X**	**X**	**X**
A430063P04Rik	Chr13:89902607-89905712 (-)		lncRNA gene					
Gm24498	Chr13:89927442-89927543 (-)	MGI:5454275	snRNA gene					

Table 4.3. Cortical total glutathione candidate genes and their relevant annotations (Chr13: 83.983 − 89.354 ± 1 Mbp; GRCm38/mm10).[a]

[a] Resource abbreviations: **EEA**, EBI Expression Atlas; **PW** PheWeb; **GO**, Gene Ontology; **GXD**, Gene eXpression Database; **MGI**, Mouse Genome Informatics; **MP**, Mammalian Phenotype.

				Expression		Functional	Phenotypic	
MGI Gene Symbol	**Genome Coordinates (strand)**	**MGI Gene/Marker ID**	**Feature Type**	**EEA (EMBL-EBI)**	**GXD (MGI)**	**GO (MGI)**	**MP**	**PW**
2310067P03Rik	Chr13:83065457-83194347 (+)	MGI:1917536	lncRNA gene	**X**	**X**	**X**		
Gm33073	Chr13:83071742-83120537 (-)	MGI:5592232	lncRNA gene					
Gm48156	Chr13:83189565-83189709 (-)	MGI:6097525	Pseudogene	**X**	**X**			
Gm33217	Chr13:83314533-833564 (-)	MGI:5592376	lncRNA gene					
Gm33274	Chr13:83427681-83446408 (-)	MGI:5592433	lncRNA gene					
Gm33317	Chr13:83498349-83503901 (-)	MGI:5592476	lncRNA gene					
Mef2c	Chr13:83504017-8366708 (+)	MGI:99458	protein coding gene	**X**	**X**			
Gm52043	Chr13:83592977-83625269 (-)	MGI:6366025	lncRNA gene					
Gm10759	Chr13:83601246-83602668 (+)		unclassified gene					
Gm52044	Chr13:83636274-83662307 (-)	MGI:6366027	lncRNA gene					
Gm48067	Chr13:83687222-83687441 (+)	MGI:6097396	Pseudogene	**X**	**X**			
Gm52046	Chr13:83714932-83721655 (-)	MGI:6366031	lncRNA gene					
C130071C03Rik	Chr13:83721381-83884194 (+)	MGI:2443574	lncRNA gene	**X**	**X**			

Gm26803	Chr13:83723442-83729582 (-)	MGI:5477297	lncRNA gene	**X**	**X**			
Gm33366	Chr13:83734709-83738535 (-)	MGI:5592525	unclassified non-coding RNA gene	**X**	**X**			
Mir9-2	Chr13:83738814-83738885 (+)	MGI:3619442	miRNA gene		**X**			
Gm51268	Chr13:83738821-83738876 (-)	MGI:6364935	miRNA gene					
Gm6411	Chr13:83761132-83762335 (-)	MGI:3643659	Pseudogene	**X**	**X**			
Gm5452	Chr13:83832241-83833845 (+)	MGI:3645281	Pseudogene	**X**	**X**			
Gm52045	Chr13:83872776-83883184 (-)	MGI:6366029	lncRNA gene					
2810049E08Rik	Chr13:83891208-8392871 (+)	MGI:1919927	lncRNA gene	**X**	**X**			
Gm4241	Chr13:83971355-83987991 (-)	MGI:3782418	lncRNA gene	**X**	**X**			
Gm8447	Chr13:83987991-83998485 (-)	MGI:3647954	Pseudogene	**X**	**X**			
Gm17750	Chr13:84025297-84064774 (-)	MGI:5009828	lncRNA gene	**X**	**X**			
Gm8456	Chr13:84166453-84166911 (+)	MGI:3647453	Pseudogene	**X**	**X**			
Gm24331	Chr13:84182278-84182344 (+)	MGI:5454108	miRNA gene					
A230107N01Rik	Chr13:84219581-84219581 (-)	MGI:2445042	lncRNA gene	**X**	**X**			
Tmem161b	Chr13:84222195-84296141 (+)	MGI:1919995	protein coding gene	**X**	**X**	**X**	**X**	**X**
Gm49223	Chr13:84274844-84280817 (+)	MGI:6118679	lncRNA gene	**X**	**X**			
Gm46432	Chr13:84281176-84281876 (-)	MGI:5826069	Pseudogene	**X**	**X**			

Gm26927	Chr13:84339149-84340113 (-)	MGI:5504042	Pseudogene	**X**	**X**	
Gm41011	Chr13:84343893-84357771 (+)	MGI:5623896	lncRNA gene			
Gm17618	Chr13:84404839-84405472 (+)		protein coding gene			
Gm34196	Chr13:84573766-84906191 (-)	MGI:5593355	lncRNA gene			
Gm34246	Chr13:84675411-84699672 (+)	MGI:5593405	lncRNA gene			
Gm26913	Chr13:8469021-84690941 (-)	MGI:5504028	Pseudogene	**X**	**X**	
Gm4059	Chr13:84973709-84974317 (-)	MGI:3782234	Pseudogene	**X**	**X**	
Gm4066	Chr13:85024162-85025436 (-)	MGI:3782241	Pseudogene	**X**	**X**	
Gm47745	Chr13:85094335-85095373 (+)	MGI:6096889	Pseudogene	**X**	**X**	
Gm4076	Chr13:8512655-85127514 (-)	MGI:3782251	Pseudogene	**X**	**X**	
Gm47746	Chr13:8514072-85141102 (+)	MGI:6096890	Pseudogene		**X**	
Ccnh	Chr13:85189377-85223469 (+)	MGI:1913921	protein coding gene	**X**	**X**	**X**
Rasa1	Chr13:85214699-85289486 (-)	MGI:97860	protein coding gene	**X**	**X**	
Gm37641	Chr13:85411681-85411919 (-)	MGI:5610869	unclassified gene		**X**	
Gm47635	Chr13:85516402-85516619 (+)	MGI:6096708	pseudogene	**X**	**X**	
Gm5666	Chr13:85572776-85573677 (-)	MGI:3648664	pseudogene	**X**	**X**	
Gm47636	Chr13:85865112-85865333 (-)	MGI:6096709	pseudogene	**X**	**X**	
Gm46396	Chr13:85891742-85892128 (+)	MGI:5826033	pseudogene	**X**	**X**	

Gm34526	Chr13:86017038-86037981 (-)	MGI:5593685	lncRNA gene			
Cox7c	Chr13:86044798-86046904 (-)	MGI:103226	protein coding gene	**X**	**X**	**X**
Gm22574	Chr13:86044989-86045048 (-)	MGI:5452351	snoRNA gene	**X**	**X**	
Gm27025	Chr13:86235827-86237727 (+)	MGI:5504140	pseudogene		**X**	
Gm25700	Chr13:86725823-86725932 (-)	MGI:5455477	miRNA gene			
Gm51420	Chr13:86748548-86748616 (-)	MGI:6365007	pseudogene			
Gm47642	Chr13:87234439-87234594 (-)	MGI:6096719	pseudogene	**X**	**X**	
Gm18265	Chr13:87307726-87308524 (+)	MGI:5010450	pseudogene	**X**	**X**	
Gm24935	Chr13:87456778-87456887 (+)	MGI:5454712	miRNA gene			
Gm21232	Chr13:87782971-87783976 (+)	MGI:5434587	pseudogene	**X**	**X**	
Gm41012	Chr13:87793851-87799957 (-)	MGI:5623897	lncRNA gene			
Gm19239	Chr13:87826532-87827257 (+)	MGI:5011424	pseudogene	**X**	**X**	
Gm47649	Chr13:87977497-87980299 (-)	MGI:6096731	unclassified gene	**X**	**X**	
Gm27044	Chr13:88184661-88185456 (-)	MGI:5504159	pseudogene	**X**	**X**	
Gm47651	Chr13:88382346-88382622 (+)	MGI:6096734	pseudogene		**X**	
Gm8526	Chr13:8847858-88479054 (+)	MGI:3645225	pseudogene	**X**	**X**	
Gm47653	Chr13:88480632-88480791 (+)	MGI:6096737	pseudogene	**X**	**X**	
Gm19139	Chr13:8850928-88511428 (-)	MGI:5011324	pseudogene	**X**	**X**	

Gm34585	Chr13:8852119-88578175 (+)	MGI:5593744	lncRNA gene	**X**	**X**			
Gm5667	Chr13:88547216-8854827 (+)	MGI:3648667	pseudogene	**X**	**X**			
Edil3	Chr13:88821472-89323225 (+)	MGI:1329025	protein coding gene	**X**	**X**			
Gm38504	Chr13:88824224-8883612 (+)	MGI:5621389	lncRNA gene					
Gm18317	Chr13:88843574-88844576 (+)	MGI:5010502	pseudogene					
Gm46433	Chr13:88870746-88887998 (+)	MGI:5826070	lncRNA gene					
Gm34699	Chr13:8949922-89539669 (-)	MGI:5593858	lncRNA gene					
Hapln1	Chr13:89539796-89611832 (+)	MGI:1337006	protein coding gene	**X**	**X**	**X**		
Gm8546	Chr13:89576959-89578463 (-)	MGI:3647346	pseudogene	**X**	**X**			
Vcan	Chr13:89655309-89743027 (-)	MGI:102889	protein coding gene	**X**	**X**			
Gm16318	Chr13:89662669-89663573 (+)	MGI:3826563	pseudogene	**X**	**X**			
Gm4117	Chr13:89733697-89887166 (+)	MGI:3782293	lncRNA gene	**X**	**X**			
Xrcc4	Chr13:89774027-90089608 (-)	MGI:1333799	protein coding gene	**X**	**X**	**X**	**X**	**X**
A430063P04Rik	Chr13:89902607-89905712 (-)		lncRNA gene					
Gm24498	Chr13:89927442-89927543 (-)	MGI:5454275	snRNA gene					

Table 4.4. Compilation of renal, hepatic, and cortical GSH system QTL intervals.

	Phenotype	LOD	Chr	QTL Position (Mbp)	QTL Position (cM)
Renal	Total Glutathione	6.298	2	52.657 (19.817 – 61.128)	30.193 (14.085 – 35.317)
	Total Glutathione	6.428	11	100.804 (100.059 – 101.369)	63.671 (63.395 – 64.832)
	Total Glutathione	7.105	X	51.602 (49.234 – 51.892)	28.205 (25.870 – 28.316)
	GSH	6.249	2	52.657 (19.817 – 64.003)	30.193 (14.085 – 37.364)
	GSH	6.664	11	100.810 (100.059 – 101.369)	63.682 (63.395 – 64.832)
	GSH	6.962	X	51.602 (49.234 – 51.892)	28.205 (25.870 – 28.316)
	GSSG	6.044	1	144.970 (143.603 – 148.590)	63.069 (62.513 – 63.371)
	GSSG	6.048	16	62.938 (61.291 – 72.202)	36.457 (36.121 – 40.793)
	GSH/GSSG	6.032	13	71.522 (71.458 – 72.209)	38.009 (37.975 – 38.731)
	E_h	6.258	14	22.959 (22.359 – 23.926)	12.791 (12.204 – 14.152)
	BUN	6.06	6	127.602 (125.386 – 128.618)	62.438 (59.395 – 63.065)
	Total Glutathione	6.748	14	22.506 (22.058 – 22.528)	12.355 (12.035 – 12.377)

Hepatic	Total Glutathione	6.011	18	51.537 (35.120 – 76.532)	28.097 (18.887 – 51.726)
	GSH	6.755	14	22.506 (22.058 – 22.528)	12.355 (12.035 – 12.377)
	GSSG	6.283	1	21.043 (18.793 – 22.050)	6.502 (5.847 – 8.186)
	GSSG	6.178	2	91.523 (78.897 – 91.656)	50.598 (47.166 – 50.641)
	GSSG	6.149	18	53.075 (50.199 – 82.487)	28.328 (27.234 – 55.913)
	GSH/GSSG	6.407	11	6.017 (5.568 – 7.583)	3.906 (3.664 – 4.782)
	GSH/GSSG	8.224	16	8.998 (8.865 – 10.077)	4.779 (4.433 – 5.470)
	E_h	6.48	16	6.997 (3.526 – 8.225)	3.373 (2.074 – 3.621)
	E_h	8.598	16	8.998 (8.865 – 10.324)	4.779 (4.433 – 5.579)
	NADPH	6.352	2	173.408 (173.133 – 174.508)	96.424 (95.769 – 97.976)
	NADPH	6.612	12	28.626 (28.578 – 29.450)	10.987 (10.975 – 11.927)
	NADPH	6.287	17	51.366 (50.164 – 52.542)	26.684 (25.861 – 27.425)
	$NADP^+$	7.032	3	110.517 (109.677 – 115.729)	48.547 (48.380 – 50.024)

	$NADP^+$	6.59	8	61.237 (60.722 – 65.378)	30.937 (30.901 – 32.757)
	$NADP^+$/NADPH	7.637	12	28.626 (28.562 – 29.394)	10.987 (10.972 – 11.864)
	NADH	6.062	14	100.731 (99.320 – 102.809)	50.508 (49.350 – 52.844)
Cortical	GSH	6.45	13	87.365 (83.909 – 89.354)	45.155 (44.142 – 45.434)
	Total Glutathione	6.78	13	87.317 (83.983 – 89.354)	45.15 (44.171 – 45.434)
	GSH/GSSG	6.09	6	112.423 (104.813 – 112.481)	52.26 (48.728 – 52.284)
	GSH/GSSG	7.28	6	112.491 (112.481 – 112.496)	52.288 (52.284 – 52.29)
	GSH/GSSG	6.30	6	112.524 (112.499 – 112.978)	52.302 (52.292 – 52.719)
	GSH/GSSG	6.67	11	90.585 (90.189 – 93.675)	55.199 (54.873 – 58.815)
	GSH/GSSG	6.15	19	58.739 (48.103 – 59.072)	54.494 (41.116 – 54.587)
	E_h	7.51	11	90.585 (48.103 – 59.054)	55.199 (54.893 – 56.567)
	E_h	6.32	19	58.74 (58.654 – 59.054)	54.495 (54.448 – 54.582)

Figure 4.3. High-resolution association mapping for cortical total glutathione concentrations reveals a suggestive peak on chromosome 13. A) Genome-wide scan of cortical total glutathione concentrations (nmol/mg protein) exhibits a QTL with a peak LOD score 6.781 at 87.317 Mbp (45.15 cM) on mouse chromosome 13. Permutation-derived significance thresholds are indicated by colored lines at significance (α) levels 0.05 (blue), 0.1 (red), and 0.2 (purple). **B)** The founder allele QTL effects indicate that the PWK, 129, NOD, and WSB alleles contribute to a higher cortical total glutathione concentration (nmol/mg protein), while the NZO and B6 alleles contribute to a lower cortical total glutathione concentration (nmol/mg protein). Each colored line represents one of eight DO founder alleles as indicated in the legend. The differences between strains are considered significant when the LOD score (bottom plot) crosses significance thresholds established in panel A. **C)** Candidate genes found within the QTL interval relative to the MGI database. The cortical GSH genome scan resulted in the same suggestive QTL interval on mouse chromosome 13 compared to cortical total glutathione (Figure 4.2)

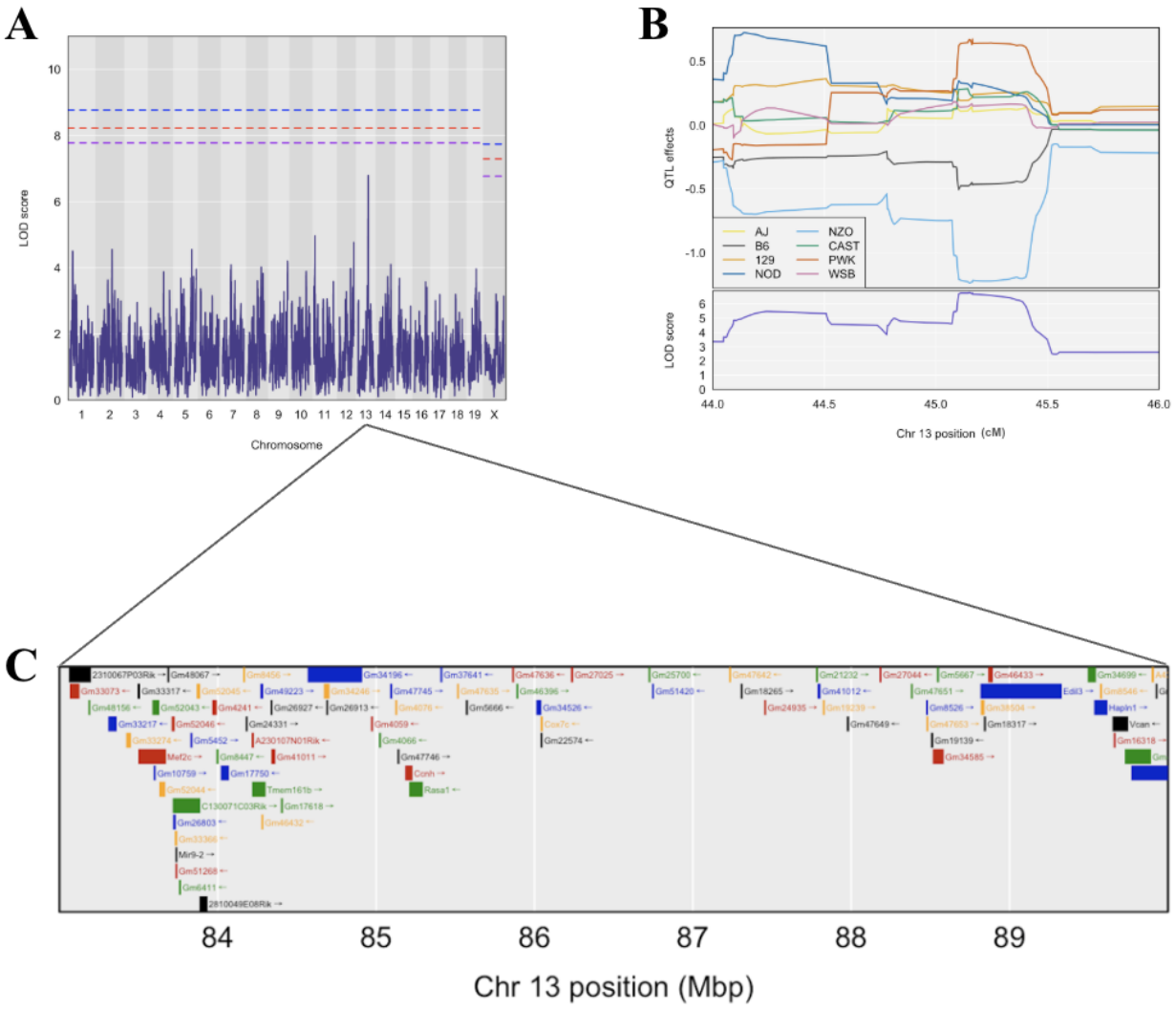

Figure 4.4. High-resolution association mapping for cortical GSH/GSSG reveals a suggestive peak on chromosome 6. A) Genome-wide scan of cortical GSH/GSSG exhibits a QTL with a peak LOD score 7.284 at 112.491 Mbp (52.288 cM) on mouse chromosome 6. Permutation-derived significance thresholds are indicated by colored lines at significance (α) levels 0.05 (blue), 0.1 (red), and 0.2 (purple). **B)** Founder allele QTL effects for this locus. Each colored line represents one of eight DO founder alleles as indicated in the legend. The differences between strains are considered significant when the LOD score (bottom plot) crosses significance thresholds established in panel A. **C)** Candidate genes found within the QTL interval relative to the MGI database.

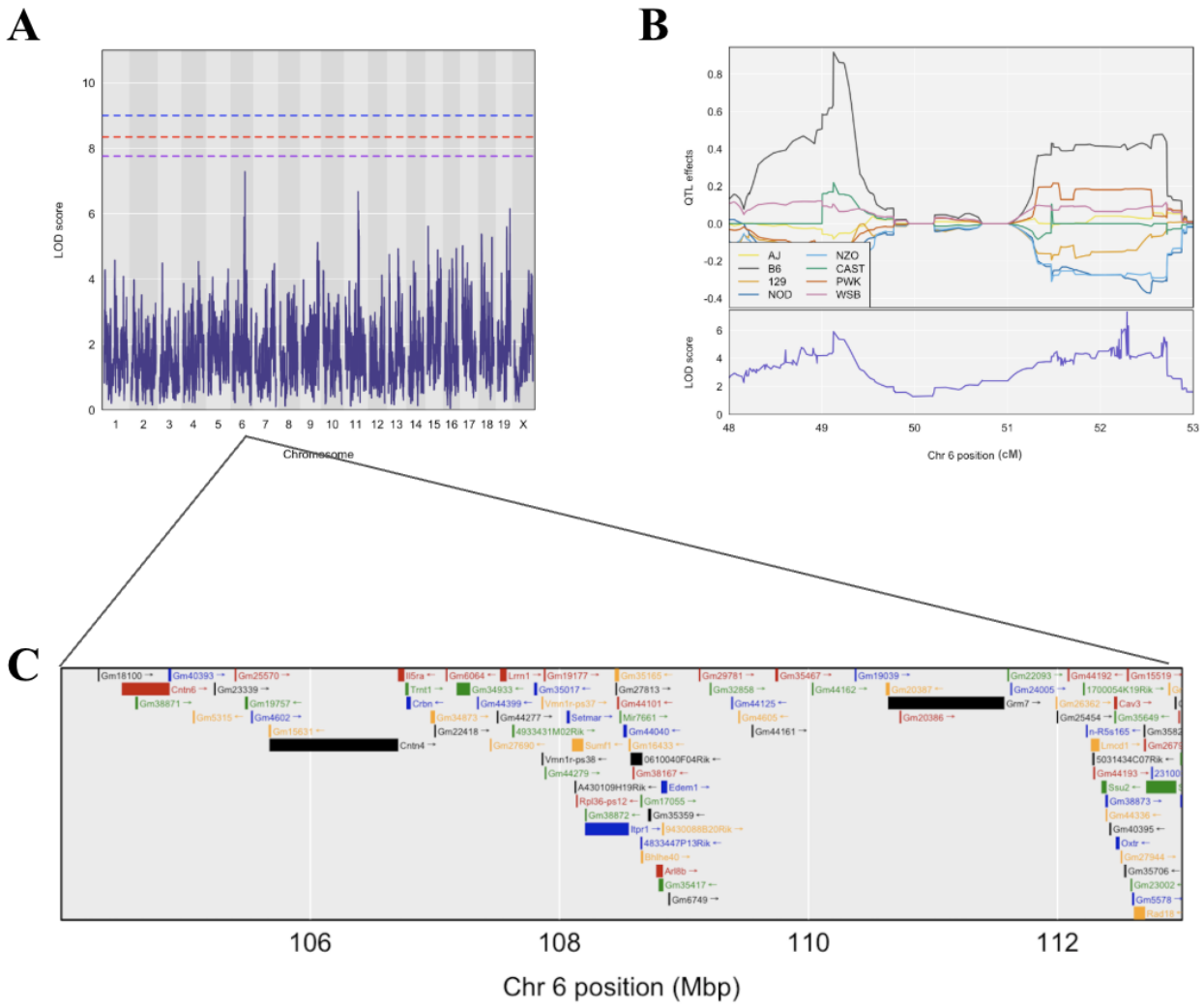

Figure 4.5. High-resolution association mapping for cortical GSH/GSSG reveals a suggestive peak on chromosome 11. A) Genome-wide scan of cortical GSH/GSSG exhibits a QTL with a peak LOD score 6.674 at 90.585 Mbp (55.199 cM) on mouse chromosome 11. Permutation-derived significance thresholds are indicated by colored lines at significance (α) levels 0.05 (blue), 0.1 (red), and 0.2 (purple). **B)** Founder allele QTL effects for this locus. Each colored line represents one of eight DO founder alleles as indicated in the legend. The differences between strains are considered significant when the LOD score (bottom plot) crosses significance thresholds established in panel A. **C)** Candidate genes found within the QTL interval relative to the MGI database.

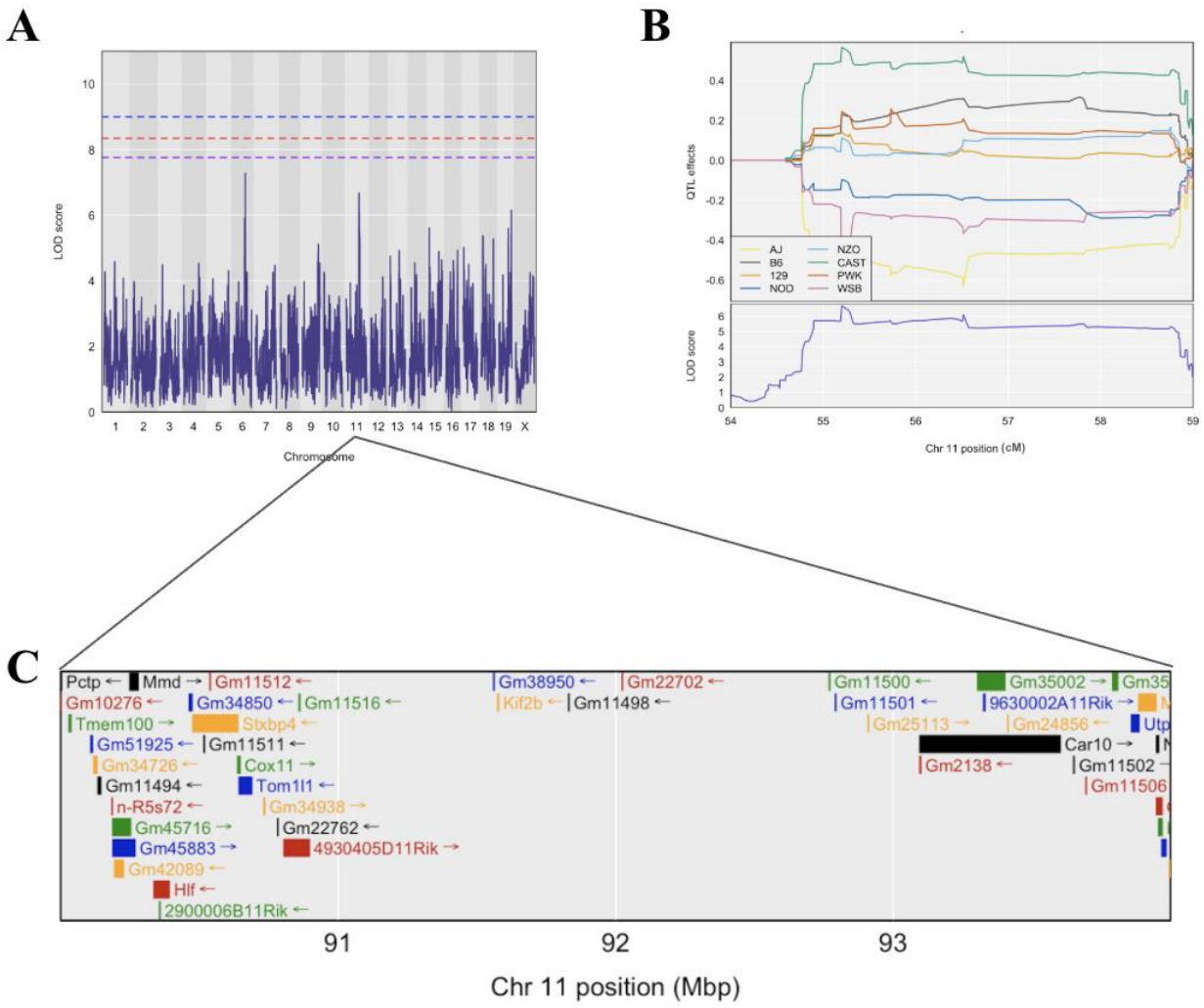

Figure 4.6. High-resolution association mapping for cortical GSH/GSSG reveals a suggestive peak on chromosome 19. A) Genome-wide scan of cortical GSH/GSSG exhibits a QTL with a peak LOD score 6.153 at 58.738 Mbp (54.494 cM) on mouse chromosome 19. Permutation-derived significance thresholds are indicated by colored lines at significance (α) levels 0.05 (blue), 0.1 (red), and 0.2 (purple). **B)** Founder allele QTL effects for this locus. Each colored line represents one of eight DO founder alleles as indicated in the legend. The differences between strains are considered significant when the LOD score (bottom plot) crosses significance thresholds established in panel A. **C)** Candidate genes found within the QTL interval relative to the MGI database.

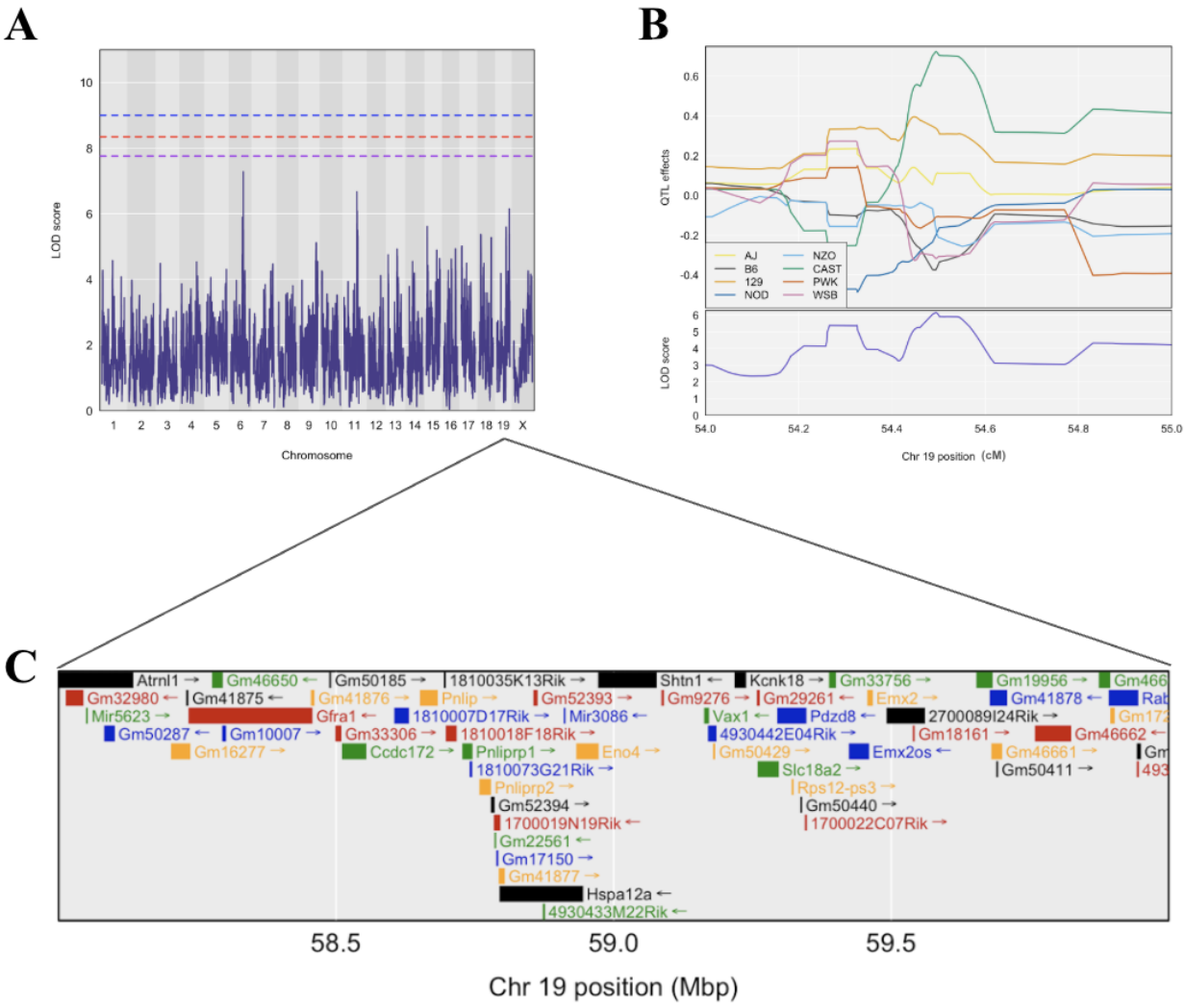

Figure 4.7. High-resolution association mapping for cortical redox potential reveals a suggestive peak on chromosome 11. A) Genome-wide scan of cortical redox potential exhibits a QTL with a peak LOD score 7.514 at 90.585 Mbp (55.199 cM) on mouse chromosome 11. Permutation-derived significance thresholds are indicated by colored lines at significance (α) levels 0.05 (blue), 0.1 (red), and 0.2 (purple). **B)** Founder allele QTL effects for this locus. Each colored line represents one of eight DO founder alleles as indicated in the legend. The differences between strains are considered significant when the LOD score (bottom plot) crosses significance thresholds established in panel A. **C)** Candidate genes found within the QTL interval relative to the MGI database.

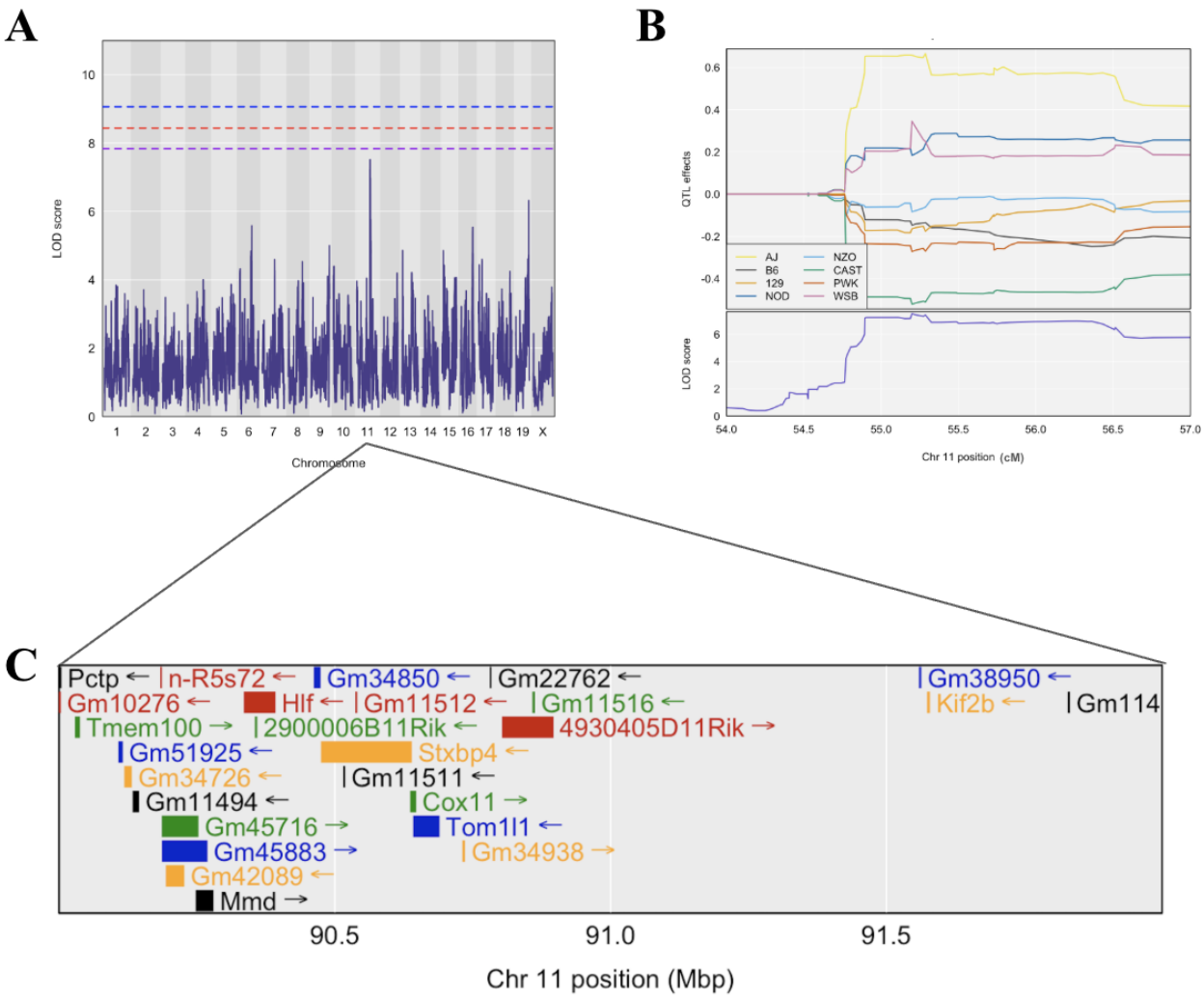

Figure 4.8. High-resolution association mapping for cortical redox potential reveals a suggestive peak on chromosome 19. A) Genome-wide scan of cortical redox potential exhibits a QTL with a peak LOD score 6.321at 58.743 Mbp (54.495 cM) on mouse chromosome 19. Permutation-derived significance thresholds are indicated by colored lines at significance (α) levels 0.05 (blue), 0.1 (red), and 0.2 (purple). **B)** Founder allele QTL effects for this locus. Each colored line represents one of eight DO founder alleles as indicated in the legend. The differences between strains are considered significant when the LOD score (bottom plot) crosses significance thresholds established in panel A. **C)** Candidate genes found within the QTL interval relative to the MGI database.

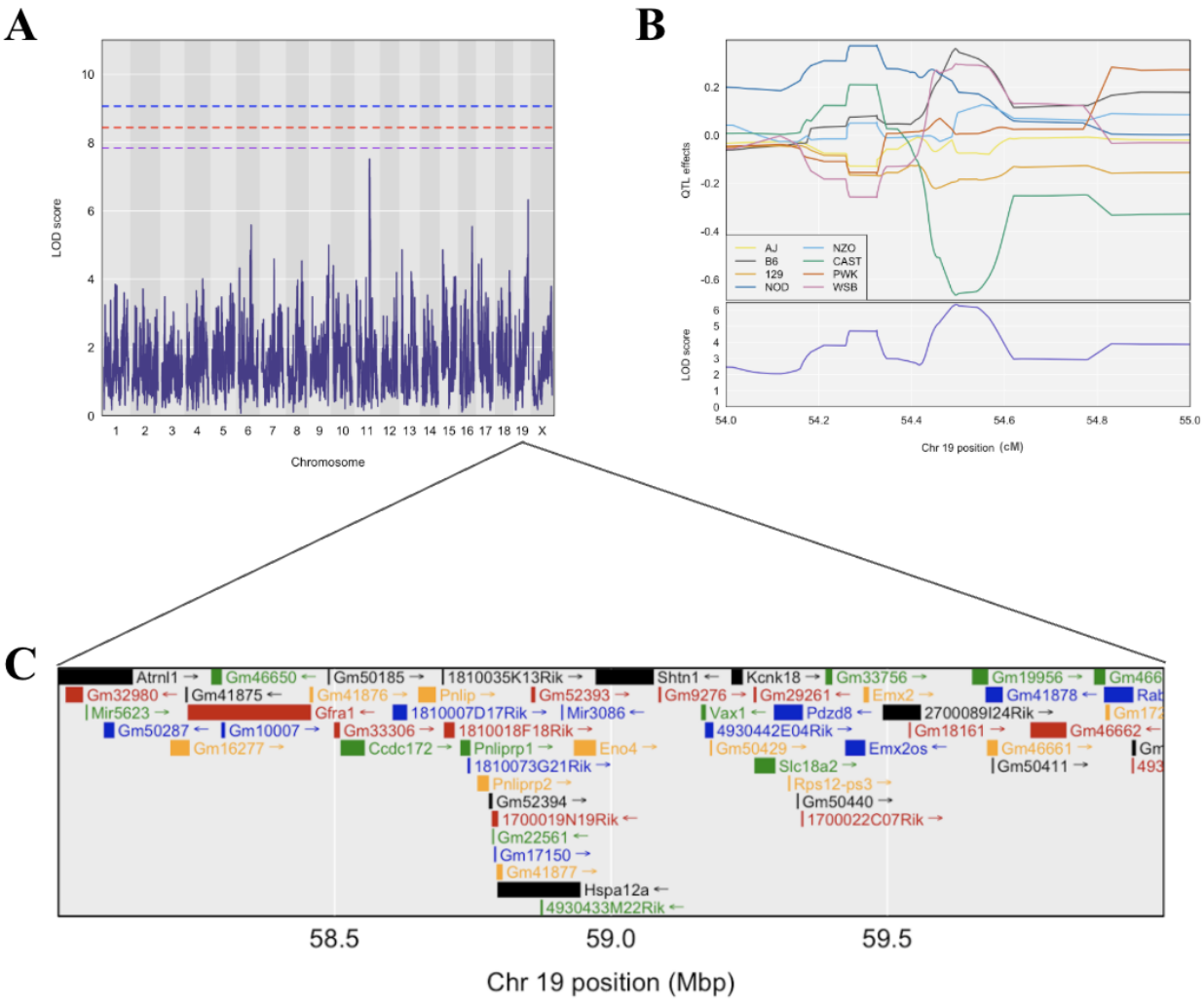

Figure 4.9. Investigating founder allele effects on genes involved in glutathione metabolism using high-resolution mapping for cortical total glutathione.
Each colored line represents one of eight DO founder alleles as indicated in the legend. The differences between strains are considered significant when the LOD score (bottom plot) is large enough to surpass phenotype-specific permutation-derived significance thresholds. The founder allele QTL effects indicate that there are no alleles found in proximity to the **A)** *Gpx1* gene location (Chromosome 9, 59.24 cM), **B)** *Glcl* gene location (Chromosome 9, 43.36 cM), **C)** *Gclm* gene location (Chromosome 3, 52.94 cM), **D)** *Gx* gene location (Chromosome 2, 77.26), and **E)** *Gr* gene location (Chromosome 8, 20.69) that contribute to a significantly lower or higher total glutathione concentration.

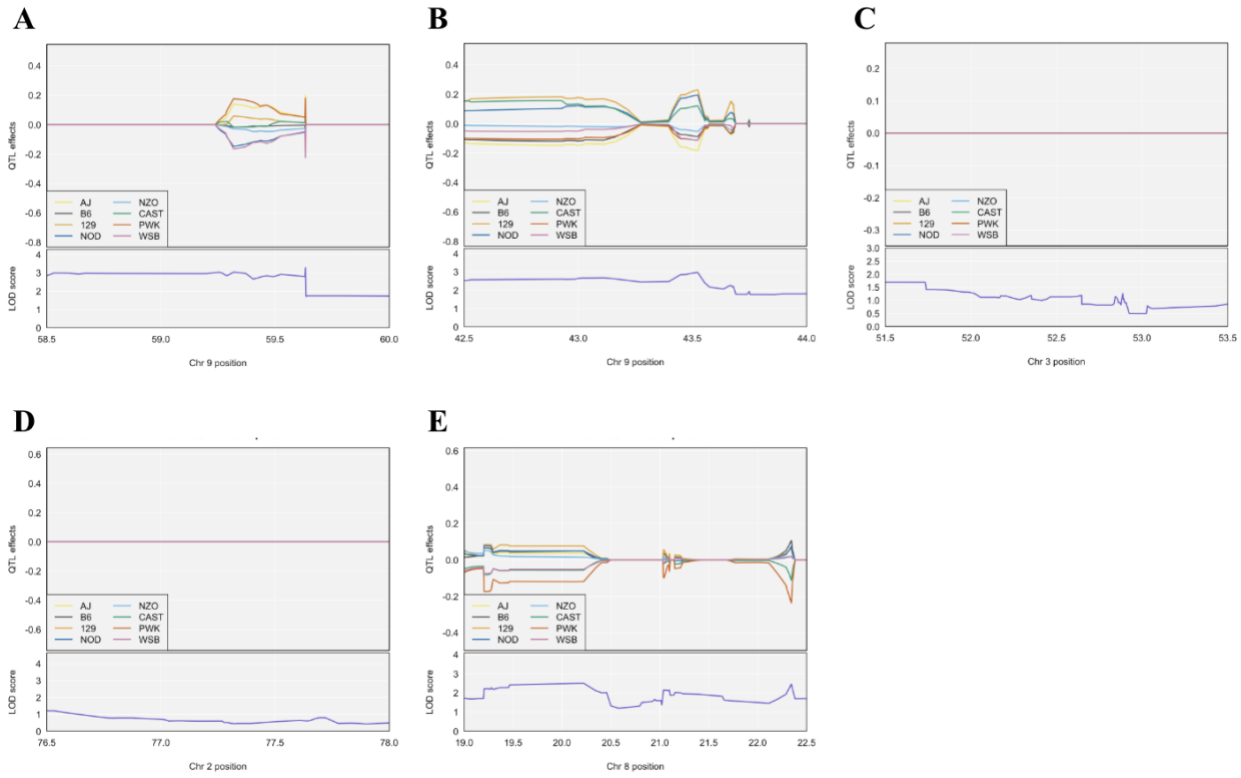

Figure 4.10. Investigating founder allele effects on genes involved in glutathione metabolism using high-resolution mapping for cortical GSH.
Each colored line represents one of eight DO founder alleles as indicated in the legend. The differences between strains are considered significant when the LOD score (bottom plot) is large enough to surpass phenotype-specific permutation-derived significance thresholds. The founder allele QTL effects indicate that there are no alleles found in proximity to the **A)** *Gpx1* gene location (Chromosome 9, 59.24 cM), **B)** *Glcl* gene location (Chromosome 9, 43.36 cM), **C)** *Gclm* gene location (Chromosome 3, 52.94 cM), **D)** *Gx* gene location (Chromosome 2, 77.26), and **E)** *Gr* gene location (Chromosome 8, 20.69) that contribute to a significantly lower or higher total glutathione concentration.

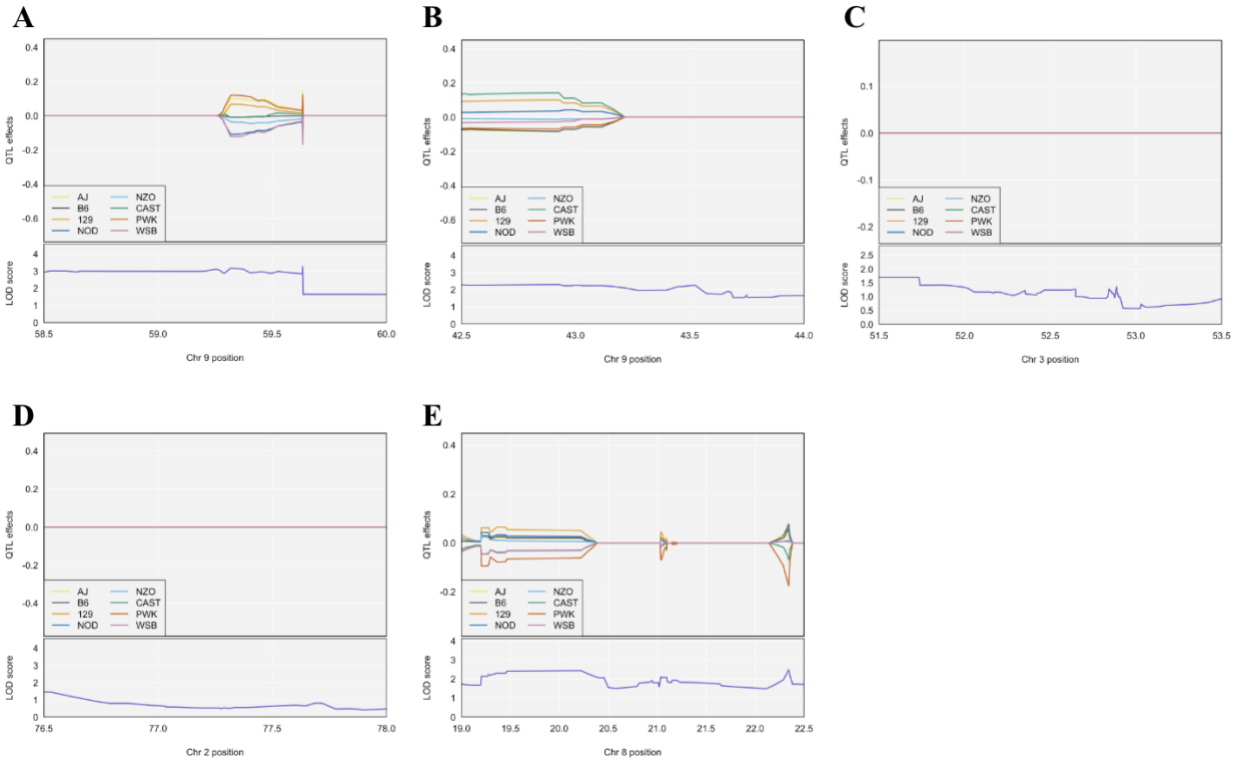

Figure 4.11. Investigating founder allele effects on genes involved in glutathione metabolism using high-resolution mapping for cortical GSSG.
Each colored line represents one of eight DO founder alleles as indicated in the legend. The differences between strains are considered significant when the LOD score (bottom plot) is large enough to surpass phenotype-specific permutation-derived significance thresholds. The founder allele QTL effects indicate that there are no alleles found in proximity to the **A)** *Gpx1* gene location (Chromosome 9, 59.24 cM), **B)** *Glcl* gene location (Chromosome 9, 43.36 cM), **C)** *Gclm* gene location (Chromosome 3, 52.94 cM), **D)** *Gx* gene location (Chromosome 2, 77.26), and **E)** *Gr* gene location (Chromosome 8, 20.69) that contribute to a significantly lower or higher total glutathione concentration.

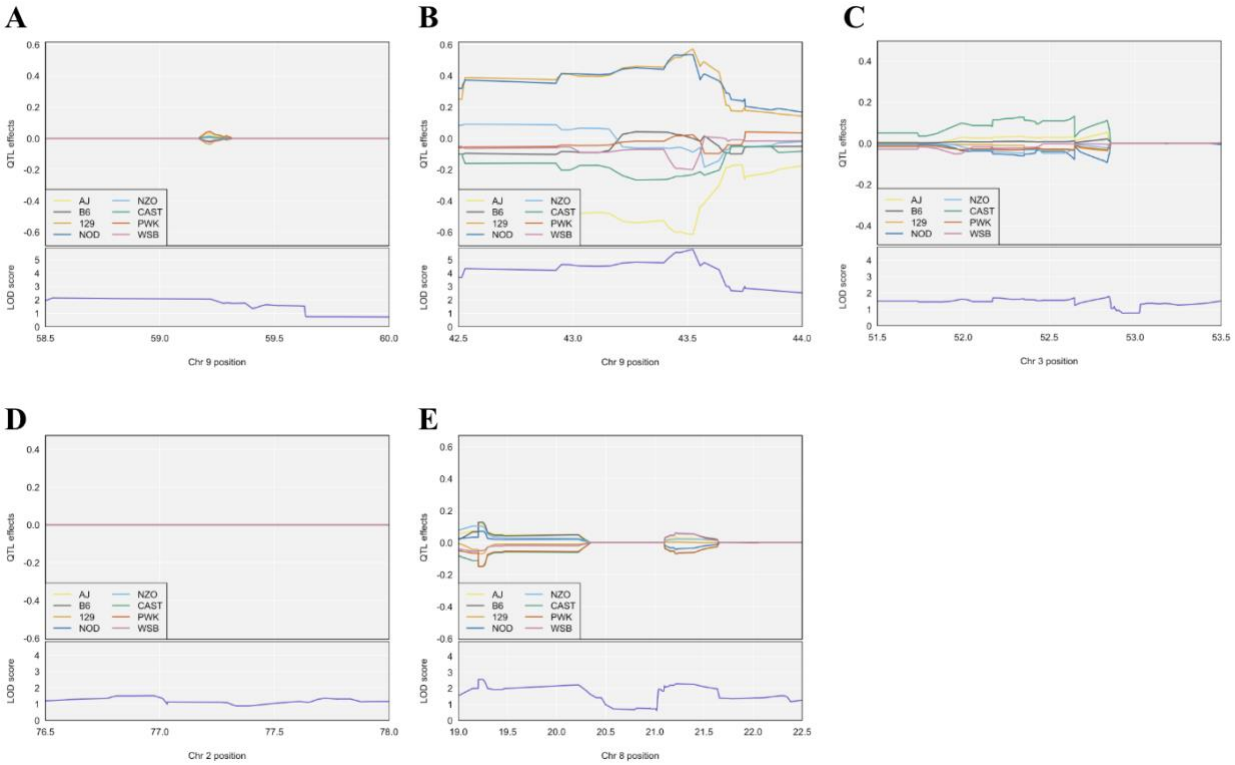

Figure 4.12. Investigating founder allele effects on genes involved in glutathione metabolism using high-resolution mapping for cortical GSH/GSSG.
Each colored line represents one of eight DO founder alleles as indicated in the legend. The differences between strains are considered significant when the LOD score (bottom plot) is large enough to surpass phenotype-specific permutation-derived significance thresholds. The founder allele QTL effects indicate that there are no alleles found in proximity to the **A)** *Gpx1* gene location (Chromosome 9, 59.24 cM), **B)** *Glcl* gene location (Chromosome 9, 43.36 cM), **C)** *Gclm* gene location (Chromosome 3, 52.94 cM), **D)** *Gx* gene location (Chromosome 2, 77.26), and **E)** *Gr* gene location (Chromosome 8, 20.69) that contribute to a significantly lower or higher total glutathione concentration.

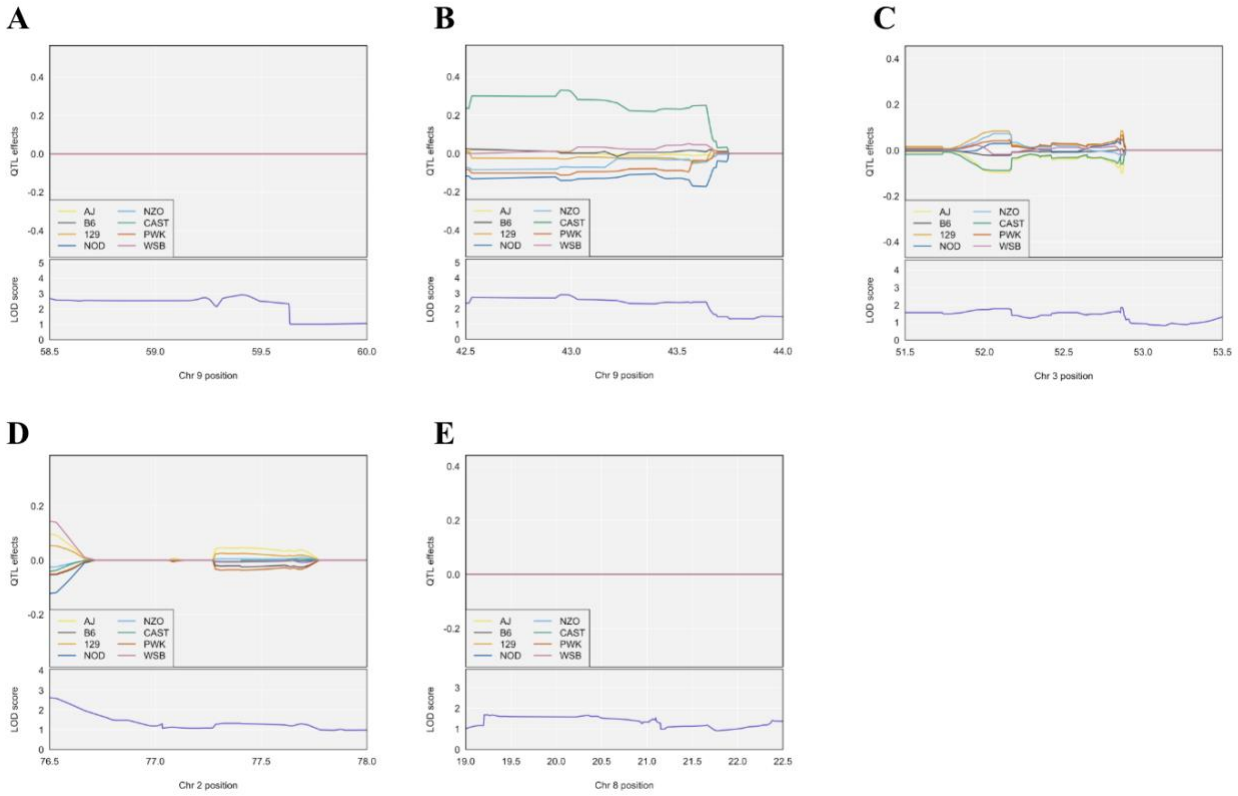

Figure 4.13. Investigating founder allele effects on genes involved in glutathione metabolism using high-resolution mapping for cortical redox potential.
Each colored line represents one of eight DO founder alleles as indicated in the legend. The differences between strains are considered significant when the LOD score (bottom plot) is large enough to surpass phenotype-specific permutation-derived significance thresholds. The founder allele QTL effects indicate that there are no alleles found in proximity to the **A)** *Gpx1* gene location (Chromosome 9, 59.24 cM), **B)** *Glcl* gene location (Chromosome 9, 43.36 cM), **C)** *Gclm* gene location (Chromosome 3, 52.94 cM), **D)** *Gx* gene location (Chromosome 2, 77.26), and **E)** *Gr* gene location (Chromosome 8, 20.69) that contribute to a significantly lower or higher total glutathione concentration.

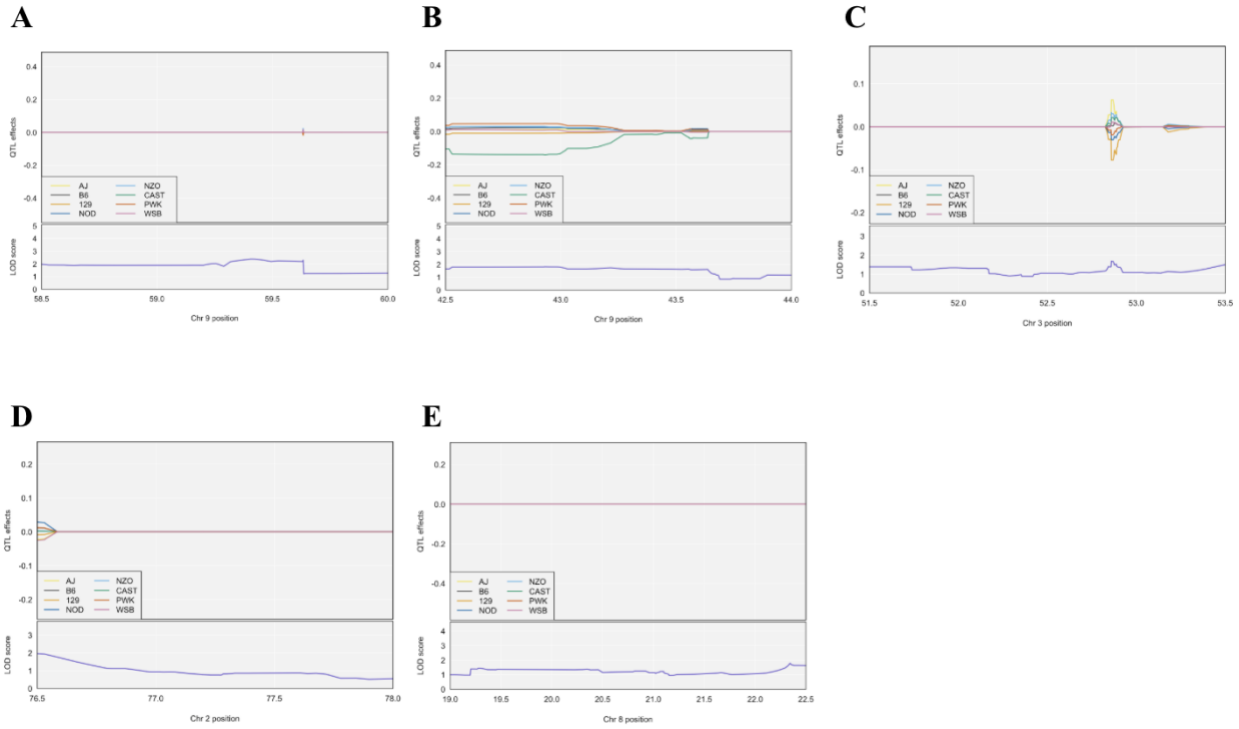

CHAPTER 5

CONCLUSION

Glutathione (GSH), a ubiquitous tripeptide composed of cysteine, glutamate, and glycine, is an essential antioxidant that functions to protect major tissues from oxidative stress and maintain redox homeostasis. GSH is known to be the most abundant non-protein thiol and can be found in its reduced form (GSH) and oxidized form (GSSG). GSH and GSSG form a redox cycle to neutralize free radicals and prevent damage to lipids, carbohydrates, proteins, and nucleic acids. An imbalance in the cell's antioxidant defense system can elevate levels of oxidative stress, which is implicated in numerous chronic diseases. It is evident in inbred mice studies that GSH regulation is dictated by canonical GSH genes, however, recent literature suggests that genes outside of the canonical GSH pathway may have tissue-specific effects on GSH status. Due to limited genetic diversity in inbred mice, findings have limited translatability to the human population, therefore this work utilizes a Diversity Outbred (DO) mouse stock to first, compare levels and regulation of glutathione in the brain and other major tissues, and second, investigate genes in the genome influencing brain glutathione regulation.

Chapter 3 of this thesis explores the statistical relationships between GSH phenotypes of the cortical GSH system, as well as its relationship to other major tissues – specifically the kidneys and liver. Previous work in our laboratory have established correlations between the hepatic and renal GSH systems using a large cohort of DO mice, so this present study builds upon current knowledge within the same DO cohort by assessing the correlation of the cortical GSH system to those of the kidneys and liver. We found significant variation in all cortical GSH

phenotypes, regardless of sex, in addition to numerous significant associations discovered among variables. Between the cortical, hepatic, and renal GSH phenotypes, statistical analysis reveal cortical GSH variables significantly associated with multiple renal GSH variables but not as significant with the hepatic GSH system. The substantial variation found in cortical GSH phenotypes and associations found between cortical, renal, and hepatic GSH status suggest genetic regulatory mechanisms in play, which will support future studies using the DO mouse stock to further understand the genetic background of GSH redox systems.

Chapter 4 of this thesis uncovers potential candidate genes governing the cortical GSH system by using a high-resolution genetic mapping approach. Within a large cohort of DO mice, we identified a novel QTL peak underlying cortical GSH and total glutathione concentrations on murine chromosome 13 at 87.365 Mbp and 87.317 Mbp, respectively. Expression, functional, and phenotypic annotations were utilized to narrow down candidate genes. which revealed *transmembrane protein 161B* (*Tmem161b*) and *X-ray repair complementing defective repair in Chinese hamster cells 4* (*Xrcc4*) to be the most plausible candidate genes controlling cortical GSH regulation based on their relevance to brain function. The discovery of these two genes expands our knowledge of the complex genetic background inherent to the cortical GSH systems and serves as the cornerstone for future studies to further interrogate *Tmem161b* and *Xrcc4* as a genetic regulator of cortical GSH status.

Overall, this work harnesses the DO mouse stock to present findings that are translatable to human health. We provide unique findings pertaining to the cortical GSH system, which include significant variation among its GSH phenotypes, its relationship with GSH systems of the kidneys and liver, and novel candidate genes associated with cortical GSH regulation. Future studies are advised to use the DO mouse model to explore statistical analysis of the GSH redox

system in other tissues, such as adipose tissue, to expand on existing knowledge of GSH variation and relationships with cortical, renal, and hepatic GSH systems. The discoveries found in the entirety of this thesis supports future research efforts to develop therapeutic interventions and treatments for improving human health.

REFERENCES

1. Pizzino, G., et al., *Oxidative Stress: Harms and Benefits for Human Health.* Oxid Med Cell Longev, 2017. **2017**: p. 8416763.
2. Lopez-Alarcon, C. and A. Denicola, *Evaluating the antioxidant capacity of natural products: a review on chemical and cellular-based assays.* Anal Chim Acta, 2013. **763**: p. 1-10.
3. Pisoschi, A.M. and A. Pop, *The role of antioxidants in the chemistry of oxidative stress: A review.* Eur J Med Chem, 2015. **97**: p. 55-74.
4. Sharifi-Rad, M., et al., *Lifestyle, Oxidative Stress, and Antioxidants: Back and Forth in the Pathophysiology of Chronic Diseases.* Front Physiol, 2020. **11**: p. 694.
5. Sies, H., *Oxidative stress: oxidants and antioxidants.* Exp Physiol, 1997. **82**(2): p. 291-5.
6. Poljsak, B., D. Suput, and I. Milisav, *Achieving the balance between ROS and antioxidants: when to use the synthetic antioxidants.* Oxid Med Cell Longev, 2013. **2013**: p. 956792.
7. Fang, Y.Z., S. Yang, and G. Wu, *Free radicals, antioxidants, and nutrition.* Nutrition, 2002. **18**(10): p. 872-9.
8. Lobo, V., et al., *Free radicals, antioxidants and functional foods: Impact on human health.* Pharmacogn Rev, 2010. **4**(8): p. 118-26.
9. Tvrdá, E. and F. Benko, *Chapter 1 - Free radicals: what they are and what they do*, in *Pathology*, V.R. Preedy, Editor. 2020, Academic Press. p. 3-13.
10. Valko, M., et al., *Free radicals and antioxidants in normal physiological functions and human disease.* Int J Biochem Cell Biol, 2007. **39**(1): p. 44-84.
11. Droge, W., *Free radicals in the physiological control of cell function.* Physiol Rev, 2002. **82**(1): p. 47-95.
12. Brand, M.D., *The sites and topology of mitochondrial superoxide production.* Exp Gerontol, 2010. **45**(7-8): p. 466-72.
13. Turrens, J.F., *Mitochondrial formation of reactive oxygen species.* J Physiol, 2003. **552**(Pt 2): p. 335-44.
14. Chen, Q., et al., *Production of reactive oxygen species by mitochondria: central role of complex III.* J Biol Chem, 2003. **278**(38): p. 36027-31.
15. Kushnareva, Y., A.N. Murphy, and A. Andreyev, *Complex I-mediated reactive oxygen species generation: modulation by cytochrome c and NAD(P)+ oxidation–reduction state.* Biochemical Journal, 2002. **368**(2): p. 545-553.
16. Bartz, R.R. and C.A. Piantadosi, *Clinical review: oxygen as a signaling molecule.* Crit Care, 2010. **14**(5): p. 234.
17. Carr, A.C., M.R. McCall, and B. Frei, *Oxidation of LDL by myeloperoxidase and reactive nitrogen species: reaction pathways and antioxidant protection.* Arterioscler Thromb Vasc Biol, 2000. **20**(7): p. 1716-23.
18. Juan, C.A., et al., *The Chemistry of Reactive Oxygen Species (ROS) Revisited: Outlining Their Role in Biological Macromolecules (DNA, Lipids and Proteins) and Induced Pathologies.* Int J Mol Sci, 2021. **22**(9).
19. Abe, C., T. Miyazawa, and T. Miyazawa, *Current Use of Fenton Reaction in Drugs and Food.* Molecules, 2022. **27**(17).

20. Valko, M., et al., *Free radicals, metals and antioxidants in oxidative stress-induced cancer.* Chem Biol Interact, 2006. **160**(1): p. 1-40.
21. Yadav, D.K., et al., *Molecular dynamic simulations of oxidized skin lipid bilayer and permeability of reactive oxygen species.* Sci Rep, 2019. **9**(1): p. 4496.
22. Ayala, A., M.F. Munoz, and S. Arguelles, *Lipid peroxidation: production, metabolism, and signaling mechanisms of malondialdehyde and 4-hydroxy-2-nonenal.* Oxid Med Cell Longev, 2014. **2014**: p. 360438.
23. Yin, H., L. Xu, and N.A. Porter, *Free radical lipid peroxidation: mechanisms and analysis.* Chem Rev, 2011. **111**(10): p. 5944-72.
24. Liu, W., J.D. Morrow, and H. Yin, *Quantification of F2-isoprostanes as a reliable index of oxidative stress in vivo using gas chromatography-mass spectrometry (GC-MS) method.* Free Radic Biol Med, 2009. **47**(8): p. 1101-7.
25. Rodriguez-Garcia, A., et al., *Protein Carbonylation and Lipid Peroxidation in Hematological Malignancies.* Antioxidants (Basel), 2020. **9**(12).
26. Grimm, S., A. Hohn, and T. Grune, *Oxidative protein damage and the proteasome.* Amino Acids, 2012. **42**(1): p. 23-38.
27. Zhou, M., et al., *Activation and modulation of the AGEs-RAGE axis: Implications for inflammatory pathologies and therapeutic interventions – A review.* Pharmacological Research, 2024. **206**: p. 107282.
28. Vistoli, G., et al., *Advanced glycoxidation and lipoxidation end products (AGEs and ALEs): an overview of their mechanisms of formation.* Free Radic Res, 2013. **47 Suppl 1**: p. 3-27.
29. Twarda-Clapa, A., et al., *Advanced Glycation End-Products (AGEs): Formation, Chemistry, Classification, Receptors, and Diseases Related to AGEs.* Cells, 2022. **11**(8).
30. Cervellati, C. and A. Pecorelli, *Chapter 4 - Fluid redox biomarkers in neurological disease*, in *Modulation of Oxidative Stress*, L. Saso, et al., Editors. 2023, Academic Press. p. 43-57.
31. Gonzalez-Hunt, C.P., M. Wadhwa, and L.H. Sanders, *DNA damage by oxidative stress: Measurement strategies for two genomes.* Current Opinion in Toxicology, 2018. **7**: p. 87-94.
32. Cooke, M.S., et al., *Oxidative DNA damage: mechanisms, mutation, and disease.* FASEB J, 2003. **17**(10): p. 1195-214.
33. Poetsch, A.R., *The genomics of oxidative DNA damage, repair, and resulting mutagenesis.* Computational and Structural Biotechnology Journal, 2020. **18**: p. 207-219.
34. Kong, Q. and C.L. Lin, *Oxidative damage to RNA: mechanisms, consequences, and diseases.* Cell Mol Life Sci, 2010. **67**(11): p. 1817-29.
35. Chen, X., et al., *Oxidative RNA Damage in the Pathogenesis and Treatment of Type 2 Diabetes.* Front Physiol, 2022. **13**: p. 725919.
36. Fisher, A.B., *Peroxiredoxin 6 in the repair of peroxidized cell membranes and cell signaling.* Arch Biochem Biophys, 2017. **617**: p. 68-83.
37. van Kuijk, F.J.G.M., et al., *A new role for phospholipase A2: protection of membranes from lipid peroxidation damage.* Trends in Biochemical Sciences, 1987. **12**: p. 31-34.
38. Cadet, J. and K.J.A. Davies, *Oxidative DNA damage & repair: An introduction.* Free Radic Biol Med, 2017. **107**: p. 2-12.
39. Ngo, J.K. and K.J. Davies, *Importance of the lon protease in mitochondrial maintenance and the significance of declining lon in aging.* Ann N Y Acad Sci, 2007. **1119**: p. 78-87.

40. Kramer, L., C. Groh, and J.M. Herrmann, *The proteasome: friend and foe of mitochondrial biogenesis.* FEBS Lett, 2021. **595**(8): p. 1223-1238.
41. Chatterjee, N. and G.C. Walker, *Mechanisms of DNA damage, repair, and mutagenesis.* Environ Mol Mutagen, 2017. **58**(5): p. 235-263.
42. Kusakabe, M., et al., *Mechanism and regulation of DNA damage recognition in nucleotide excision repair.* Genes Environ, 2019. **41**: p. 2.
43. Petruseva, I.O., A.N. Evdokimov, and O.I. Lavrik, *Molecular mechanism of global genome nucleotide excision repair.* Acta Naturae, 2014. **6**(1): p. 23-34.
44. Hoag, A., M. Duan, and P. Mao, *The role of Transcription Factor IIH complex in nucleotide excision repair.* Environ Mol Mutagen, 2024. **65 Suppl 1**(Suppl 1): p. 72-81.
45. Cardoso, M.A., H.M.R. Goncalves, and F. Davis, *Reactive oxygen species in biological media are they friend or foe? Major In vivo and In vitro sensing challenges.* Talanta, 2023. **260**: p. 124648.
46. Liu, T., et al., *NF-κB signaling in inflammation.* Signal Transduction and Targeted Therapy, 2017. **2**(1): p. 17023.
47. Sun, S.C., *Non-canonical NF-kappaB signaling pathway.* Cell Res, 2011. **21**(1): p. 71-85.
48. Ngo, V. and M.L. Duennwald, *Nrf2 and Oxidative Stress: A General Overview of Mechanisms and Implications in Human Disease.* Antioxidants (Basel), 2022. **11**(12).
49. Chaudhary, P., et al., *Oxidative stress, free radicals and antioxidants: potential crosstalk in the pathophysiology of human diseases.* Front Chem, 2023. **11**: p. 1158198.
50. Kurutas, E.B., *The importance of antioxidants which play the role in cellular response against oxidative/nitrosative stress: current state.* Nutr J, 2016. **15**(1): p. 71.
51. Korczowska-Lacka, I., et al., *Disorders of Endogenous and Exogenous Antioxidants in Neurological Diseases.* Antioxidants (Basel), 2023. **12**(10).
52. Health, N.R.C.C.o.D.a., *Fat-Soluble Vitamins*, in *Diet and Health: Implications for Reducing Chronic Disease Risk*. 1989, National Academies Press (US).
53. Shastak, Y., G. Alvaro, and W. and Pelletier, *The relationship between vitamin A status and oxidative stress in animal production.* Journal of Applied Animal Research, 2023. **51**(1): p. 546-553.
54. Li, J., et al., *Novel role of vitamin k in preventing oxidative injury to developing oligodendrocytes and neurons.* J Neurosci, 2003. **23**(13): p. 5816-26.
55. Kawashima, A., et al., *Vitamin C Induces the Reduction of Oxidative Stress and Paradoxically Stimulates the Apoptotic Gene Expression in Extravillous Trophoblasts Derived From First-Trimester Tissue.* Reprod Sci, 2015. **22**(7): p. 783-90.
56. Gegotek, A. and E. Skrzydlewska, *Ascorbic acid as antioxidant.* Vitam Horm, 2023. **121**: p. 247-270.
57. Kaulmann, A. and T. Bohn, *Carotenoids, inflammation, and oxidative stress--implications of cellular signaling pathways and relation to chronic disease prevention.* Nutr Res, 2014. **34**(11): p. 907-29.
58. *Office of Dietary Supplements - Vitamin A and Carotenoids.*
59. Rudrapal, M., et al., *Dietary Polyphenols and Their Role in Oxidative Stress-Induced Human Diseases: Insights Into Protective Effects, Antioxidant Potentials and Mechanism(s) of Action.* Front Pharmacol, 2022. **13**: p. 806470.
60. Tinggi, U., *Selenium: its role as antioxidant in human health.* Environ Health Prev Med, 2008. **13**(2): p. 102-8.

61. Tan, B.L., et al., *Antioxidant and Oxidative Stress: A Mutual Interplay in Age-Related Diseases.* Front Pharmacol, 2018. **9**: p. 1162.
62. Jiang, S., H. Liu, and C. Li, *Dietary Regulation of Oxidative Stress in Chronic Metabolic Diseases.* Foods, 2021. **10**(8).
63. Ighodaro, O.M. and O.A. Akinloye, *First line defence antioxidants-superoxide dismutase (SOD), catalase (CAT) and glutathione peroxidase (GPX): Their fundamental role in the entire antioxidant defence grid.* Alexandria Journal of Medicine, 2018. **54**(4): p. 287-293.
64. Koju, N., et al., *Pharmacological strategies to lower crosstalk between nicotinamide adenine dinucleotide phosphate (NADPH) oxidase and mitochondria.* Biomedicine & Pharmacotherapy, 2019. **111**: p. 1478-1498.
65. Brigelius-Flohé, R. and M. Maiorino, *Glutathione peroxidases.* Biochimica et Biophysica Acta (BBA) - General Subjects, 2013. **1830**(5): p. 3289-3303.
66. Pei, J., et al., *Research progress of glutathione peroxidase family (GPX) in redoxidation.* Front Pharmacol, 2023. **14**: p. 1147414.
67. Couto, N., J. Wood, and J. Barber, *The role of glutathione reductase and related enzymes on cellular redox homoeostasis network.* Free Radical Biology and Medicine, 2016. **95**: p. 27-42.
68. Singhal, S.S., et al., *Antioxidant role of glutathione S-transferases: 4-Hydroxynonenal, a key molecule in stress-mediated signaling.* Toxicol Appl Pharmacol, 2015. **289**(3): p. 361-70.
69. Valencia, E., A. Marin, and G. Hardy, *Glutathione--nutritional and pharmacological viewpoints: part II.* Nutrition, 2001. **17**(6): p. 485-6.
70. Cassier-Chauvat, C., et al., *The Glutathione System: A Journey from Cyanobacteria to Higher Eukaryotes.* Antioxidants (Basel), 2023. **12**(6).
71. Meister, A., *On the discovery of glutathione.* Trends Biochem Sci, 1988. **13**(5): p. 185-8.
72. Averill-Bates, D.A., *Chapter Five - The antioxidant glutathione*, in *Vitamins and Hormones*, G. Litwack, Editor. 2023, Academic Press. p. 109-141.
73. Lu, S.C., *Regulation of glutathione synthesis.* Mol Aspects Med, 2009. **30**(1-2): p. 42-59.
74. Labarrere, C.A. and G.S. Kassab, *Glutathione: A Samsonian life-sustaining small molecule that protects against oxidative stress, ageing and damaging inflammation.* Front Nutr, 2022. **9**: p. 1007816.
75. Mistry, D. and R.A. Stockley, *Gamma-glutamyl transferase: the silent partner?* COPD, 2010. **7**(4): p. 285-90.
76. Zhang, H., H.J. Forman, and J. Choi, *Gamma-glutamyl transpeptidase in glutathione biosynthesis.* Methods Enzymol, 2005. **401**: p. 468-83.
77. Xiao, W. and J. Loscalzo, *Metabolic Responses to Reductive Stress.* Antioxid Redox Signal, 2020. **32**(18): p. 1330-1347.
78. Gasmi, A., et al., *An Update on Glutathione's Biosynthesis, Metabolism, Functions, and Medicinal Purposes.* Curr Med Chem, 2024. **31**(29): p. 4579-4601.
79. Sharma, D.K. and P. Sharma, *Augmented Glutathione Absorption from Oral Mucosa and its Effect on Skin Pigmentation: A Clinical Review.* Clin Cosmet Investig Dermatol, 2022. **15**: p. 1853-1862.
80. Gould, R.L. and R. Pazdro, *Impact of Supplementary Amino Acids, Micronutrients, and Overall Diet on Glutathione Homeostasis.* Nutrients, 2019. **11**(5): p. 1056.

81. Liu, Y., et al., *Supplementation with γ-glutamylcysteine (γ-GC) lessens oxidative stress, brain inflammation and amyloid pathology and improves spatial memory in a murine model of AD.* Neurochemistry International, 2021. **144**: p. 104931.
82. Lu, S.C., *Glutathione synthesis.* Biochimica et Biophysica Acta (BBA) - General Subjects, 2013. **1830**(5): p. 3143-3153.
83. Vázquez-Meza, H., et al., *Cellular Compartmentalization, Glutathione Transport and Its Relevance in Some Pathologies.* Antioxidants, 2023. **12**(4): p. 834.
84. Wu, G., et al., *Glutathione Metabolism and Its Implications for Health.* The Journal of Nutrition, 2004. **134**(3): p. 489-492.
85. Bachhawat, A.K., et al., *Glutathione transporters.* Biochimica et Biophysica Acta (BBA) - General Subjects, 2013. **1830**(5): p. 3154-3164.
86. Nuhu, F., et al., *Measurement of Glutathione as a Tool for Oxidative Stress Studies by High Performance Liquid Chromatography.* Molecules, 2020. **25**(18).
87. Yap, L.P., et al., *Determination of GSH, GSSG, and GSNO using HPLC with electrochemical detection.* Methods Enzymol, 2010. **473**: p. 137-47.
88. David, V., S.C. Moldoveanu, and T. Galaon, *Derivatization procedures and their analytical performances for HPLC determination in bioanalysis.* Biomed Chromatogr, 2021. **35**(1): p. e5008.
89. Krull, I.S. and R.S. Strong, *CHROMATOGRAPHY: LIQUID | Derivatization*, in *Encyclopedia of Separation Science*, I.D. Wilson, Editor. 2000, Academic Press: Oxford. p. 583-591.
90. Squellerio, I., et al., *Direct glutathione quantification in human blood by LC–MS/MS: comparison with HPLC with electrochemical detection.* Journal of Pharmaceutical and Biomedical Analysis, 2012. **71**: p. 111-118.
91. Seger, C., *Usage and limitations of liquid chromatography-tandem mass spectrometry (LC-MS/MS) in clinical routine laboratories.* Wien Med Wochenschr, 2012. **162**(21-22): p. 499-504.
92. Asantewaa, G. and I.S. Harris, *Glutathione and its precursors in cancer.* Current Opinion in Biotechnology, 2021. **68**: p. 292-299.
93. Lewerenz, J., et al., *The cystine/glutamate antiporter system x(c)(-) in health and disease: from molecular mechanisms to novel therapeutic opportunities.* Antioxid Redox Signal, 2013. **18**(5): p. 522-55.
94. Baba, S.P. and A. Bhatnagar, *Role of Thiols in Oxidative Stress.* Curr Opin Toxicol, 2018. **7**: p. 133-139.
95. Chiang, F.-F., et al. *Cysteine Regulates Oxidative Stress and Glutathione-Related Antioxidative Capacity before and after Colorectal Tumor Resection*. International Journal of Molecular Sciences, 2022. **23**, DOI: 10.3390/ijms23179581.
96. Fra, A., E.D. Yoboue, and R. Sitia, *Cysteines as Redox Molecular Switches and Targets of Disease.* Front Mol Neurosci, 2017. **10**: p. 167.
97. Go, Y.-M., J.D. Chandler, and D.P. Jones, *The cysteine proteome.* Free Radical Biology and Medicine, 2015. **84**: p. 227-245.
98. Raghu, G., et al., *The Multifaceted Therapeutic Role of N-Acetylcysteine (NAC) in Disorders Characterized by Oxidative Stress.* Curr Neuropharmacol, 2021. **19**(8): p. 1202-1224.

99. Ezerina, D., et al., *N-Acetyl Cysteine Functions as a Fast-Acting Antioxidant by Triggering Intracellular H(2)S and Sulfane Sulfur Production.* Cell Chem Biol, 2018. **25**(4): p. 447-459 e4.
100. Mokhtari, V., et al., *A Review on Various Uses of N-Acetyl Cysteine.* Cell J, 2017. **19**(1): p. 11-17.
101. Dodd, S., et al., *N-acetylcysteine for antioxidant therapy: pharmacology and clinical utility.* Expert Opin Biol Ther, 2008. **8**(12): p. 1955-62.
102. McCarty, M.F., J.H. O'Keefe, and J.J. DiNicolantonio, *Dietary Glycine Is Rate-Limiting for Glutathione Synthesis and May Have Broad Potential for Health Protection.* Ochsner J, 2018. **18**(1): p. 81-87.
103. Pedre, B., et al., *The mechanism of action of N-acetylcysteine (NAC): The emerging role of H2S and sulfane sulfur species.* Pharmacology & Therapeutics, 2021. **228**: p. 107916.
104. Falach-Malik, A., et al., *N-Acetyl-L-Cysteine inhibits the development of glucose intolerance and hepatic steatosis in diabetes-prone mice.* Am J Transl Res, 2016. **8**(9): p. 3744-3756.
105. Har-Zahav, A., et al., *Oral N-acetylcysteine ameliorates liver fibrosis and enhances regenerative responses in Mdr2 knockout mice.* Sci Rep, 2024. **14**(1): p. 26513.
106. Chevez-Barrios, P., et al., *Cataract development in gamma-glutamyl transpeptidase-deficient mice.* Exp Eye Res, 2000. **71**(6): p. 575-82.
107. Tardiolo, G., P. Bramanti, and E. Mazzon, *Overview on the Effects of N-Acetylcysteine in Neurodegenerative Diseases.* Molecules, 2018. **23**(12).
108. Eakin, K., et al., *Efficacy of N-acetyl cysteine in traumatic brain injury.* PLoS One, 2014. **9**(4): p. e90617.
109. Farr, S.A., et al., *The antioxidants alpha-lipoic acid and N-acetylcysteine reverse memory impairment and brain oxidative stress in aged SAMP8 mice.* J Neurochem, 2003. **84**(5): p. 1173-83.
110. More, J., et al., *N-Acetylcysteine Prevents the Spatial Memory Deficits and the Redox-Dependent RyR2 Decrease Displayed by an Alzheimer's Disease Rat Model.* Front Aging Neurosci, 2018. **10**: p. 399.
111. Schuurman, M., et al., *N-acetyl-L-cysteine treatment reduces beta-cell oxidative stress and pancreatic stellate cell activity in a high fat diet-induced diabetic mouse model.* Front Endocrinol (Lausanne), 2022. **13**: p. 938680.
112. Xing, S., et al., *N-Acetyl-l-cysteine ameliorates gestational diabetes mellitus by inhibiting oxidative stress.* Gynecol Endocrinol, 2023. **39**(1): p. 2189969.
113. Lasram, M.M., et al., *A review on the possible molecular mechanism of action of N-acetylcysteine against insulin resistance and type-2 diabetes development.* Clin Biochem, 2015. **48**(16-17): p. 1200-8.
114. Cui, Y., et al., *N-Acetylcysteine and Atherosclerosis: Promises and Challenges.* Antioxidants (Basel), 2023. **12**(12).
115. Badawy, A., O. State, and S. Abdelgawad, *N-Acetyl cysteine and clomiphene citrate for induction of ovulation in polycystic ovary syndrome: a cross-over trial.* Acta Obstet Gynecol Scand, 2007. **86**(2): p. 218-22.
116. Bedaiwy, M.A., A. RezkH. Al Inany, and T. Falcone, *N-acetyl cystein improves pregnancy rate in long standing unexplained infertility: A novel mechanism of ovulation induction.* Fertility and Sterility, 2004. **82**: p. S228.

117. Devi, N., et al., *N-acetyl-cysteine as adjuvant therapy in female infertility: a systematic review and meta-analysis.* J Basic Clin Physiol Pharmacol, 2020. **32**(5): p. 899-910.
118. Tenório, M.C.D.S., et al., *N-Acetylcysteine (NAC): Impacts on Human Health.* Antioxidants, 2021. **10**(6): p. 967.
119. Bavarsad Shahripour, R., M.R. Harrigan, and A.V. Alexandrov, *N-acetylcysteine (NAC) in neurological disorders: mechanisms of action and therapeutic opportunities.* Brain Behav, 2014. **4**(2): p. 108-22.
120. Adair, J.C., J.E. Knoefel, and N. Morgan, *Controlled trial of N-acetylcysteine for patients with probable Alzheimer's disease.* Neurology, 2001. **57**(8): p. 1515-7.
121. Lavoie, S., et al., *Glutathione precursor, N-acetyl-cysteine, improves mismatch negativity in schizophrenia patients.* Neuropsychopharmacology, 2008. **33**(9): p. 2187-99.
122. Yang, Y.S., et al., *N-Acetylcysteine effects on glutathione and glutamate in schizophrenia: A preliminary MRS study.* Psychiatry Res Neuroimaging, 2022. **325**: p. 111515.
123. Berk, M., et al., *N-Acetyl Cysteine as a Glutathione Precursor for Schizophrenia—A Double-Blind, Randomized, Placebo-Controlled Trial.* Biological Psychiatry, 2008. **64**(5): p. 361-368.
124. Walayat, S., et al., *Role of N-acetylcysteine in non-acetaminophen-related acute liver failure: an updated meta-analysis and systematic review.* Ann Gastroenterol, 2021. **34**(2): p. 235-240.
125. Ghabril, M., N. Chalasani, and E. Bjornsson, *Drug-induced liver injury: a clinical update.* Curr Opin Gastroenterol, 2010. **26**(3): p. 222-6.
126. Stey, C., et al., *The effect of oral N-acetylcysteine in chronic bronchitis: a quantitative systematic review.* Eur Respir J, 2000. **16**(2): p. 253-62.
127. Sutherland, E.R., J.D. Crapo, and R.P. Bowler, *N-acetylcysteine and exacerbations of chronic obstructive pulmonary disease.* COPD, 2006. **3**(4): p. 195-202.
128. Drager, L.F., et al., *Renal effects of N-acetylcysteine in patients at risk for contrast nephropathy: decrease in oxidant stress-mediated renal tubular injury.* Nephrol Dial Transplant, 2004. **19**(7): p. 1803-7.
129. Deepmala, et al., *Clinical trials of N-acetylcysteine in psychiatry and neurology: A systematic review.* Neuroscience & Biobehavioral Reviews, 2015. **55**: p. 294-321.
130. Oldham, J.M., et al., *TOLLIP, MUC5B, and the Response to N-Acetylcysteine among Individuals with Idiopathic Pulmonary Fibrosis.* Am J Respir Crit Care Med, 2015. **192**(12): p. 1475-82.
131. Gopika, M.G., et al., *Unveiling thiol biomarkers: Glutathione and cysteamine.* Clinica Chimica Acta, 2024. **563**: p. 119915.
132. Paul, B.D. and S.H. Snyder, *Therapeutic Applications of Cysteamine and Cystamine in Neurodegenerative and Neuropsychiatric Diseases.* Front Neurol, 2019. **10**: p. 1315.
133. Giustarini, D., et al., *How to Increase Cellular Glutathione.* Antioxidants (Basel), 2023. **12**(5).
134. Kalamkar, S., et al., *Randomized Clinical Trial of How Long-Term Glutathione Supplementation Offers Protection from Oxidative Damage and Improves HbA1c in Elderly Type 2 Diabetic Patients.* Antioxidants (Basel), 2022. **11**(5).
135. Richie, J.P., Jr., et al., *Randomized controlled trial of oral glutathione supplementation on body stores of glutathione.* Eur J Nutr, 2015. **54**(2): p. 251-63.

136. Mischley, L.K., et al., *Central nervous system uptake of intranasal glutathione in Parkinson's disease.* npj Parkinson's Disease, 2016. **2**(1): p. 16002.
137. Schmitt, B., et al., *Effects of N-acetylcysteine, oral glutathione (GSH) and a novel sublingual form of GSH on oxidative stress markers: A comparative crossover study.* Redox Biology, 2015. **6**: p. 198-205.
138. Jain, S.K., R. McVie, and T. Smith, *Vitamin E supplementation restores glutathione and malondialdehyde to normal concentrations in erythrocytes of type 1 diabetic children.* Diabetes Care, 2000. **23**(9): p. 1389-1394.
139. Barbagallo, M., et al., *Effects of vitamin E and glutathione on glucose metabolism: role of magnesium.* Hypertension, 1999. **34**(4 Pt 2): p. 1002-6.
140. Tefagh, G., et al., *Effect of vitamin E supplementation on cardiometabolic risk factors, inflammatory and oxidative markers and hormonal functions in PCOS (polycystic ovary syndrome): a systematic review and meta-analysis.* Sci Rep, 2022. **12**(1): p. 5770.
141. Hsu, C.C., et al., *Role of vitamin B6 status on antioxidant defenses, glutathione, and related enzyme activities in mice with homocysteine-induced oxidative stress.* Food Nutr Res, 2015. **59**: p. 25702.
142. Mahfouz, M.M. and F.A. Kummerow, *Vitamin C or Vitamin B6 supplementation prevent the oxidative stress and decrease of prostacyclin generation in homocysteinemic rats.* The International Journal of Biochemistry & Cell Biology, 2004. **36**(10): p. 1919-1932.
143. Anand, S.S., *Pyridoxine attenuates chromium-induced oxidative stress in rat kidney.* Basic Clin Pharmacol Toxicol, 2005. **97**(1): p. 58-60.
144. Lai, C.Y., et al., *Impact of Glutathione and Vitamin B-6 in Cirrhosis Patients: A Randomized Controlled Trial and Follow-Up Study.* Nutrients, 2020. **12**(7).
145. DiFrancisco-Donoghue, J., et al., *Effects of exercise and B vitamins on homocysteine and glutathione in Parkinson's disease: a randomized trial.* Neurodegener Dis, 2012. **10**(1-4): p. 127-34.
146. Lee, E., et al., *Vitamin C and glutathione supplementation: a review of their additive effects on exercise performance.* Phys Act Nutr, 2023. **27**(3): p. 36-43.
147. Lenton, K.J., et al., *Direct correlation of glutathione and ascorbate and their dependence on age and season in human lymphocytes123.* The American Journal of Clinical Nutrition, 2000. **71**(5): p. 1194-1200.
148. Lal, H., et al., *Effect of methionine and vitamin C supplementation on pulmonary glutathione-s-transferase and glutathione levels in ageing rats.* Indian Journal of Clinical Biochemistry, 1993. **8**(1): p. 33-35.
149. Chen, L.H. and R.R. Thacker, *An increase in glutathione peroxidase activity induced by high supplementation of vitamin C in rats.* Nutrition Research, 1984. **4**(4): p. 657-664.
150. Rojas, C., et al., *Effect of vitamin C on antioxidants, lipid peroxidation, and GSH system in the normal guinea pig heart.* J Nutr Sci Vitaminol (Tokyo), 1994. **40**(5): p. 411-20.
151. Lenton, K.J., et al., *Vitamin C augments lymphocyte glutathione in subjects with ascorbate deficiency.* Am J Clin Nutr, 2003. **77**(1): p. 189-95.
152. Johnston, C.S., C.G. Meyer, and J.C. Srilakshmi, *Vitamin C elevates red blood cell glutathione in healthy adults.* Am J Clin Nutr, 1993. **58**(1): p. 103-5.
153. Karajibani, M., et al., *Effect of vitamin E and C supplements on antioxidant defense system in cardiovascular disease patients in Zahedan, southeast Iran.* J Nutr Sci Vitaminol (Tokyo), 2010. **56**(6): p. 436-40.

154. Ryan, M.J., et al., *Vitamin E and C supplementation reduces oxidative stress, improves antioxidant enzymes and positive muscle work in chronically loaded muscles of aged rats.* Experimental Gerontology, 2010. **45**(11): p. 882-895.
155. Rayman, M.P., *Selenium intake, status, and health: a complex relationship.* Hormones (Athens), 2020. **19**(1): p. 9-14.
156. Bermingham, E.N., et al., *Selenium-enriched foods are more effective at increasing glutathione peroxidase (GPx) activity compared with selenomethionine: a meta-analysis.* Nutrients, 2014. **6**(10): p. 4002-31.
157. Nogales, F., et al., *Role of selenium and glutathione peroxidase on development, growth, and oxidative balance in rat offspring.* Reproduction, 2013. **146**(6): p. 659-67.
158. Kang, B.P., M.P. Bansal, and U. Mehta, *Selenium supplementation and diet induced hypercholesterolemia in the rat: changes in lipid levels, malonyldialdehyde production and the nitric oxide synthase activity.* Gen Physiol Biophys, 1998. **17**(1): p. 71-8.
159. Sedighi, O., M. Zargari, and G. Varshi, *Effect of selenium supplementation on glutathione peroxidase enzyme activity in patients with chronic kidney disease: a randomized clinical trial.* Nephrourol Mon, 2014. **6**(3): p. e17945.
160. Zachara, B.A., et al., *Selenium and glutathione levels, and glutathione peroxidase activities in blood components of uremic patients on hemodialysis supplemented with selenium and treated with erythropoietin.* J Trace Elem Med Biol, 2001. **15**(4): p. 201-8.
161. Nève, J., F. Vertongen, and P. Capel, *Selenium supplementation in healthy Belgian adults: response in platelet glutathione peroxidase activity and other blood indices.* The American Journal of Clinical Nutrition, 1988. **48**(1): p. 139-143.
162. Mohammadi, H., et al., *Effects of zinc supplementation on inflammatory biomarkers and oxidative stress in adults: A systematic review and meta-analysis of randomized controlled trials.* Journal of Trace Elements in Medicine and Biology, 2021. **68**: p. 126857.
163. Oteiza, P.I., *Zinc and the modulation of redox homeostasis.* Free Radic Biol Med, 2012. **53**(9): p. 1748-59.
164. Hübner, C. and H. Haase, *Interactions of zinc- and redox-signaling pathways.* Redox Biology, 2021. **41**: p. 101916.
165. Zhou, Z., et al., *Zinc supplementation prevents alcoholic liver injury in mice through attenuation of oxidative stress.* Am J Pathol, 2005. **166**(6): p. 1681-90.
166. Galażyn-Sidorczuk, M., et al., *Effect of zinc supplementation on glutathione peroxidase activity and selenium concentration in the serum, liver and kidney of rats chronically exposed to cadmium.* Journal of Trace Elements in Medicine and Biology, 2012. **26**(1): p. 46-52.
167. Amores-Sánchez, M.a.I. and M.Á. Medina, *Glutamine, as a Precursor of Glutathione, and Oxidative Stress.* Molecular Genetics and Metabolism, 1999. **67**(2): p. 100-105.
168. Cruzat, V.F. and J. Tirapegui, *Effects of oral supplementation with glutamine and alanyl-glutamine on glutamine, glutamate, and glutathione status in trained rats and subjected to long-duration exercise.* Nutrition, 2009. **25**(4): p. 428-435.
169. Belmonte, L., et al., *Effects of glutamine supplementation on gut barrier, glutathione content and acute phase response in malnourished rats during inflammatory shock.* World J Gastroenterol, 2007. **13**(20): p. 2833-40.
170. Manhart, N., et al., *Oral feeding with glutamine prevents lymphocyte and glutathione depletion of Peyer's patches in endotoxemic mice.* Ann Surg, 2001. **234**(1): p. 92-7.

171. Humbert, B., et al., *Effect of glutamine on glutathione kinetics in vivo in dogs.* The Journal of Nutritional Biochemistry, 2007. **18**(1): p. 10-16.
172. Pires, R.S., et al., *l-Glutamine supplementation enhances glutathione peroxidase and paraoxonase-1 activities in HDL of exercising older individuals.* Experimental Gerontology, 2021. **156**: p. 111584.
173. Borges-Santos, M.D., et al., *Plasma glutathione of HIV+ patients responded positively and differently to dietary supplementation with cysteine or glutamine.* Nutrition, 2012. **28**(7): p. 753-756.
174. Valencia, E., A. Marin, and G. Hardy, *Impact of oral l-glutamine on glutathione, glutamine, and glutamate blood levels in volunteers.* Nutrition, 2002. **18**(5): p. 367-370.
175. Wang, W., et al., *Glycine is a nutritionally essential amino acid for maximal growth of milk-fed young pigs.* Amino Acids, 2014. **46**(8): p. 2037-45.
176. Zhang, Y., et al., *Effects of glycine supplementation on myocardial damage and cardiac function after severe burn.* Burns, 2013. **39**(4): p. 729-735.
177. Senthilkumar, R., P. Viswanathan, and N. Nalini, *Effect of glycine on oxidative stress in rats with alcohol induced liver injury.* Pharmazie, 2004. **59**(1): p. 55-60.
178. Ruiz-Ramirez, A., et al., *Glycine restores glutathione and protects against oxidative stress in vascular tissue from sucrose-fed rats.* Clin Sci (Lond), 2014. **126**(1): p. 19-29.
179. Gut, P., et al., *Effects of glycine and n-acetylcysteine on glutathione levels and mitochondrial energy metabolism in healthy aging.* Innovation in Aging, 2021. **5**(Supplement_1): p. 685-685.
180. Lizzo, G., et al., *A Randomized Controlled Clinical Trial in Healthy Older Adults to Determine Efficacy of Glycine and N-Acetylcysteine Supplementation on Glutathione Redox Status and Oxidative Damage.* Front Aging, 2022. **3**: p. 852569.
181. Sekhar, R.V., et al., *Deficient synthesis of glutathione underlies oxidative stress in aging and can be corrected by dietary cysteine and glycine supplementation1234.* The American Journal of Clinical Nutrition, 2011. **94**(3): p. 847-853.
182. Hristov, B.D., *The Role of Glutathione Metabolism in Chronic Illness Development and Its Potential Use as a Novel Therapeutic Target.* Cureus, 2022. **14**(9): p. e29696.
183. Townsend, D.M., K.D. Tew, and H. Tapiero, *The importance of glutathione in human disease.* Biomed Pharmacother, 2003. **57**(3-4): p. 145-55.
184. Matuz-Mares, D., et al., *Glutathione Participation in the Prevention of Cardiovascular Diseases.* Antioxidants (Basel), 2021. **10**(8).
185. Rosenblat, M., et al., *Anti-oxidant and anti-atherogenic properties of liposomal glutathione: studies in vitro, and in the atherosclerotic apolipoprotein E-deficient mice.* Atherosclerosis, 2007. **195**(2): p. e61-8.
186. Rosenblat, M., R. Coleman, and M. Aviram, *Increased macrophage glutathione content reduces cell-mediated oxidation of LDL and atherosclerosis in apolipoprotein E-deficient mice.* Atherosclerosis, 2002. **163**(1): p. 17-28.
187. Lin, C.C., et al., *Effect of five cysteine-containing compounds on three lipogenic enzymes in Balb/cA mice consuming a high saturated fat diet.* Lipids, 2004. **39**(9): p. 843-8.
188. Shimizu, H., et al., *Relationship between plasma glutathione levels and cardiovascular disease in a defined population: the Hisayama study.* Stroke, 2004. **35**(9): p. 2072-7.
189. Sekhar, R.V., et al., *Glutathione synthesis is diminished in patients with uncontrolled diabetes and restored by dietary supplementation with cysteine and glycine.* Diabetes Care, 2011. **34**(1): p. 162-7.

190. Tuell, D., et al., *The Role of Glutathione and Its Precursors in Type 2 Diabetes.* Antioxidants (Basel), 2024. **13**(2).
191. De Mattia, G., et al., *Reduction of oxidative stress by oral N-acetyl-L-cysteine treatment decreases plasma soluble vascular cell adhesion molecule-1 concentrations in non-obese, non-dyslipidaemic, normotensive, patients with non-insulin-dependent diabetes.* Diabetologia, 1998. **41**(11): p. 1392-6.
192. Szkudlinska, M.A., A.D. von Frankenberg, and K.M. Utzschneider, *The antioxidant N-Acetylcysteine does not improve glucose tolerance or β-cell function in type 2 diabetes.* Journal of Diabetes and its Complications, 2016. **30**(4): p. 618-622.
193. Sekhar, R.V., *GlyNAC (Glycine and N-Acetylcysteine) Supplementation Improves Impaired Mitochondrial Fuel Oxidation and Lowers Insulin Resistance in Patients with Type 2 Diabetes: Results of a Pilot Study.* Antioxidants (Basel), 2022. **11**(1).
194. Kumar, P., et al., *Supplementing Glycine and N-Acetylcysteine (GlyNAC) in Older Adults Improves Glutathione Deficiency, Oxidative Stress, Mitochondrial Dysfunction, Inflammation, Physical Function, and Aging Hallmarks: A Randomized Clinical Trial.* J Gerontol A Biol Sci Med Sci, 2023. **78**(1): p. 75-89.
195. Di Giorno, C., et al., *Beneficial Effect of N-Acetyl-Cysteine on Renal Injury Triggered by Ischemia and Reperfusion.* Transplantation Proceedings, 2006. **38**(9): p. 2774-2776.
196. Subramaniam, R.M., et al., *Effectiveness of Prevention Strategies for Contrast-Induced Nephropathy: A Systematic Review and Meta-analysis.* Ann Intern Med, 2016. **164**(6): p. 406-16.
197. Tsai, J.-P., et al., *Effect of Intravenous N-acetylcysteine on Plasma Total Homocysteine and Inflammatory Cytokines During High Flux Hemodialysis.* Tzu Chi Medical Journal, 2010. **22**(2): p. 90-95.
198. Thaha, M., M. Yogiantoro, and Y. Tomino, *Intravenous N-acetylcysteine during haemodialysis reduces the plasma concentration of homocysteine in patients with end-stage renal disease.* Clin Drug Investig, 2006. **26**(4): p. 195-202.
199. Giannikouris, I., *The effect of N-acetylcysteine on oxidative serum biomarkers of hemodialysis patients.* Hippokratia, 2015. **19**(2): p. 131-5.
200. Ahmadi, F., et al., *Effectiveness of N-acetylcysteine for preserving residual renal function in patients undergoing maintenance hemodialysis: multicenter randomized clinical trial.* Clin Exp Nephrol, 2017. **21**(2): p. 342-349.
201. Smilkstein, M.J., et al., *Efficacy of oral N-acetylcysteine in the treatment of acetaminophen overdose. Analysis of the national multicenter study (1976 to 1985).* N Engl J Med, 1988. **319**(24): p. 1557-62.
202. Nabi, T., et al., *Role of N-acetylcysteine treatment in non-acetaminophen-induced acute liver failure: A prospective study.* Saudi J Gastroenterol, 2017. **23**(3): p. 169-175.
203. Lee, W.M., et al., *Intravenous N-acetylcysteine improves transplant-free survival in early stage non-acetaminophen acute liver failure.* Gastroenterology, 2009. **137**(3): p. 856-64, 864 e1.
204. Wang, M.L., et al., *Retrospective Analysis of the Clinical Efficacy of N-Acetylcysteine in the Treatment of Hepatitis B Virus Related Acute-on-Chronic Liver Failure.* Front Med (Lausanne), 2021. **8**: p. 724224.
205. Wei, Q. and J. Zhao, *Therapeutic effects of reduced glutathione on liver function, fibrosis, and HBV DNA clearance in chronic hepatitis B patients.* BMC Gastroenterol, 2025. **25**(1): p. 68.

206. Khoshbaten, M., et al., *N-acetylcysteine improves liver function in patients with non-alcoholic Fatty liver disease.* Hepat Mon, 2010. **10**(1): p. 12-6.
207. Honda, Y., et al., *Efficacy of glutathione for the treatment of nonalcoholic fatty liver disease: an open-label, single-arm, multicenter, pilot study.* BMC Gastroenterol, 2017. **17**(1): p. 96.
208. Ozaras, R., et al., *N-acetylcysteine attenuates alcohol-induced oxidative stress in the rat.* World J Gastroenterol, 2003. **9**(1): p. 125-8.
209. Johnson, W.M., A.L. Wilson-Delfosse, and J.J. Mieyal, *Dysregulation of glutathione homeostasis in neurodegenerative diseases.* Nutrients, 2012. **4**(10): p. 1399-440.
210. Hashimoto, S., et al., *Neuronal glutathione loss leads to neurodegeneration involving gasdermin activation.* Sci Rep, 2023. **13**(1): p. 1109.
211. Huang, Q., et al., *Potential in vivo amelioration by N-acetyl-L-cysteine of oxidative stress in brain in human double mutant APP/PS-1 knock-in mice: toward therapeutic modulation of mild cognitive impairment.* J Neurosci Res, 2010. **88**(12): p. 2618-29.
212. Alkandari, A.F., S. Madhyastha, and M.S. Rao, *N-Acetylcysteine Amide against Abeta-Induced Alzheimer's-like Pathology in Rats.* Int J Mol Sci, 2023. **24**(16).
213. Clark, J., et al., *Oral N-acetyl-cysteine attenuates loss of dopaminergic terminals in alpha-synuclein overexpressing mice.* PLoS One, 2010. **5**(8): p. e12333.
214. Monti, D.A., et al., *N-Acetyl Cysteine Is Associated With Dopaminergic Improvement in Parkinson's Disease.* Clin Pharmacol Ther, 2019. **106**(4): p. 884-890.
215. Kennedy, L., et al., *Role of Glutathione in Cancer: From Mechanisms to Therapies.* Biomolecules, 2020. **10**(10).
216. Monti, D., et al., *Pilot study demonstrating metabolic and anti-proliferative effects of in vivo anti-oxidant supplementation with N-Acetylcysteine in Breast Cancer.* Seminars in Oncology, 2017. **44**(3): p. 226-232.
217. Deng, J., et al., *N-acetylcysteine decreases malignant characteristics of glioblastoma cells by inhibiting Notch2 signaling.* J Exp Clin Cancer Res, 2019. **38**(1): p. 2.
218. Kwon, Y., *Possible Beneficial Effects of N-Acetylcysteine for Treatment of Triple-Negative Breast Cancer.* Antioxidants (Basel), 2021. **10**(2).
219. Sayin, V.I., et al., *Antioxidants accelerate lung cancer progression in mice.* Sci Transl Med, 2014. **6**(221): p. 221ra15.
220. Le Gal, K., et al., *Antioxidants can increase melanoma metastasis in mice.* Sci Transl Med, 2015. **7**(308): p. 308re8.
221. Lu, S.C., et al., *Hormonal regulation of glutathione efflux.* J Biol Chem, 1990. **265**(27): p. 16088-95.
222. Dasgupta, A., S. Das, and P. Kumar Sarkar, *Thyroid hormone promotes glutathione synthesis in astrocytes by up regulation of glutamate cysteine ligase through differential stimulation of its catalytic and modulator subunit mRNAs.* Free Radical Biology and Medicine, 2007. **42**(5): p. 617-626.
223. Rahaman, S.O., et al., *Hypothyroidism in the developing rat brain is associated with marked oxidative stress and aberrant intraneuronal accumulation of neurofilaments.* Neuroscience Research, 2001. **40**(3): p. 273-279.
224. Dasgupta, A., S. Das, and P.K. Sarkar, *Thyroid hormone stimulates gamma-glutamyl transpeptidase in the developing rat cerebra and in astroglial cultures.* J Neurosci Res, 2005. **82**(6): p. 851-7.

225. Coecke, S., et al., *Hormonal regulation of glutathione S-transferase expression in co-cultured adult rat hepatocytes.* J Endocrinol, 2000. **166**(2): p. 363-71.
226. Patarrao, R.S., W.W. Lautt, and M.P. Macedo, *Acute glucagon induces postprandial peripheral insulin resistance.* PLoS One, 2015. **10**(5): p. e0127221.
227. Kim, S.K., K.J. Woodcroft, and R.F. Novak, *Insulin and Glucagon Regulation of Glutathione S-Transferase Expression in Primary Cultured Rat Hepatocytes.* The Journal of Pharmacology and Experimental Therapeutics, 2003. **305**(1): p. 353-361.
228. Kim, B.-H., et al., *Effects of Glucagon and Insulin on Glutathione Homeostasis: Role of Cellular Signaling Pathways and Glutathione Transport System.* Environmental Analysis Health and Toxicology, 2007.
229. Lu, S.C., et al., *Hormone-mediated down-regulation of hepatic glutathione synthesis in the rat.* J Clin Invest, 1991. **88**(1): p. 260-9.
230. Allison, C., C.R. Michael, and H.F. Nijhout, *Sex differences in glutathione metabolism and acetaminophen toxicity.* Metabolism and Target Organ Damage, 2024. **4**(2): p. 17.
231. Cruz-Topete, D., P. Dominic, and K.Y. Stokes, *Uncovering sex-specific mechanisms of action of testosterone and redox balance.* Redox Biol, 2020. **31**: p. 101490.
232. Bellanti, F., et al., *Sex hormones modulate circulating antioxidant enzymes: Impact of estrogen therapy.* Redox Biology, 2013. **1**(1): p. 340-346.
233. Suojanen, J.N., R.J. Gay, and R. Hilf, *Influence of estrogen on glutathione levels and glutathione-metabolizing enzymes in uteri and R3230AC mammary tumors of rats.* Biochimica et Biophysica Acta (BBA) - General Subjects, 1980. **630**(4): p. 485-496.
234. Ohwada, M., et al., *Glutathione peroxidase activity in endometrium: effects of sex hormones and cancer.* Gynecol Oncol, 1996. **60**(2): p. 277-82.
235. Zhang, L., et al., *Testosterone suppresses oxidative stress via androgen receptor-independent pathway in murine cardiomyocytes.* Mol Med Rep, 2011. **4**(6): p. 1183-8.
236. Lopes, R.A., et al., *Testosterone induces apoptosis in vascular smooth muscle cells via extrinsic apoptotic pathway with mitochondria-generated reactive oxygen species involvement.* Am J Physiol Heart Circ Physiol, 2014. **306**(11): p. H1485-94.
237. Rojanathammanee, L., S. Rakoczy, and H.M. Brown-Borg, *Growth hormone alters the glutathione S-transferase and mitochondrial thioredoxin systems in long-living Ames dwarf mice.* J Gerontol A Biol Sci Med Sci, 2014. **69**(10): p. 1199-211.
238. Brown-Borg, H.M., S.G. Rakoczy, and E.O. Uthus, *Growth hormone alters methionine and glutathione metabolism in Ames dwarf mice.* Mech Ageing Dev, 2005. **126**(3): p. 389-98.
239. Staffas, L., et al., *Further characterization of hormonal regulation of glutathione transferase in rat liver and adrenal glands. Sex differences and demonstration that growth hormone regulates the hepatic levels.* Biochem J, 1992. **286 (Pt 1)**(Pt 1): p. 65-72.
240. Donahue, A.N., et al., *Growth hormone administration to aged animals reduces disulfide glutathione levels in hippocampus.* Mechanisms of Ageing and Development, 2006. **127**(1): p. 57-63.
241. Zhou, Y., et al., *Genetic analysis of tissue glutathione concentrations and redox balance.* Free Radic Biol Med, 2014. **71**: p. 157-164.
242. Yamashita, R., et al., *Cell line-dependent difference in glutathione levels affects the cigarette sidestream smoke-induced inhibition of nucleotide excision repair.* Mutation

Research/Genetic Toxicology and Environmental Mutagenesis, 2020. **858-860**: p. 503273.
243. Gould, R.L., et al., *Heritability of the aged glutathione phenotype is dependent on tissue of origin.* Mamm Genome, 2018. **29**(9-10): p. 619-631.
244. Norris, K.M., et al., *A high-fat diet differentially regulates glutathione phenotypes in the obesity-prone mouse strains DBA/2J, C57BL/6J, and AKR/J.* Nutr Res, 2016. **36**(12): p. 1316-1324.
245. van 't Erve, T.J., et al., *The concentration of glutathione in human erythrocytes is a heritable trait.* Free Radical Biology and Medicine, 2013. **65**: p. 742-749.
246. Rebrin, I., M.J. Forster, and R.S. Sohal, *Effects of age and caloric intake on glutathione redox state in different brain regions of C57BL/6 and DBA/2 mice.* Brain Research, 2007. **1127**: p. 10-18.
247. Rebrin, I., M.J. Forster, and R.S. Sohal, *Association between life-span extension by caloric restriction and thiol redox state in two different strains of mice.* Free Radical Biology and Medicine, 2011. **51**(1): p. 225-233.
248. Tsuchiya, M., et al., *Interstrain differences in liver injury and one-carbon metabolism in alcohol-fed mice.* Hepatology, 2012. **56**(1): p. 130-9.
249. *Mouse Model.*
250. Fang, Z. and G. Peltz, *Twenty-first century mouse genetics is again at an inflection point.* Lab Anim (NY), 2025. **54**(1): p. 9-15.
251. Brown, S.D.M., *Advances in mouse genetics for the study of human disease.* Hum Mol Genet, 2021. **30**(R2): p. R274-R284.
252. Russell, E.S., *Origins of Inbred Mice.*
253. Beck, J.A., et al., *Genealogies of mouse inbred strains.* Nat Genet, 2000. **24**(1): p. 23-5.
254. Tuttle, A.H., et al., *Comparing phenotypic variation between inbred and outbred mice.* Nat Methods, 2018. **15**(12): p. 994-996.
255. Churchill, G.A., et al., *The Diversity Outbred mouse population.* Mamm Genome, 2012. **23**(9-10): p. 713-8.
256. Saul, M.C., et al., *High-Diversity Mouse Populations for Complex Traits.* Trends in Genetics, 2019. **35**(7): p. 501-514.
257. Logan, R.W., et al., *High-precision genetic mapping of behavioral traits in the diversity outbred mouse population.* Genes Brain Behav, 2013. **12**(4): p. 424-37.
258. Cheng, R., et al., *QTLRel: an R package for genome-wide association studies in which relatedness is a concern.* BMC Genet, 2011. **12**: p. 66.
259. Broman, K.W., et al., *R/qtl: QTL mapping in experimental crosses.* Bioinformatics, 2003. **19**(7): p. 889-890.
260. Gould, R.L., et al., *Quantitative trait mapping in Diversity Outbred mice identifies novel genomic regions associated with the hepatic glutathione redox system.* Redox Biology, 2021. **46**: p. 102093.
261. Gould, R.L., et al., *Genetic mapping of renal glutathione suggests a novel regulatory locus on the murine X chromosome and overlap with hepatic glutathione regulation.* Free Radical Biology and Medicine, 2021. **174**: p. 28-39.
262. Bayat, A., *Science, medicine, and the future: Bioinformatics.* BMJ, 2002. **324**(7344): p. 1018-22.

263. Uffelmann, E., D. Posthuma, and W.J. Peyrot, *Genome-wide association studies of polygenic risk score-derived phenotypes may lead to inflated false positive rates.* Sci Rep, 2023. **13**(1): p. 4219.
264. Robinson, J.R., et al., *Genome-wide and Phenome-wide Approaches to Understand Variable Drug Actions in Electronic Health Records.* Clin Transl Sci, 2018. **11**(2): p. 112-122.
265. Berg, J.J., et al., *Reduced signal for polygenic adaptation of height in UK Biobank.* Elife, 2019. **8**.
266. Elliott, L.T., et al., *Genome-wide association studies of brain imaging phenotypes in UK Biobank.* Nature, 2018. **562**(7726): p. 210-216.
267. Smith, S.M., et al., *An expanded set of genome-wide association studies of brain imaging phenotypes in UK Biobank.* Nat Neurosci, 2021. **24**(5): p. 737-745.
268. Canela-Xandri, O., K. Rawlik, and A. Tenesa, *An atlas of genetic associations in UK Biobank.* Nat Genet, 2018. **50**(11): p. 1593-1599.
269. Tan, V.Y. and N.J. Timpson, *The UK Biobank: A Shining Example of Genome-Wide Association Study Science with the Power to Detect the Murky Complications of Real-World Epidemiology.* Annu Rev Genomics Hum Genet, 2022. **23**: p. 569-589.
270. Winkler, T.W., et al., *Genetic-by-age interaction analyses on complex traits in UK Biobank and their potential to identify effects on longitudinal trait change.* Genome Biol, 2024. **25**(1): p. 300.
271. Neuraz, A., et al., *Phenome-wide association studies on a quantitative trait: application to TPMT enzyme activity and thiopurine therapy in pharmacogenomics.* PLoS Comput Biol, 2013. **9**(12): p. e1003405.
272. Diogo, D., et al., *TYK2 protein-coding variants protect against rheumatoid arthritis and autoimmunity, with no evidence of major pleiotropic effects on non-autoimmune complex traits.* PLoS One, 2015. **10**(4): p. e0122271.
273. Bastarache, L., J.C. Denny, and D.M. Roden, *Phenome-Wide Association Studies.* JAMA, 2022. **327**(1): p. 75-76.
274. Denny, J.C., et al., *Systematic comparison of phenome-wide association study of electronic medical record data and genome-wide association study data.* Nat Biotechnol, 2013. **31**(12): p. 1102-10.
275. Verma, A., et al., *Human-Disease Phenotype Map Derived from PheWAS across 38,682 Individuals.* Am J Hum Genet, 2019. **104**(1): p. 55-64.
276. Iskusnykh, I.Y., A.A. Zakharova, and D. Pathak, *Glutathione in Brain Disorders and Aging.* Molecules, 2022. **27**(1).
277. Dwivedi, D., et al., *Glutathione in Brain: Overview of Its Conformations, Functions, Biochemical Characteristics, Quantitation and Potential Therapeutic Role in Brain Disorders.* Neurochemical Research, 2020. **45**(7): p. 1461-1480.
278. Aoyama, K., *Glutathione in the Brain.* Int J Mol Sci, 2021. **22**(9).
279. Dringen, R., *Metabolism and functions of glutathione in brain.* Progress in Neurobiology, 2000. **62**(6): p. 649-671.
280. Gu, M., et al., *Mitochondrial function, GSH and iron in neurodegeneration and Lewy body diseases.* J Neurol Sci, 1998. **158**(1): p. 24-9.
281. Ansari, M.A. and S.W. Scheff, *Oxidative stress in the progression of Alzheimer disease in the frontal cortex.* J Neuropathol Exp Neurol, 2010. **69**(2): p. 155-67.

282. Mandal, P.K., et al., *Brain glutathione levels--a novel biomarker for mild cognitive impairment and Alzheimer's disease.* Biol Psychiatry, 2015. **78**(10): p. 702-10.
283. Sultana, R., et al., *Protein levels and activity of some antioxidant enzymes in hippocampus of subjects with amnestic mild cognitive impairment.* Neurochem Res, 2008. **33**(12): p. 2540-6.
284. Puertas, M.C., et al., *Plasma oxidative stress parameters in men and women with early stage Alzheimer type dementia.* Experimental Gerontology, 2012. **47**(8): p. 625-630.
285. Rinaldi, P., et al., *Plasma antioxidants are similarly depleted in mild cognitive impairment and in Alzheimer's disease.* Neurobiology of Aging, 2003. **24**(7): p. 915-919.
286. Lovell, M.A., C. Xie, and W.R. Markesbery, *Decreased glutathione transferase activity in brain and ventricular fluid in Alzheimer's disease.* Neurology, 1998. **51**(6): p. 1562-6.
287. Sofic, E., et al., *Reduced and oxidized glutathione in the substantia nigra of patients with Parkinson's disease.* Neurosci Lett, 1992. **142**(2): p. 128-30.
288. Pearce, R.K., et al., *Alterations in the distribution of glutathione in the substantia nigra in Parkinson's disease.* J Neural Transm (Vienna), 1997. **104**(6-7): p. 661-77.
289. Hambright, W.S., et al., *Ablation of ferroptosis regulator glutathione peroxidase 4 in forebrain neurons promotes cognitive impairment and neurodegeneration.* Redox Biol, 2017. **12**: p. 8-17.
290. Shin, E.J., et al., *Glutathione Peroxidase-1 Knockout Facilitates Memory Impairment Induced by beta-Amyloid (1-42) in Mice via Inhibition of PKC betaII-Mediated ERK Signaling; Application with Glutathione Peroxidase-1 Gene-Encoded Adenovirus Vector.* Neurochem Res, 2020. **45**(12): p. 2991-3002.
291. Hazelton, G.A. and C.A. Lang, *Glutathione contents of tissues in the aging mouse.* Biochem J, 1980. **188**(1): p. 25-30.
292. Lash, L.H., *Role of glutathione transport processes in kidney function.* Toxicol Appl Pharmacol, 2005. **204**(3): p. 329-42.
293. Sun, X., et al., *Two-photon imaging of glutathione levels in intact brain indicates enhanced redox buffering in developing neurons and cells at the cerebrospinal fluid and blood-brain interface.* J Biol Chem, 2006. **281**(25): p. 17420-17431.
294. Richie, J.P., Jr., et al., *Blood glutathione concentrations in a large-scale human study.* Clin Chem, 1996. **42**(1): p. 64-70.
295. Cantin, A.M., et al., *Normal alveolar epithelial lining fluid contains high levels of glutathione.* J Appl Physiol (1985), 1987. **63**(1): p. 152-7.
296. Park, H.J., E. Mah, and R.S. Bruno, *Validation of high-performance liquid chromatography–boron-doped diamond detection for assessing hepatic glutathione redox status.* Analytical Biochemistry, 2010. **407**(2): p. 151-159.
297. Wang, X., et al., *Intramucosal pH and oxygen extraction in the gastrointestinal tract after major liver resection in rats.* The European journal of surgery = Acta chirurgica, 1993. **159**(2): p. 81-87.
298. Ziegler, T.R., et al., *REGULATION OF GLUTATHIONE REDOX STATUS IN LUNG AND LIVER BY CONDITIONING REGIMENS AND KERATINOCYTE GROWTH FACTOR IN MURINE ALLOGENEIC BONE MARROW TRANSPLANTATION1.* Transplantation, 2001. **72**(8).
299. Rost, J. and S. Rapoport, *Reduction-potential of Glutathione.* Nature, 1964. **201**(4915): p. 185-185.

300. Wang, L., Y.J. Ahn, and R. Asmis, *Sexual dimorphism in glutathione metabolism and glutathione-dependent responses.* Redox Biol, 2020. **31**: p. 101410.
301. Wang, H., H. Liu, and R.-M. Liu, *Gender difference in glutathione metabolism during aging in mice.* Experimental Gerontology, 2003. **38**(5): p. 507-517.
302. Chen, X., C. Guo, and J. Kong, *Oxidative stress in neurodegenerative diseases.* Neural Regen Res, 2012. **7**(5): p. 376-85.
303. Crack, P.J., et al., *Potential Contribution of NF-κB in Neuronal Cell Death in the Glutathione Peroxidase-1 Knockout Mouse in Response to Ischemia-Reperfusion Injury.* Stroke, 2006. **37**(6): p. 1533-1538.
304. Crack, P.J., et al., *Lack of glutathione peroxidase-1 exacerbates Abeta-mediated neurotoxicity in cortical neurons.* J Neural Transm (Vienna), 2006. **113**(5): p. 645-57.
305. Solodilova, M., et al., *The discovery of GGT1 as a novel gene for ischemic stroke conferring protection against disease risk in non-smokers and non-abusers of alcohol.* Journal of Stroke and Cerebrovascular Diseases, 2024. **33**(6): p. 107685.
306. Shao, X., et al., *Association Between Glutathione Peroxidase-1 (GPx-1) Polymorphisms and Schizophrenia in the Chinese Han Population.* Neuropsychiatr Dis Treat, 2020. **16**: p. 2297-2305.
307. Sian, J., et al., *Alterations in glutathione levels in Parkinson's disease and other neurodegenerative disorders affecting basal ganglia.* Annals of Neurology, 1994. **36**(3): p. 348-355.
308. Morgan, A.P., et al., *The Mouse Universal Genotyping Array: From Substrains to Subspecies.* G3 Genes|Genomes|Genetics, 2016. **6**(2): p. 263-279.
309. Broman, K.W., et al., *R/qtl2: Software for Mapping Quantitative Trait Loci with High-Dimensional Data and Multiparent Populations.* Genetics, 2019. **211**(2): p. 495-502.
310. Svenson, K.L., et al., *High-resolution genetic mapping using the Mouse Diversity outbred population.* Genetics, 2012. **190**(2): p. 437-47.
311. Yang, J., et al., *Advantages and pitfalls in the application of mixed-model association methods.* Nature Genetics, 2014. **46**(2): p. 100-106.
312. Sen, Ś. and G.A. Churchill, *A Statistical Framework for Quantitative Trait Mapping.* Genetics, 2001. **159**(1): p. 371-387.
313. Churchill, G.A. and R.W. Doerge, *Empirical threshold values for quantitative trait mapping.* Genetics, 1994. **138**(3): p. 963-971.
314. Robinson, G.K., *That BLUP is a Good Thing: The Estimation of Random Effects.* Statistical Science, 1991. **6**(1): p. 15-32.
315. Recla, J.M., et al., *Precise genetic mapping and integrative bioinformatics in Diversity Outbred mice reveals Hydin as a novel pain gene.* Mammalian Genome, 2014. **25**(5): p. 211-222.
316. Spanidis, Y., et al., *Assessment of the redox status in patients with metabolic syndrome and type 2 diabetes reveals great variations.* Exp Ther Med, 2016. **11**(3): p. 895-903.
317. Blake, J.A., et al., *Mouse Genome Database (MGD): Knowledgebase for mouse–human comparative biology.* Nucleic Acids Research, 2021. **49**(D1): p. D981-D987.
318. Finger, J.H., et al., *The mouse Gene Expression Database (GXD): 2017 update.* Nucleic Acids Research, 2017. **45**(D1): p. D730-D736.
319. Moreno, P., et al., *Expression Atlas update: gene and protein expression in multiple species.* Nucleic Acids Research, 2022. **50**(D1): p. D129-D140.

320. Ashburner, M., et al., *Gene Ontology: tool for the unification of biology.* Nature Genetics, 2000. **25**(1): p. 25-29.
321. The Gene Ontology Consortium, *Expansion of the Gene Ontology knowledgebase and resources.* Nucleic Acids Research, 2017. **45**(D1): p. D331-D338.
322. Smith, C.L., C.-A.W. Goldsmith, and J.T. Eppig, *The Mammalian Phenotype Ontology as a tool for annotating, analyzing and comparing phenotypic information.* Genome Biology, 2004. **6**(1): p. R7.
323. Gagliano Taliun, S.A., et al., *Exploring and visualizing large-scale genetic associations by using PheWeb.* Nature Genetics, 2020. **52**(6): p. 550-552.
324. Luo, L., et al., *The interaction between TMEM161B (rs768705) and paranoid personality traits in relation to the risk of major depressive disorder: Results form a longitudinal study of 7642 Chinese freshmen.* J Affect Disord, 2024. **365**: p. 171-177.
325. Hou, B., et al., *Role of rs454214 in Personality mediated Depression and Subjective Well-being.* Sci Rep, 2020. **10**(1): p. 5702.
326. Muench, C., et al., *The major depressive disorder GWAS-supported variant rs10514299 in TMEM161B-MEF2C predicts putamen activation during reward processing in alcohol dependence.* Transl Psychiatry, 2018. **8**(1): p. 131.
327. Hyde, C.L., et al., *Identification of 15 genetic loci associated with risk of major depression in individuals of European descent.* Nat Genet, 2016. **48**(9): p. 1031-6.
328. Wang, L., et al., *TMEM161B modulates radial glial scaffolding in neocortical development.* Proc Natl Acad Sci U S A, 2023. **120**(4): p. e2209983120.
329. Akula, S.K., et al., *TMEM161B regulates cerebral cortical gyration, Sonic Hedgehog signaling, and ciliary structure in the developing central nervous system.* Proc Natl Acad Sci U S A, 2023. **120**(4): p. e2209964120.
330. Guo, C., et al., *XRCC4 deficiency in human subjects causes a marked neurological phenotype but no overt immunodeficiency.* Journal of Allergy and Clinical Immunology, 2015. **136**(4): p. 1007-1017.
331. Mazaheri, H. and M. Saadat, *Susceptibility to schizophrenia and insertion/deletion polymorphism in intron 3 of the XRCC4 gene.* Psychiatry Research, 2015. **228**(3): p. 972-973.
332. Pehlivan, S., et al., *eNOS and XRCC4 VNTR variants contribute to formation of nicotine dependence and/or schizophrenia.* Bratisl Lek Listy, 2017. **118**(8): p. 467-471.
333. Dasdemir, S., et al., *DNA repair gene XPD Asp312Asn and XRCC4 G-1394T polymorphisms and the risk of autism spectrum disorder.* Cell Mol Biol (Noisy-le-grand), 2016. **62**(3): p. 46-50.
334. Zhao, P., et al., *Genetic polymorphisms of DNA double-strand break repair pathway genes and glioma susceptibility.* BMC Cancer, 2013. **13**: p. 234.
335. Ahel, I., et al., *The neurodegenerative disease protein aprataxin resolves abortive DNA ligation intermediates.* Nature, 2006. **443**(7112): p. 713-716.
336. Nurdiana, S., et al., *Improvement of spatial learning and memory, cortical gyrification patterns and brain oxidative stress markers in diabetic rats treated with Ficus deltoidea leaf extract and vitexin.* Journal of Traditional and Complementary Medicine, 2018. **8**(1): p. 190-202.
337. Chui, A., et al., *Oxidative stress regulates progenitor behavior and cortical neurogenesis.* Development, 2020. **147**(5).

338. Gao, Y., et al., *A Critical Role for DNA End-Joining Proteins in Both Lymphogenesis and Neurogenesis.* Cell, 1998. **95**(7): p. 891-902.
339. Gao, Y., et al., *Interplay of p53 and DNA-repair protein XRCC4 in tumorigenesis, genomic stability and development.* Nature, 2000. **404**(6780): p. 897-900.
340. Junop, M.S., et al., *Crystal structure of the Xrcc4 DNA repair protein and implications for end joining.* The EMBO Journal, 2000. **19**(22): p. 5962-5970-5970.
341. Shackelford, D.A., *DNA end joining activity is reduced in Alzheimer's disease.* Neurobiology of Aging, 2006. **27**(4): p. 596-605.
342. Koch, R.L., et al., *Discovery of genomic loci for liver health and steatosis reveals overlap with glutathione redox genetics.* Redox Biology, 2024. **75**: p. 103248.
343. Raho, S., et al., *KRAS-regulated glutamine metabolism requires UCP2-mediated aspartate transport to support pancreatic cancer growth.* Nature Metabolism, 2020. **2**(12): p. 1373-1381.
344. Qiu, P., et al., *Sirt1 deficiency upregulates glutathione metabolism to prevent hepatocellular carcinoma initiation in mice.* Oncogene, 2021. **40**(41): p. 6023-6033.
345. Chen, Y., et al., *The role of nuclear factor E2-Related factor 2 and uncoupling protein 2 in glutathione metabolism: Evidence from an in vivo gene knockout study.* Biochem Biophys Res Commun, 2016. **478**(1): p. 87-92.
346. Gatti, D.M., et al., *Quantitative trait locus mapping methods for diversity outbred mice.* G3 (Bethesda), 2014. **4**(9): p. 1623-33.